Universitat de Girona
Escola Politècnica Superior

Treball final de grau

Estudi: Grau en Enginyeria Biomèdica

Títol:
Tumor-on-a-chip: new strategies of *in-vitro* cancer cell culture.

Document: Memòria

Alumne: Antoni Ignasi Cànaves Llabrés

Tutor: Quim de Ciurana Gay
Departament: Enginyeria Mecànica i de la Construcció Industrial
Àrea: Enginyeria dels Processos de Fabricació

Convocatòria (mes/any): Juny 2022

INDEX

1. INTRODUCTION

I had the opportunity to intern at the TargetsLab research centre during the summer of 2021. This group, affiliated with the University of Girona, has been exploring new ways for the treatment of Triple Negative Breast Cancer (TNBC) and lung cancer during the past few years. I was tasked with assisting former doctoral-level researchers in the production of specialised scaffolds that could be utilised for the growth of the MDA-MB-231 TNBC cell line, and which would hopefully permit and enhance the formation of highly specific cell structures known as tumoroids by imitating the human extracellular matrix. These formations could be interpreted as early form tumours or a functional tumoral mass on a very small scale; they are currently viewed as a promising tool for cost-effective studies on new cancer treatments that will be used in the field of oncology's precision medicine.

Despite what I knew about the basic cell culture methods currently employed in the world of scientific research, I was continually struck by the fact that the design and functioning of culture equipment had not been updated to accommodate the biomedical field's growing complexity.

During my internship, I learnt that the key to obtaining the needed structures or any organ-like cell culture consisted of mimicking the conditions and dynamics of the human body as accurately as possible, given the technical constraints. However, many other parameters must be applied to the culture in order to achieve a successful simulation of the dynamics of the human internal environment, including the flow and pressure of the liquids in contact with the cells or the concentration of oxygen and carbon dioxide in the culture vessel, among others.

At that time, I began exploring existing dynamic culture methods and became familiar with the concept of "Organ-on-a-Chip," a micro-scale system designed to imitate the human body environment in order to build human tissue models for disease modelling and medication testing. Despite its many advantages, a brief market analysis revealed that very few businesses were devoted to the development of dynamic culture equipment and that, in reality, this feature had a substantial impact on the prices of this equipment, which began at approximately $20,000.

Since I began my degree, one of my professional goals has been to participate in the development of strategies to shape a more accessible, sustainable, and decentralised science. Therefore, after the investigation, I began to consider how universities or research groups, with significantly fewer resources than large pharmaceutical multinationals or large educational institutions, might be able to utilise these new techniques and technologies. Thus, the idea arose to design a system with the same objectives and fundamental features as existing dynamic culture equipment, but at a significantly cheaper cost, and whose production could be handled by the same groups in a simple and cost-effective manner.

The following is a proposal for a device for the production of dynamic 3D cell cultures that aims to meet the aforementioned affordability and functionality requirements. AutoDesk's AutoCAD platform will be used for the design, while fused filament fabrication technique has been selected for the manufacture. To realise the full potential of personalised medicine, it is natural and necessary for personalised and cost-effective manufacturing and medicine to converge.

2. PREVIOUS CONCEPTS

2.1. BIOMEDICINE

2.1.1. CANCER

Cancer is one of the main pathologies affecting the population worldwide, with more than 19.3 million diagnoses and a mortality rate of almost 10 million by 2020 according to the World Health Organization, which represents more than 10% of total deaths worldwide [1]. This year, the most common (in terms of cancer diagnosis) were:

- Breast (2.26 million cases)
- Pulmonary (2.21 million deaths)
- Colorectal (1.93 million cases)
- Prostate (1.41 million cases)
- Skin (non-melanoma) (1.20 million cases)
- Gastric (1.09 million cases)

The types of cancer that caused a highest number of deaths in 2020 were:

- Pulmonary (1.8 million deaths)
- Colorectal (935,000 deaths)
- Liver disease (830,000 deaths)
- Gastric (769,000 deaths)
- Breast (685,000 deaths)

In our country, it represents the second cause of death after cardiovascular diseases, it is estimated that by the end of 2021, 276.239 cases were detected according to the calculations of REDECAN (Spanish Network of Cancer Registries)[2].

Getting to know and describing the pathophysiological mechanisms of cancer is a complex task. In 1838, at the beginning of its research, cancerous tissue was described as the one made up of cells with altered morphology and it was postulated that the cause of the pathology was cellular damage. Currently, cancer is considered a disorder of cells that are abnormally divided, which leads to the formation of aggregates that create lesions to the adjacent tissues, they nourish from the body and alter its physiology; in addition to these factors, aggregates can migrate and invade distant tissues, continue their growth and thus give rise to the well-known metastasis [3].

2.1.2. CELL CULTURE

The term cell culture refers to laboratory methods that allow the growth of prokaryotic or eukaryotic cells under physiological conditions. Its origins date to the early 20th century, when it was introduced to study tissue growth and maturation, viral biology and vaccine development, the role of genes in disease and health, and the use of large-scale hybrid cell lines to produce biopharmaceuticals.

The experimental applications of cultured cells are as diverse as the cell types that can be grown in vitro. However, in the clinical context, cell culture is most often associated with the creation of model systems used to study basic cell biology, mimic disease mechanisms, or investigate the toxicity of novel drugs. One of the advantages of using cell cultures for these applications is the ability to manipulate genes and molecular signalling pathways. In addition, the homogeneity of clonal cell populations or specific cell types and well-defined culture systems eliminates

confounding genetic or environmental variables, generating data with high reproducibility and consistency that cannot be guaranteed when whole organ systems are studied [4].

Cell culture systems are indispensable tools for a variety of in vitro clinical studies and for basic research. The classically preferred model is a static dish culture. This approach generates mainly adherent two-dimensional (2D) cell monolayers that do not reflect the situation in vivo, where cells grow in a complex three-dimensional (3D) microenvironment [5]. Although it is known that static 2D cell culture systems resemble the complexity of the physiologic conditions only to a limited extend, the expansion and differentiation of cells on plastic surfaces is still "gold standard" in many cell culture applications.

2.1.3. 3D CELL CULTURE

The use of 3D cell culture refers to the process of growing cells in their natural environment or in vivo. This is done by adding a third dimension that can mimic the complex interactions between cells and between cells and the extracellular matrix (ECM). In living tissues, cells exist in 3D microenvironments with complicated cell-cell and cell-matrix interactions and complex transport dynamics for nutrients and cells. Standard 2D or monolayer cell cultures poorly represent these environments, often making them unreliable predictors of drug efficacy and toxicity in vivo. Cells cultured in simplified monolayers lose their original phenotypic and functional properties, often become dedifferentiated, and are very different from the tissues from which they are derived. As a result, the biological responses of these cells may not be physiologically relevant, which can greatly affect their predictability and thus their utility for drug discovery.

3D spheroids are more similar to tissues in vivo in terms of cellular communication and development of extracellular matrices. These matrices contribute to the ability of cells to move within their spheroid, similar to cells in living tissue. The spheroids are thus improved models for cell migration, differentiation, survival, and growth. Because of their architectural similarity to in vivo tissues, 3D cells cultures retain the phenotypic and functional properties of their in vivo counterparts, providing a more physiologically relevant in vitro system for evaluating biological responses. In addition, 3D cells cultures provide a more accurate representation of cell polarization, as cells can only be partially polarized in 2D. In addition, cells grown in 3D exhibit different gene expression than cells grown in 2D.

In the world of drug discovery and development, 3D cell culture systems are rapidly replacing 2D cell cultures due to their reliability as an in vitro approach to predicting in vivo responses [5][6].

2.1.4. DYNAMIC CULTURING SYSTEM

Dynamic cell culture describes the in vitro culture of cells in the presence of applied mechanical stress. Of great emerging interest is the ability to control the flow of fluid, such as medium, over cells while they grow. Flow rate can be generated very precisely using microfluidic instruments and is an ideal way to better replicate the dynamic environment that cells normally reside in. The use of bioreactors bears the potential to achieve a more organ or tissue-specific dynamic culture by providing physical cues, improved nutrient supply (by enhancing the removal of waste products through the circulation of medium), and adding shear stress to cell [7][8].

2.1.5. TUMOROID

One of the most important recent advances in biological science research is the development of 3D cell culture systems, such as organoids, spheroids, and chip models of organs. A 3D cell culture is an artificial environment in which cells can grow and interact with their environment in all three dimensions. These conditions are similar to an in vivo state.

Organoids are a type of 3D cell culture that contains organ-specific cell types that can show spatial organization and replicate some of the functions of the organ in question. They recreate a very relevant system from a physiological point of view that allows researchers to analyse complex and multidimensional issues, such as the onset of a disease, tissue regeneration, and organ-to-organ interaction.

The term "tumoroid" means "tumor-like organoid"; tumors are generally derived from primary tumors harvested from cancer patients and may mimic the human tumor microenvironment (TME). They are currently considered a promising tool for cost-effective studies on new cancer drugs that will be used in precision medicine in the field of oncology [9].

2.1.6. SCAFFOLD

Scaffolds are structures engineered to induce desirable cellular interactions that contribute to the formation of new functional tissues for medical purposes. Cells are often 'seeded' into these structures, which can support the formation of three-dimensional tissue. Scaffolds mimic the extracellular matrix of native tissue by reconstructing the in vivo environment and allowing cells to influence their own microenvironment. They typically serve at least one of the following purposes: enable cell attachment and migration (as seen in *Figure 1*), transport and retain cells and biochemical factors, allow diffusion of vital cell nutrients and expressed products, and exert certain mechanical and biological influences to alter cell phase behaviour.

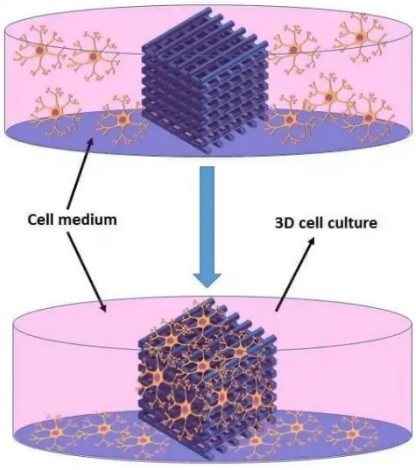

Figure 1. *Graphic representation of cell adhesion to a scaffold* [187].

To achieve the goal of tissue reconstruction, scaffolds must meet some specific requirements. High porosity and adequate pore size are necessary to facilitate cell seeding and diffusion of cells and nutrients throughout the structure. They are critical for tissue engineering because they must provide a suitable mechanical and chemical environment in which seeded cells can thrive and function as expected and eventually form fully functional tissue. These requirements place high demands on the materials used to fabricate the scaffolds, which must be naturally biocompatible and biodegradable. The rate at which degradation occurs must match the rate of tissue formation as closely as possible [6], [10]–[12].

2.1.7. HIDROGEL

Hydrogels are hydrophilic polymer networks that are able to swell, store large amounts of water and maintain three-dimensional, swollen structures. These properties form the basis for various applications, especially in the biomedical field. Many hydrogels are synthetic, but some are derived from nature [13].

The cross-links that bind the polymers of a hydrogel fall into two general categories: physical and chemical. Chemical hydrogels have covalent cross-linking bonds, while physical hydrogels have non-covalent bonds. A covalent bond is a chemical bond in which pairs of electrons are exchanged between atoms. These electron pairs are called common pairs or bond pairs. The stable balance between attractive and repulsive forces between atoms when they share electrons is called a covalent bond. A non-covalent interaction differs from a covalent bond in that it is not a sharing

of electrons, but rather scattered variations of electromagnetic interactions between molecules or within a molecule [14].

Chemical hydrogels result in strong, irreversible gels due to covalent bonding. They can also have harmful properties, making them unfavourable for medical applications. Physical hydrogels, on the other hand, have high biocompatibility, are non-toxic and are also easily reversed by simply changing an external stimulus such as pH or temperature; therefore, they are well suited for medical applications.

Hydrogels have proven useful in a number of cell culture applications. They reveal fundamental phenomena that regulate cell behaviour and provide tools for expansion and targeted differentiation of different cell types that are not possible with conventional culture substrates. The production of hydrogels for cellular experiments usually involves either the encapsulation of viable cells in the material or the production of substrates using moulds that are later populated with cells [15]–[18] .

2.2. FABRICATION

2.2.1. ELECTROSPINNING

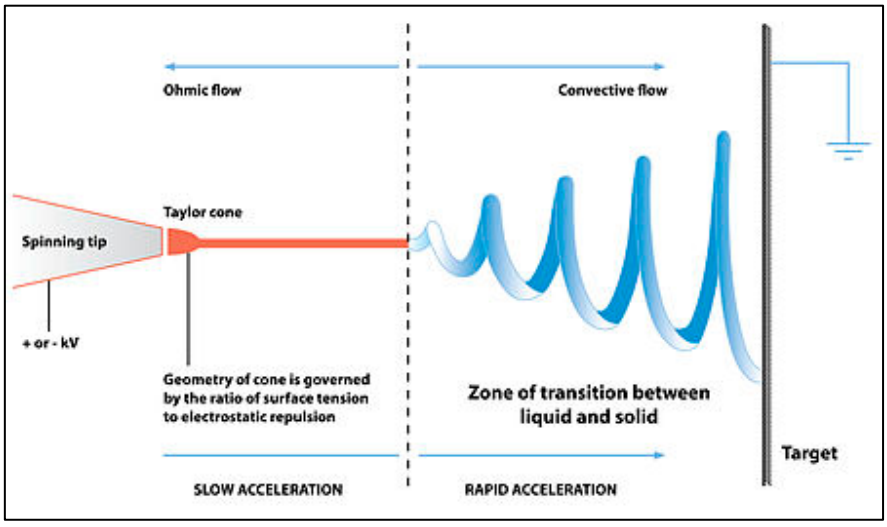

Figure 2. Electrospinning process [19].

Electrospinning is a widely used technique to produce polymer fibres with a diameter between 2 nm and several micrometres from a polymer in solution. This technique has gained interest in the last decade, mainly because of the control it can exert over the structure and size of the fibres, the versatility of the polymers used and the unique properties of the final material: high specific surface area, controllable and cross-linked porosity, high mechanical performance, flexibility etc.

The basic process is based on the combination of three main components: the current generator, the metal needle and the collector in which the fibres are deposited. The needle is in a syringe that contains the solution and the flow is controlled by a pump. When a voltage is applied (usually in the range of 1 to 30 kV), the droplet emerging from the needle is electrified and the charges are distributed on the surface so that the droplet experiences two types of forces: electrostatic, as repulsion between the surface charges, and the coulombic forces exerted by the external electric field. The surface of the droplet gradually resists the action of these forces until it begins to stretch and form an inverted cone called the Taylor cone. The stretching process reaches a limit where the concentration of the charge is so high that it exceeds the surface tension of the

solution and creates a current at the tip of the cone. This current passes through an unstable path where it undergoes a stretching process simultaneously with the evaporation of the solvent, resulting in a drastic reduction in diameter. Attracted by the charged collector, the fibres are deposited and randomly distributed to form a nonwoven fabric. The diameter of the fibres and their morphology determine the properties of the finished material [20], [21]. This process is visually represented in *Figure 2*.

2.2.2. 3D MODELING

3D modelling is the process of developing a mathematical representation of any three-dimensional object (either inanimate or animate) using specialised software. The product is called a 3D model. These 3D objects can be generated automatically or created manually by deforming the mesh that contains them or otherwise manipulating its vertices. 3D models are used for a variety of media, including video games, movies, architecture, illustration, engineering and commercial advertising.

3D modelling software is a type of 3D graphics software used to create three-dimensional models. Although complex mathematical formulae form the basis of 3D modelling software, the programmes automate the calculations for users and have tool-based user interfaces. 3D models represent a three-dimensional object through a collection of points in 3D space connected by various geometric entities such as triangles, lines, curved surfaces, etc. Because they are a collection of data (points and other information), 3D models can be created by hand, by algorithms or by scanning. They can be displayed as a two-dimensional image through a process called 3D rendering or used in a computer simulation of physical phenomena. The model can also be created physically using 3D printing equipment [22]–[24].

2.2.3. ADDITIVE MANUFACTURING

Additive manufacturing is the process of building up an object layer by layer. It is the opposite of subtractive manufacturing, where an object is created by removing a solid block of material until the final product is ready.

Technically, additive manufacturing can refer to any process where a product is created by building something up, such as casting, but it usually refers to 3D printing (see the more used additive manufacturing methods in *Figure 3*). 3D printing is the construction of a three-dimensional object from a CAD model or a 3D digital model. The term "3D printing" can refer to a variety of processes in which material is applied, bonded or solidified by computer control to create a three-dimensional object, usually adding the material layer by layer.

Additive manufacturing was first used in the 1980s to develop prototypes but these objects were usually non-functional. This process was called rapid prototyping because it allowed a scale model of the final object to be created quickly, without the typical set-up process and costs associated with creating a prototype. As additive manufacturing improved, its application expanded to include rapid tooling, which was used to create moulds for final products. In the early 2000s, additive manufacturing was used to produce functional products. Today, the precision, repeatability and material diversity of 3D printing have increased to the point where some 3D printing processes are considered viable technology for industrial production, and the term additive manufacturing can be used synonymously with 3D printing. One of the main advantages of 3D printing is the ability to produce very complex shapes or geometries that would otherwise be impossible to construct by hand, including hollow parts or parts with internal truss structures to reduce weight. Fused Deposition Modelling (FDM), which uses a continuous filament of a

thermoplastic material, is the most commonly used 3D printing process [25]–[27]. This term is a Trademark of Stratasys Inc. [28], thus the technology is known in the community as Fused Filament Fabrication or FFF.

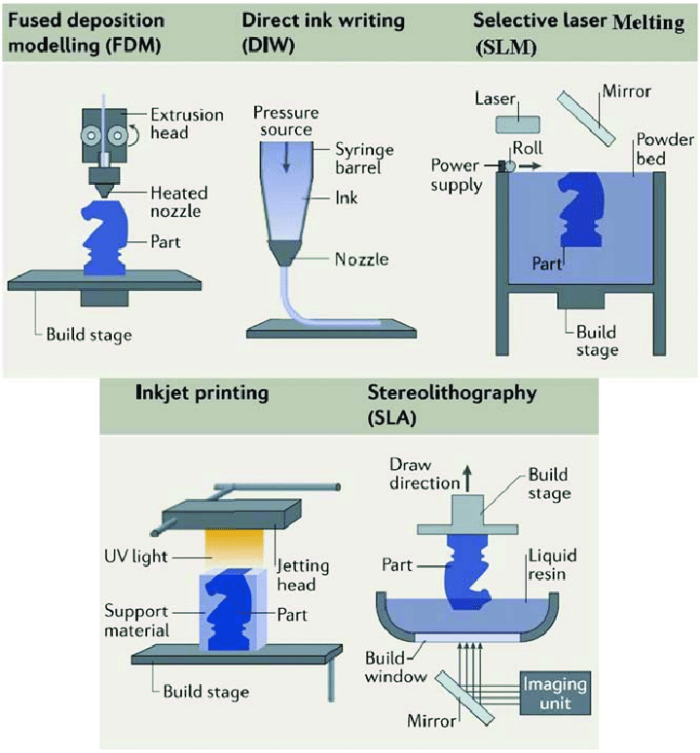

Figure 3. Popular additive manufacturing methods [29].

2.2.4. FUSED FILAMENT FABRICATION

Fused Filament Fabrication (FFF) is a 3D printing process that uses a continuous filament made of a thermoplastic material. The plastic filament is wound on a spool and feeds the heater (hot end). The resulting molten material is then ejected through a nozzle in the form of 'drops', while the incoming filament, still in the solid phase, acts as a 'trigger'. The nozzle is mounted on a mechanical support that can be moved in the X-Y plane. As the nozzle is moved on the table in a predetermined geometry, it applies a thin grain of molten plastic that solidifies on contact with the substrate and/or previous layers of the object. Once a layer is complete, the platform is lowered in the Z direction to begin the next layer. This process continues until the object is completed. The 3D printer head or printer extruder is responsible for melting the material to form the layers of the object. The extrusion is done by a part called the cold end, which pulls the filament, and a hot end, which melts it and applies it to the object being constructed [30], [31].

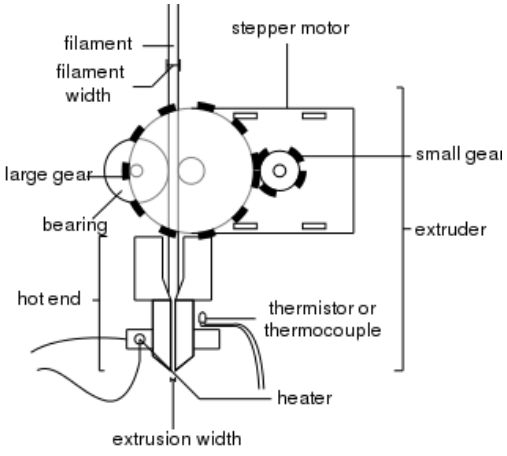

Figure 4. Illustration of an extruder [188].

The cold end usually consists of a stepper motor, a small gear, a large gear and a bearing. The hot end consists of the heater and the thermistor sensor, as seen in *Figure 4*. The speed of the print

head must be controlled so that the deposition can be stopped and started and a layer without holes or build-up is produced [32]. We distinguish between two varieties of extruders:

- Direct extruder: The filament runs directly from the sprocket to the hot end, which are in close proximity. This proximity allows you to manage the extrusion of the filament, resulting in fewer errors and easier filament replacement. In addition, it is employed for flexible materials, which can fail with other types of extruders. The primary issue with direct extruders is that the filament moves abruptly with the motion of the machine, resulting in increased inertial forces and vibrations.
- Bowden Extruder: A Teflon tube separates the sprocket from the hot end. This tube is used to introduce the filament till it reaches the nozzle. Adding one more component to the machine increases the number of parts that must be replaced and inspected. This sort of extruder can fail with flexible materials because to the difficulty in controlling the filament tension inside the Bowden tube. Removing components from moving elements and affixing them to the structure accelerates the movement of the 3D printer and can boost printing speed.

There are a variety of materials that can be used in this type of technology, including thermoplastics such as ABS (acrylonitrile butadiene styrene), PLA (polylactic acid), high impact polystyrene (HIPS), polyurethane (TPU), nylon, ...

The term Fused Filament Fabrication was coined by members of the RepRap project to avoid the patented term Fused Deposition Modelling (FDM). FFF is now the most popular technique (in terms of number of machines) in mainstream 3D printing. Other techniques, such as stereolithography, can achieve better results but are much more expensive. FDM was developed in 1988 by S. Scott Crump, the co-founder of Stratasys. When the patent on this technology expired in 2009, anyone could use this type of printing without paying Stratasys for the right to do so. This opened up commercial, "Do It Yourself" and open-source 3D printer applications [33].

2.3. MATERIALS

2.3.1. PLA

PLA (molecular structure shown in *Figure 5*), also known as polylactic acid or polylactide, is a thermoplastic that, unlike other industrial materials made mainly from petroleum, is derived from renewable resources such as corn starch, tapioca roots or sugar cane and can be semi-crystalline or amorphous depending on the purity of the polymer character. Due to its more environmentally friendly origin, this material has become very popular in the 3D printing industry. We have started to see it in medical applications and in the food industry as it has excellent organoleptic properties [34], [35].

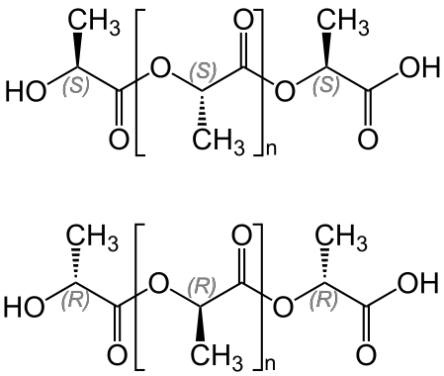

Figure 5. Structural unit of the PLA polymer [189].

Lactic acid is produced through a fermentation process from 100% renewable resources. The polymer degrades quickly in the environment and has very low toxicity as it is mainly converted into water and CO_2. PLA can be produced by condensing lactic acid and ring opening the cyclic lactic acid dimer [36].

PLA is one of the easiest materials to print on and does not require precise print settings. For practical applications, the strength of PLA is surprisingly sufficient for most lightweight prototypes and models. Especially in recent years, PLA blends have improved greatly in terms of durability.

However, research shows that for prints that need to be truly food safe / suitable for biological research, a number of post-processing procedures need to be carried out, as bacteria or microorganisms can be deposited between the layers of the model during filament printing due to the hardware used not being a sterile environment [37], [38].

2.3.2. PET-G / PCTG

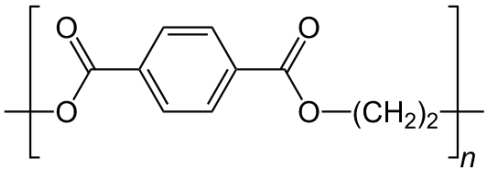

Figure 6. PET molecule [190].

Polyethylene terephthalate or PET (molecular structure shown in *Figure 6*), is a type of thermoplastic polymer obtained by a polycondensation reaction between terephthalic acid and ethylene glycol, both low molecular weight substances derived from petroleum. It is a recyclable material, but not biodegradable. This opaque or transparent linear thermoplastic polymer is very resistant, light, harmless and has a high degree of crystallisation, depending on the arrangement of the molecules that make it up. It belongs to the group of synthetic materials called polyesters.

Its main properties include high transparency, although it can absorb dyes, high resistance to wear and corrosion, very good sliding coefficient, good chemical and thermal resistance, very good barrier to carbon dioxide, acceptable barrier to oxygen and moisture, compatibility with other barrier materials, which together improve the barrier quality of packaging and therefore allow its use in certain markets, recyclability, the fact that its viscosity decreases when heated, resistance to ultraviolet (UV) radiation and approval for use in products that must come into contact with food [39]–[41].

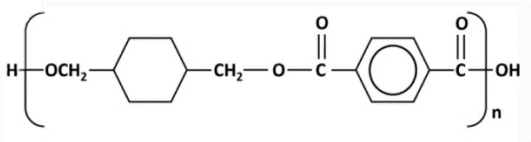

Figure 7. PETG molecule [195].

PETG (polyethylene terephthalate glycol) (molecular structure shown in *Figure 7*), is one of the types in which PET plastic polyester is presented. PETG is formed by the copolymerisation of PET. The process is based on the addition of cyclohexanedimethanol (CHDM) instead of ethylene glycol, resulting in a block with longer atoms where the adjacent chains do not fit together as in ethylene glycol. This makes it possible to stop crystallization when acting on this material, to obtain more transparent objects and to lower the melting point. These are ideal properties for producing resistant parts that are easy to mould or extrude. Due to its ease of extrusion and thermal stability, PETG and other PET derivatives are increasingly used in the world of 3D printing FDM / FFF.

One of the reasons PETG is used in 3D printing instead of PET is the problem the latter has when it heats up. When overheated, PET becomes cloudy and brittle, which is impractical for use with a 3D printer FDM / FFF, a problem that does not occur with PETG as it contains glycol. It is also more durable thanks to its higher resistance to wear and corrosion from oxidants, which comes with high impact resistance.

PETG as a material for 3D printing is characterised by a functionality very similar to that of ABS (good temperature resistance, durable, resistant) and is as easy to print as PLA. It is also characterised by good adhesion between layers, low deformation during printing, resistance at low temperatures for long periods of time, chemical resistance (bases and acids) and absence of

odour during printing. The application of this copolyester in 3D printing is focused on the production of parts that require a certain flexibility and good impact resistance (even at low temperatures) [42]–[44].

In both cases, these materials meet FDA (Food and Drug Administration, USA) requirements, so they are approved for food contact and can also be used in medical applications. PET is odourless and tasteless and can be sterilised with gamma rays or ethylene oxide; PETG can also be sterilised by radiation but not autoclaved [41], [45].

PCTG (modified cyclohexylene dimethylene glycol polyterephthalate) belongs to the same family of polyesters as the increasingly popular PETG. Compared to its better-known counterpart, PCTG offers higher impact strength, temperature resistance and clarity, making it an excellent alternative to PETG. This filament does not require a heating chamber, so it can be used in home printers. At the same time, it offers high dimensional stability and its low shrinkage prevents the model from cracking. It also meets the requirements of the FDA and could be used in the food-packaging and medical fields [46].

PCTG offers much higher impact resistance than other similar materials. It achieves results of about 90 kJ / m2 in the Izod test (PETG: 5-8 kJ / m2). PCTG also withstands higher temperatures (up to 76°C)[47].

2.3.3. TPU

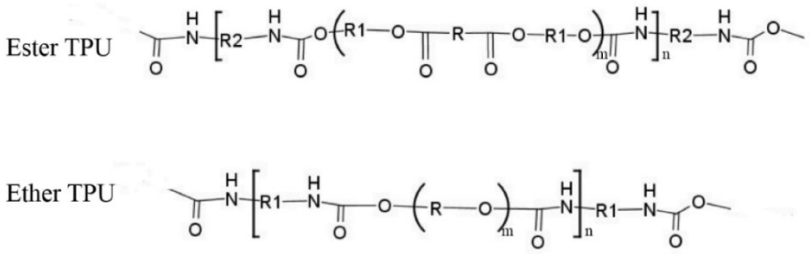

Figure 8. TPU molecules [48].

Thermoplastic polyurethane is one of the existing varieties within polyurethanes. It is a linear elastomeric polymer and therefore thermoplastic. Vulcanisation is not required for its processing, but a new process for cross-linking was introduced in 2008. This elastomer can be moulded by the usual processes for thermoplastics, such as injection moulding, extrusion and blow moulding. TPE-U is an abbreviation for urethane-based thermoplastic elastomer, but is commonly referred to as TPU. Thermoplastic polyurethane is characterised by its high resistance to abrasion, oxygen, ozone and low temperatures. This combination of properties makes thermoplastic polyurethane an engineering plastic. It is a block copolymer consisting of alternating sequences of hard and soft segments. Its conformability depends on the presence of hard and soft segments in its chemical composition. The ratio of hard and soft segments can be manipulated to produce a wide range of hardnesses.

Hard segments are isocyanates and can be classified as aliphatic or aromatic depending on the type of isocyanate. The soft segments are reactive polyol. In addition to the ratio of hard and soft segments in a given TPU product, the type of isocyanate and polyol is also responsible for the properties of the resulting TPU. The linear and long-chain polyols and the linear and short-chain diols react with the diisocyanates to form a semi-crystalline polymer with a linear structure, whereby the combination of the polyols with the diisocyanates forms the amorphous part

(flexible segment) and the combination of the short-chain diols with the diisocyanates forms the crystalline part (hard segment).

The type of raw material and the reaction conditions determine the properties of the final product. Thermoplastic polyurethane can be produced from two families of polyols: Polyester-based polyols and polyether-based polyols.

Polyester-based polyols are characterised by very good mechanical properties and good resistance to temperatures, mineral oils and hydraulic fluids. Polyether-based polyols are characterised by higher hydrolysis resistance, greater flexibility at low temperatures and better resistance to microorganisms [49]–[51]. *Figure 8* shows the molecular structure of each group.

2.3.4. POLY(METHYL METHACRYLATE)

Polymethyl methacrylate (PMMA) (molecular structure shown in *Figure 9*) is an amorphous thermoplastic. It is better known as acrylic and is sold under brands such as Plexiglas®. PMMA is a durable, highly transparent material with excellent resistance to ultraviolet radiation and weathering. It can be coloured, shaped, cut and perforated [52].

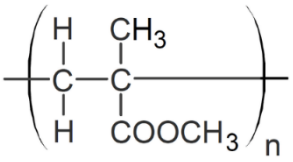

Polymethyl methacrylate: PMMA

Figure 9. PMMA molecule [191].

Acrylic compounds have a high tendency to polymerise; the reaction is very exothermic. They are produced by bulk or suspension polymerisation. Bulk polymerisation is also called in-situ polymerisation because it is carried out without solvent or water and results in semi-finished products such as sheets, blocks or pipes without the need for moulding. In this process, primers are added to the pure monomer or a higher viscosity prepolymer. Heat must be dissipated by cooling water or air to obtain a polymer without internal stresses; to achieve this, the polymerisation process can take days or weeks. PMMA obtained by bulk polymerisation has a high molecular weight, so it cannot be melted without decomposing. An isotropic product is obtained that has no orientation and has excellent optical properties [53], [54].

PMMA can be bonded with cyanoacrylate cement (commonly known as superglue), with heat (welding) or with chlorinated solvents such as dichloromethane or trichloromethane (chloroform) to dissolve the plastic at the joint, which then melts and hardens to form an almost invisible weld. Scratches can be easily removed by polishing or heating the surface of the material[55] .

You can form intricate designs from PMMA sheets by laser cutting. PMMA vaporises into gaseous compounds (including its monomers) during laser cutting, creating a very clean cut and making cutting very easy.

2.3.5. CHLOROFORM

Trichloromethane, chloroform or methyl trichloride, is a chemical compound with the chemical formula $CHCl_3$. It can be obtained by chlorination as a derivative of methane or ethyl alcohol or, more commonly in the pharmaceutical industry, using iron and acid on carbon tetrachloride.

At room temperature, it is a volatile, non-flammable, colourless liquid. It decomposes slowly by the combined action of oxygen and sunlight, converting to phosgene (COCl2) and hydrogen chloride (HCl) according to the following equation: $2\,CHCl_3 + O_2 \rightarrow 2\,COCl_2 + 2\,HCl$.

Since it is usually stable and miscible with most lipids and saponifiable organic compounds, it is often used as a solvent. It is also used in molecular biology for various processes, e.g., DNA extraction from cell lysates. Likewise, it is used in the fixation of post-mortem histological specimens [56]–[58].

It is one of the most commonly used solvents for smoothing printed PLA and PETG models, as it is stronger and faster acting than acetone. However, the fumes produced by its evaporation are more toxic than those of acetone [59].

2.3.6. PDMS

Polydimethylsiloxane (PDMS) (molecular structure shown in *Figure 10*) is a polymer derived from silicones. Common to all silicones is the repetition of siloxane units, each consisting of a $Si-O$ group. A large number of side groups can be attached to a silicon atom. In the case of PDMS, this is methyl, CH3. Different chain ends can be coupled to the polymer. Trimethylsiloxy $Si-SH_3$ usually forms the chain ends. The shortest molecule consisting of only two end groups and containing no dimethylsiloxane monomer units is hexamethyldisiloxane, HMDSO, which is very important as a process gas for hydrophobic plasma coatings. PDMS are linear polymers that exist in a liquid state with a very high molecular weight. However, they can be cross-linked to become elastic. It is a nearly inert polymer and very resistant to oxidation. It can be used as an electrical insulator in organic electronics (microelectronics or polymer electronics) as well as in biological microanalysis.

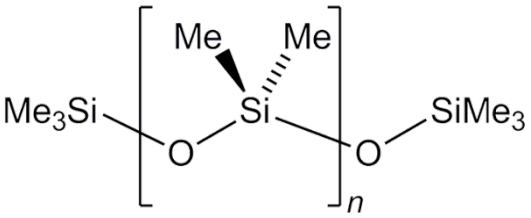

Figure 10. PDMS molecule [192].

One of the most common applications of low-pressure plasma for PDMS is in the field of microfluidic systems: The customer produces a specific polydimethylsiloxane depending on the application, then it is plasma treated and finally the PDMS chip is mounted on a glass plate, silicon surfaces or other substrates. Some of the advantages of plasma pre-treatment in microfluidic systems are the short processing time, the ability to create irreversible PDMS bonds on the substrate surface leading to the formation of impermeable channels in the microfluidic assembly, the hydrophilization of PDMS and the substrate surface with the subsequent complete wetting of the channel and the design of hydrophilic-hydrophobic regions. If we focus on the application of microfluidic systems, they will be crucial in the future for the study of chemical reactions and fluid transport on a microscopic scale, the detection of biological organisms and rapid clinical diagnosis and screening of drugs.

3. STATE OF THE ART

3.1. ORGAN-ON-A-CHIP

Organ-on-a-chip is a system that biomimetically simulates a physiological organ and is integrated into a microfluidic device. The chip's microenvironment simulates the organ in terms of tissue interactions and mechanical stimulation using cell biology, engineering and biomaterial technologies. This represents the structural and functional properties of human tissue and can be used to predict response to a variety of stimuli, including pharmacological and environmental responses. It has a wide range of applications in precision medicine and the development of biological defence strategies [60], [61].

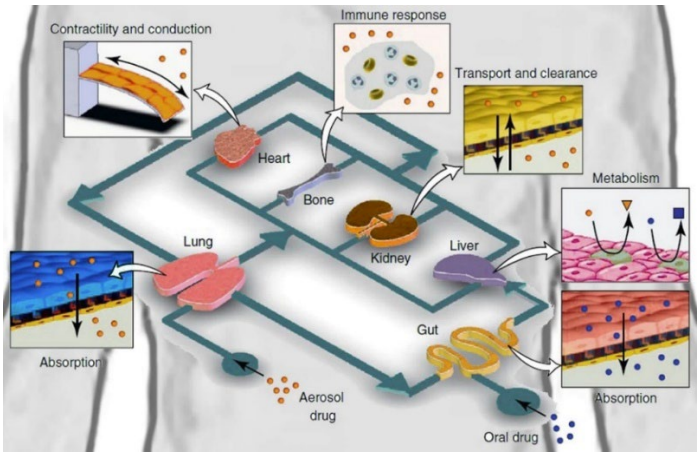

Figure 11. Example of body-on-a-chip (interconnected organs-on-a-chip) system [62].

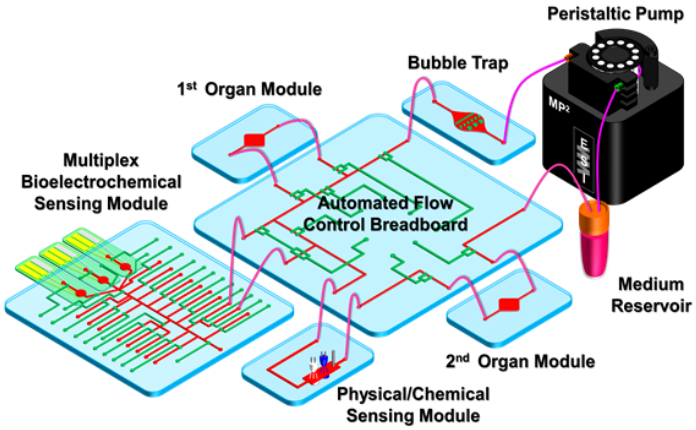

Figure 12. Diagram of an organ-on-a-chip system [63], [64].

3.1.1. DESIGN

A microfluidic system mimics complex physiological processes in the human body by varying flow rate and channel geometry with microvalves and micropumps to achieve stable two-dimensional biochemical concentration gradients. It also improves nutrient delivery and eliminates waste deposits. The dynamic environment of the cells is more similar to in vivo conditions than a static culture. In addition, the flow of the culture medium causes the polarity and arrangement of the treated cells. The microfluidics integrated into the cultivation equipment allow for a variety of biological assessments specific to each organ. The media flow in the system is controllable and modifiable and can either be constant or programmed to simulate a pulsatile format [65], [66]. The fluid behaves primarily like laminar flow at the microscale level, resulting in a stable gradient

of biochemical molecules that is controlled both spatially and temporally. Concentration gradients control various biochemical signals in biological phenomena such as angiogenesis, invasion and migration [67]. We can also control the stress to which cells are exposed. Elastic porous membranes can help with this. Mechanical stimulation is thought to be an important factor in the differentiation of physiological processes [68]. Finally, microfluidics can help us design cell patterns to create physiological in vitro models with complex geometries. Surface modifications, templates and 3D printing all contribute to on-chip cell modelling. The latter enables extensive personalisation of the patterns, structures and systems developed by the researchers [69]–[71]. An example of organ-on-a-chip implementation can be seen in *Figure 11*, and an example of body-on-a-chip implementation can be seen in *Figure 12*.

3.1.2. COMPONENTS

According to the literature, any organ-on-a-chip system consists of four basic components. The microfluidics are responsible for delivering the target cells to a predetermined location and include an inlet system for the culture fluid and the drainage of residual fluid during the culture process. Our goal is to develop a product that is miniaturised, integrated and automated. Another factor to consider is the cell tissue from which the cultured samples are taken and whether they are to be seeded in a two-dimensional or three-dimensional cell culture. Three-dimensional cellular structures can be built with three-dimensional culture structures such as scaffolds or hydrogels. Although 3D tissue structures simulate the in vivo situation more accurately than 2D models, living cells of organ tissues are still mainly cultured in 2D due to technological limitations and the cost of developing the extracellular matrix (compounds and hardware used in culture). Certain tissues require physical or chemical signals to simulate the physiological microenvironment that promotes their maturation. Finally, we need to consider the component of detection, which refers to the monitoring of substances, changes or interactions between particles in our culture system, whether desired or undesired, and which can be done with advanced sensors [72], [73].

3.1.3. APLICATIONS

Many types of healthy and diseased tissues and organs are currently being built on microfluidic chips, including models of microvascular obstruction, cystic fibrosis, heart, kidney, liver, lung, pancreas, brain, skin, eye, gut and neuropsychiatric disorders. Importantly, these organ-on-a-chip microdevices can mimic organ-level responses to toxins, drugs, radiation, pathogens and microorganisms in vitro, as well as organ-specific inflammatory responses, which is critical for preclinical modelling of drugs and diseases [74]–[100].

3.2. TUMOR-ON-A-CHIP

Despite enormous efforts to study the biology of cancer and to develop therapies against it, cancer remains one of the leading causes of death in humans. To understand the nature of cancer and develop treatments, the greatest challenges in cancer research are to create an efficient in vitro tumor microenvironment and to explore efficient methods to detect anticancer drugs. Human-specific biophysical and biochemical factors in the tumor microenvironment are difficult to replicate in traditional flat in vitro cell models and in vivo animal models. Due to the limitations of traditional models, it has been difficult to translate basic research findings into clinical applications [101].

Organ-on-a-chip technology has also been used to create 3D models of human tumors in vitro, opening new avenues for cancer research thanks to advances in organ-on-a-chip platforms and dynamic culture systems [102]–[104]. Tumor-on-a-chip has proven to be an attractive prospect

in organ-on-a-chip research for studying cancer biology and treatment options. It mimics the interactions between human tumors in vivo and tissues / organs using microfluidics and cell culture technology in a bioinspired design . Tumors have a complex microenvironment that includes a dense extracellular matrix (ECM), irregular vessels, a diverse population of stromal, immune and inflammatory cells, carcinogenic stem cells and a limited nutrient supply [105]–[110]. Several studies have shown that complex components can significantly influence cancer growth and metastasis via mechanical and biochemical factors [111]–[113].

3.2.1. MANUFACTURE

Tumor-on-a-chip developed devices so far include lung tumor chips, liver tumor chips, pancreatic tumor chips, breast tumor chips, brain tumor chips, melanoma tumor chips, and tumor metastasis chips. These tumor chips can simulate the 3D microstructure and microphysiological functions of human organs/tissues in vivo, tumor growth and spread, angiogenesis and progression from early to advanced lesions, including epithelial-mesenchymal transition (EMT), tumor cell invasion and metastasis, allowing researchers to better understand the mechanisms of action of this pathology. Multi-organ-on-a-chip systems with cell culture interactions have also shown great promise for screening cancer drugs and cancer therapies [114], [115].

To simulate the intravasation process in vivo, migrated tumor cells need to be exposed to different microenvironments and oxygen gradients in an in vitro metastasis model. To simulate the physiological effects of oxygen on tumor progression and metastasis, microfluidics-based chips can generate oxygen gradients with high spatial and temporal resolution [116], [117].

As mentioned earlier, there are several key elements in making an integrated organ-on-a-chip, including a microfluidic system, 2D/3D microtissue cultures, components that can replicate the ECM and physiological processes, and sensors to monitor the system and read out the results. The same applies to a tumor-on-chip device.

Tumor-on-a-chip devices have been fabricated using a variety of techniques. Photolithography, replica moulding, soft lithography, microcontact printing and bioprinting technology are the most commonly used. Despite the promising results of these techniques, when applied in the reality of non-privatised biological research laboratories, we find that in most cases it is necessary to collaborate with other research groups to produce the devices or, in the worst case, to acquire the necessary machinery to apply these techniques and the knowledge to use them properly and achieve optimal manufacturing.

3.2.1.1. 3D PRINTING

The advent of new technologies has created high-resolution yet low-cost manufacturing opportunities. Three-dimensional material printing is an emerging method for producing microscale 3D templates, components and devices. Interestingly, they are also capable of printing biomedical parts and tissues using cells, matrices and biomaterials. Known techniques include stereolithography, multi-jet modelling and focused deposition modelling [118]–[120], as seen in *Figure 13*. It can also be a combination of additive and subtractive manufacturing. In microfabrication, rapid prototyping is a major advantage of this approach, as it can replace master moulds made by photolithography and also allows direct fabrication of various other microstructures [121]. In bioprinting of artificial living organs [122], there are usually six steps, including imaging, design, material selection, cell selection, bioprinting and application. The advantages of 3D printing are the precise control and application of the desired cell arrangement. However, there are still limitations to the smallest dimensions that can be achieved, and it is also

not compatible with all materials . Nonetheless, the use of 3D printing technologies for the manufacture of microfluidic devices is becoming more common [123].

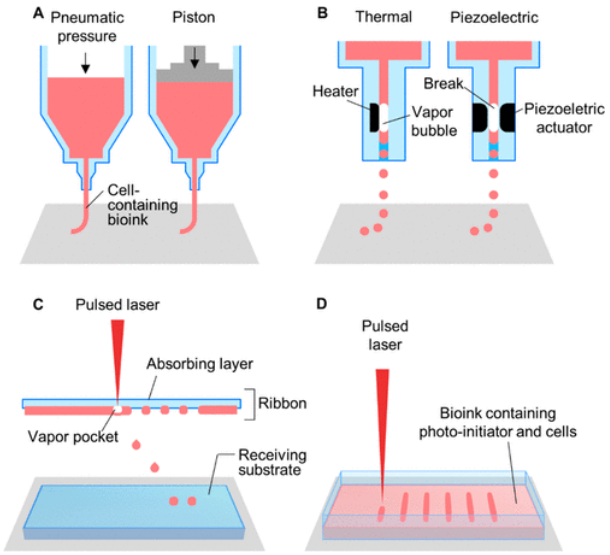

Figure 13. Schematic of currently applied 3D printing methods on organ-on-a-chip fabrication. Microextrussion (A), Inkjet (B), Laser printing (C), Stereolithography (D) [124].

3.2.1.2. HOT EMBOSSING

A very suitable and adaptable method for microfabrication of polymer-based chips. First, a master must be designed and fabricated, which is usually done by photolithography. The process is then carried out in the embossing machine, where the master is assembled by applying force and heat. The method has several advantages, including low cost and the ability to produce polymer microstructures with a high aspect ratio and micro lamellae. In order to achieve a high-quality surface, the temperature and other influencing parameters must be precisely controlled [126]–[128]. An example of fabrication of a PMMA chip using hot embossing is shown in *Figure 14.*

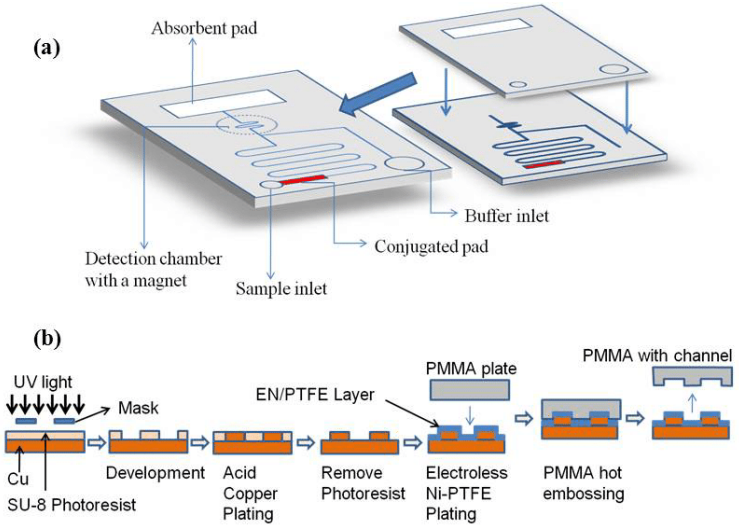

Figure 14. PMMA chip fabrication through hot embossing [125].

3.2.1.3. INJECTION MOULDING

Injection moulding is a manufacturing process in which molten material is injected into a mould. It can be performed on a variety of materials, the most common of which are metals, glasses, elastomers, confections, and thermoplastic and thermoset polymers. Further efforts to reduce microfabrication processes have led to casting and especially injection moulding techniques. The first major advantage is that the cost of high-precision microfabrication is limited to the master fabrication. This method is used for mass production of a large number of microcomponents. To ensure high production quality, temperature, pressure and injection speed must be precisely controlled [129]–[131]. An example of organ-on-a-chip implementation using injection moulding as the fabrication technique can be seen in *Figure 15*.

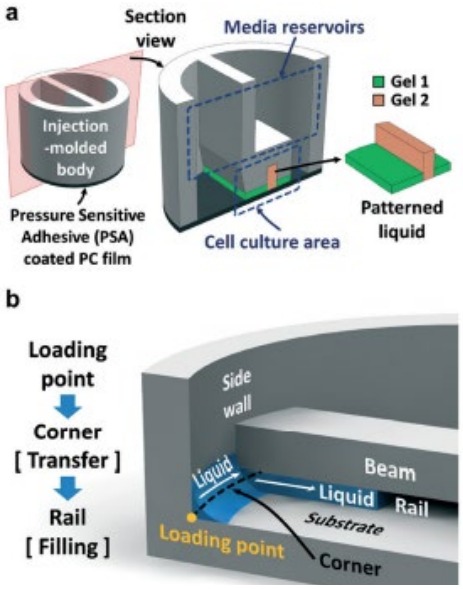

Figure 15. Organ on a chip fabricated by injection moulding [193].

3.2.1.4. SOFT LITHOGRAPHY

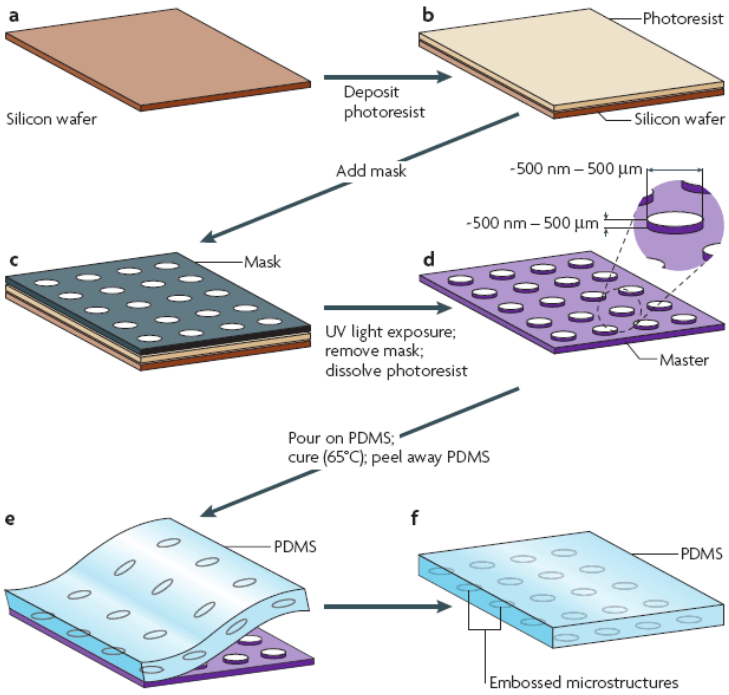

Figure 16. Manufacture of a PDMS application using soft lithography [132].

Photolithography is a general term used in integrated circuit manufacturing to describe techniques that use light to create finely patterned thin films of suitable materials on a substrate, such as a silicon wafer, to protect specific areas during subsequent etching, deposition or implantation processes. Typically, UV light is used to transfer a geometric pattern from an optical mask to a photosensitive chemical (photoresist) that is applied to the substrate. When the

photoresist is exposed to light, it is either degraded or hardened. The textured film is then created using appropriate solvents to remove the softer parts of the coating [133].

Soft lithography is a technique based on the method of photolithography and applied to a wider range of materials, especially elastomers (such as PDMS, example of implementation in *Figure 16*). The method was offered due to certain limitations of photolithography that were encountered when working with biological systems. The relatively high cost, incompatibility with curved substrates and lack of surface control are cited as limitations of photolithography. Finally, there are many cases where soft lithography has been used to make a chip to replicate an organ, e.g., kidney on a chip, brain on a chip and intestine and liver on a chip [134]–[136].

3.2.2. MATERIALS

3.2.2.1. PDMS

Polydimethylsiloxane is the most commonly used material in the manufacture of tumor-on-a-chip devices (PDMS). It is a silicon-based elastomer with highly advantageous properties such as optical transparency, breathability, biocompatibility and flexibility, which allow continuous microscopic observation of tissue constructs for real-time assessment of cell behaviour and response to treatment. It is also compatible with a wide range of microfabrication techniques, such as soft lithography and moulding, as seen in *Figure 17*. However, there are some properties of PDMS that limit its use and motivate the search for alternatives. The absorption of hydrophobic molecules is a drawback that negatively affects toxicity, efficacy and the prediction of pharmacokinetics and pharmacodynamics. It is also fluorescent to some degree and should not be used with organic solvents. Despite increasing efforts to improve the properties of PDMS chips through surface modifications such as plasma treatment, UV treatment and coating, no one has succeeded yet [137]–[142].

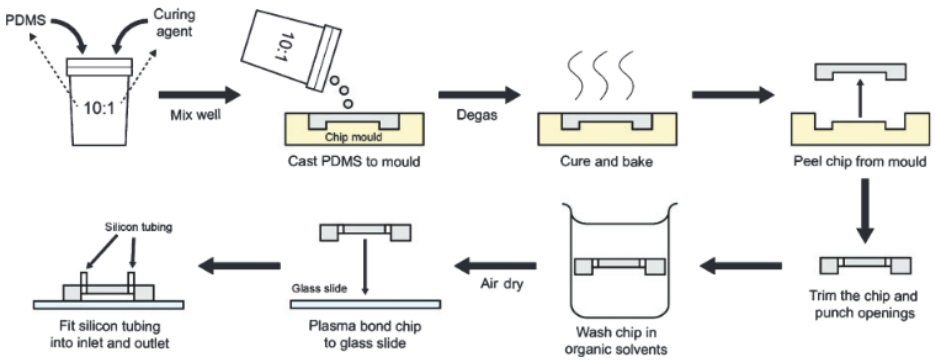

***Figure 17**. Manufacture of a microfluidics device using PDMS* [143].

3.2.2.2. THERMOPLASTICS

Thermoplastics have recently been proposed for the fabrication of microfluidic devices, as PDMS and glass-based chips have limitations in terms of surface treatment instability, processing techniques and molecular absorption. Their main advantages are low cost, low density, biocompatibility and ease of fabrication. They are more resistant to pressure and temperature fluctuations as they contain linear and branched molecules, which makes them chemically stable and suitable for biomedical/biochemical studies. This is evident in the study by Trinh et al. in which they make a lab-on-chip device for human cell cultures from PMMA, which has the advantage that it can be bonded quickly and is suitable for protecting sensors in chips [144].

Microfluidic devices based on polymers such as PMMA or copolymers (COC) have thus been developed, as well as new microfabrication techniques such as injection moulding, casting and laser cutting. The use of thermoplastic polymers has some limitations. For example, not all are transparent, making microscopic observation or imaging impossible. Some have strong autofluorescence properties that make them unsuitable for detection, and they have low gas permeability, which has a negative impact on long-term cell culture [145]–[147].

3.2.2.3. GLASS

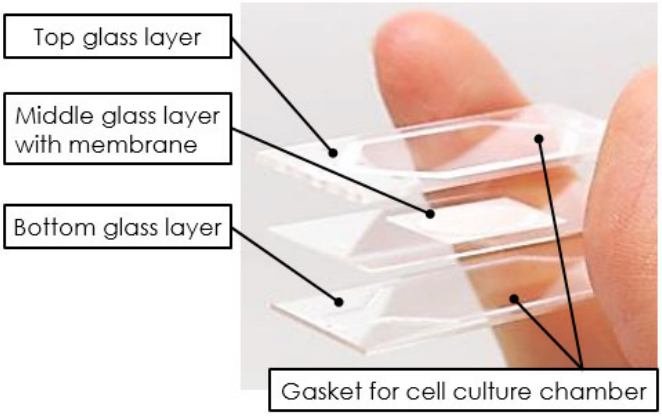

Figure 18. Layering example of a microfluidics device using glass [194].

Glass is one of the oldest materials used in the development of microfluidic devices. Soda lime, quartz and borosilicate glass are used in this field. They consist of silica (SiO_2) and other oxides (e.g., CaO, MgO...). Transparency, resistance to mechanical stress, hydrophilicity, biocompatibility and a lower drug absorption capacity have been mentioned as advantages of using glass in microfabrication. The low gas permeability of glass, on the other hand, is a major problem that can lead to channel blockage. Nevertheless, it can be an advantage in anaerobic studies. Photolithography, wet etching and laser cutting are examples of glass microfabrication techniques [148]–[150] (see glass chip implementation in *Figure 18*).

The main reason for preferring polymer materials over glass is the high manufacturing cost, as it is difficult to mould and requires cleanroom facilities for each step, which prolongs the manufacturing processes. In addition, the techniques for bonding the substrates (anodic or thermal bonding) are more demanding. However, there are some applications where glass microfluidics are highly recommended such as when sensor integration is needed, as polymers have low stiffness or require scaffolding [151].

3.2.2.4. OTHERS

Besides PDMS, glass and thermoplastics, other materials can be used to create microfluidic tumors-on-a-chip. Gelatine is a natural biopolymer derived from collagen. Due to its cellular reactivity and ability to transport a variety of biomolecules, it is often used in drug delivery models and tissue engineering. Gelatine can polymerise with proteins, growth factor nucleotides, polysaccharides and other polyionic complexes, in addition to promoting cell growth [152]. This material offers a wide range of models for the controlled, sustained and/or targeted release of bioactive molecules. Bacterial cellulose paper is another new material. It offers all the advantages of cellulose at the nanoscale and is derived from natural sources with good biocompatibility and low cost. Bacterial cellulose nanofibers are processed and dried to produce a stable paper device for model making. Some research groups have successfully fabricated vascularized 3D breast tumor models from paper by using this paper device to make various microchannels [153].

3.2.3. BIOLOGICAL IMPLICATIONS

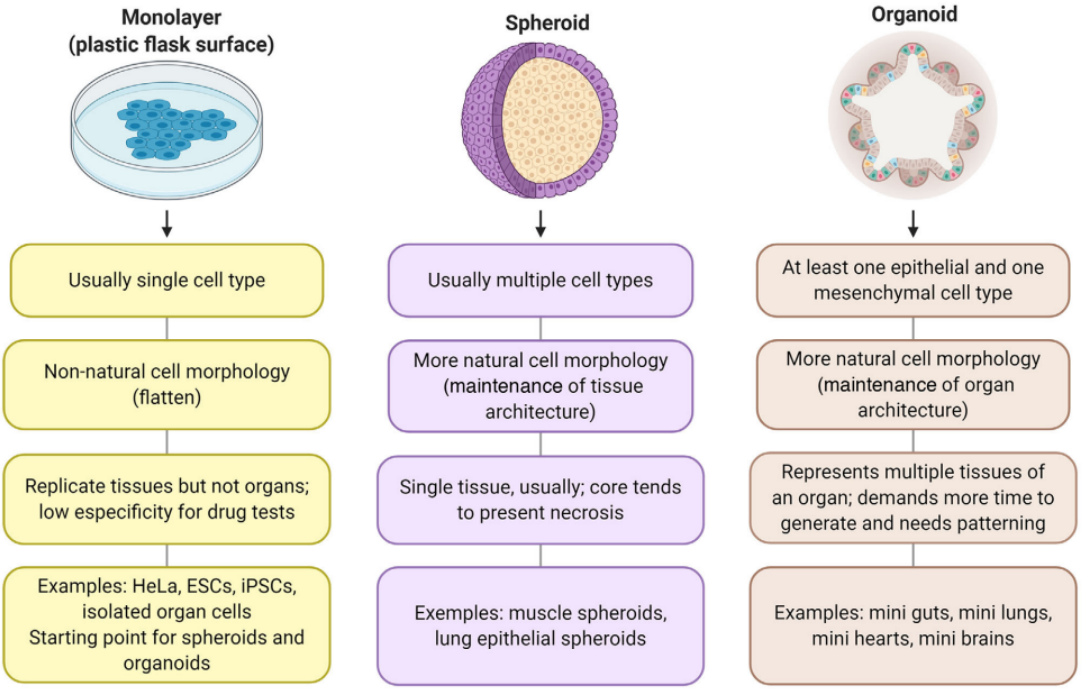

Figure 19. Similarities and differences between 2D and 3D culture [154].

With the advent of new components and production techniques, such as microfluidics and microprinting, along with stem cell technologies, it is now possible to create organoids and spheroids that resemble human tissues. They can be utilised in the study of human development, the progression of diseases and their therapies, and the creation of individualised drug delivery systems [155].

Organoids are three-dimensional cell culture models with the capacity to self-organize into complex and intricate tissues and organs. Typically, embryonic stem cells, induced pluripotent stem cells, adult stem cells, and other forms of stem cells can be utilised to generate organoid models [156]. The combination of these two technologies may allow organ-specific structures and in vivo gene expression signatures to replicate the evolution of in vivo pathology more accurately than either model alone [157]. Organoids derived from these stem cells may be incorporated into tumour chips.

A cellular spheroid is a three-dimensional aggregate of several individual cells created from cancer cell lines or clusters of cells separated from tumour tissue and deposited on non-adherent surfaces. A cancer spheroid 3D is one of the well-defined in vitro 3D cell culture models used to increase the accuracy of the predictions made during preclinical drug testing. Patra et al. performed drug detection and flow cytometry analyses on a large number of identically sized tumour spheroids. They utilised a microfluidic device to accomplish this. Utilizing experimental data from three-dimensional models of tumour spheroids, the significance of drug detection was demonstrated to be crucial. In addition, the type of cell culture (2D or 3D) and the size of the spheroid have a substantial effect on the reactions to medicines, highlighting the benefits of combining the two techniques for screening applications. These results have the potential to aid pharmaceutical researchers in gaining a more comprehensive understanding of the actions of medications in three-dimensional cell structures that more closely resemble those formed in vivo [158]–[162].

In contrast to organoids, which normally require a framework for growth, spheroids are three-dimensional cell cultures that can be created without a scaffold. Therefore, this is the most significant distinction that can be made between organoids and spheroids. Organoids are capable of both self-assembly and regeneration, whereas spheroids are incapable of doing so [163]. A proper differentiation between monolayer, spheroid and organoid cultures is shown in *Figure 19*.

3.2.4. TYPES AND DESIGN

3.2.4.1. LUNG TUMOR-ON-A-CHIP

The lung is a crucial organ for gas exchange, specifically the transport of oxygen from the air and carbon dioxide from the blood to the lungs. In addition, it is one of the most common entry points for foreign substances such as drugs, toxins, viruses, and other agents to enter the human body. The study of cell-cell, cell-blood flow, and cell-gas flow interactions in the airways is crucial for both physiological research and drug administration. Lung cancer, one of the most common types of cancer, has a very dismal prognosis for sufferers. Therefore, it is of the utmost necessity to construct a lung tumor-to-chip model in order to understand the mechanism of lung cancer and the potential treatment options. As seen in *Figure 20,* the lung-on-a-chip will typically contain two microfluidic channels that are separated by a porous extracellular matrix. On one side are human lung epithelial cells, while the opposite side contains human lung microvascular endothelial cells. This model can simulate a range of pulmonary physiological processes. Based on the lung chip, the lung tumour chip unites lung tumour cells with lung epithelial cells [165], [166].

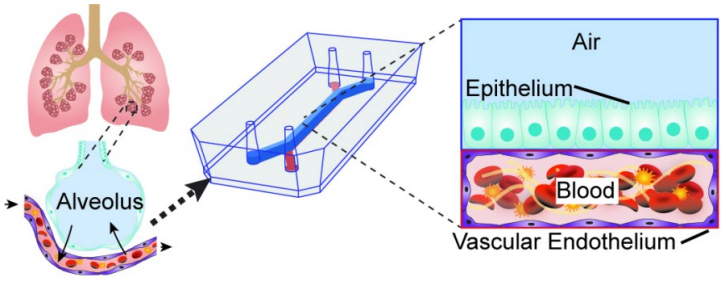

Figure 20. Example of a lung-on-a-chip [164].

3.2.4.2. COLORECTAL TUMOR-ON-A-CHIP

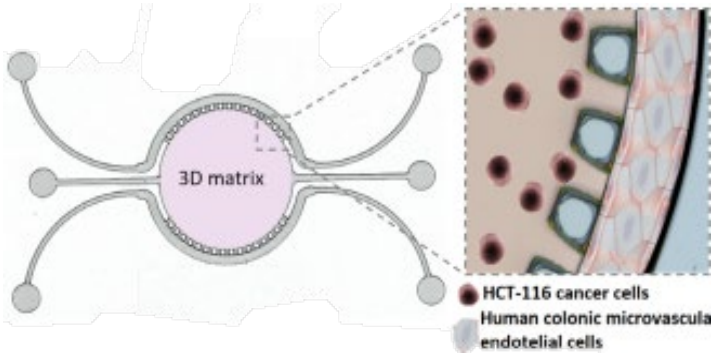

Figure 21. Example of a colorectal tumor-on-a-chip [167].

Due to the high incidence of cancer metastasis and the low treatment cure rate, colorectal cancer is the second leading cause of cancer-related death. Maintaining healthy endothelial cells in the microvasculature, which serve as gatekeepers, can prevent colorectal cancer. In order to develop a model for a microvascular system, human colonic microvascular endothelial cells are usually utilised. Carvalho et al. constructed a colorectal microfluidic chip (*Figure 21*) with three primary

components. The hydrogel-constructed circular chamber in the middle contains extracellular matrix. There is only a single entrance and exit. The remaining two perfusion channels are located on either side of the circular-shaped core chamber [167].

3.2.4.3. PANCREATIC TUMOR-ON-A-CHIP

To boost the efficacy of pancreatic drug screening prior to animal model testing and clinical trials, it is necessary to develop in vitro pancreatic tumor-on-a-chip systems. Pancreatic malignancies are invasive solid tumours with a hypovascular architecture and significant fibrosis [168]. Recently, the pancreatic tumour model developed by Nishiguchi et al. was deemed the most successful in simulating its in vivo environment [169]. This model includes a blood capillary structure that can replicate cellular morphologies and depict the loss of endothelial cells during the metastatic phase. However, the crop is static in three dimensions. Using organ-on-a-chip technology, Haque et al. have recently reported the state of the art in the development of a very similar biomodel [170]. Regarding the biological component, the spheroid three-dimensional culture cells exhibit stronger drug resistance than the two-dimensional culture cells. Moreover, the chemical environment of the 3D culture is more similar to that of the original tissues than that of the 2D culture.

3.2.4.4. LIVER TUMOR-ON-A-CHIP

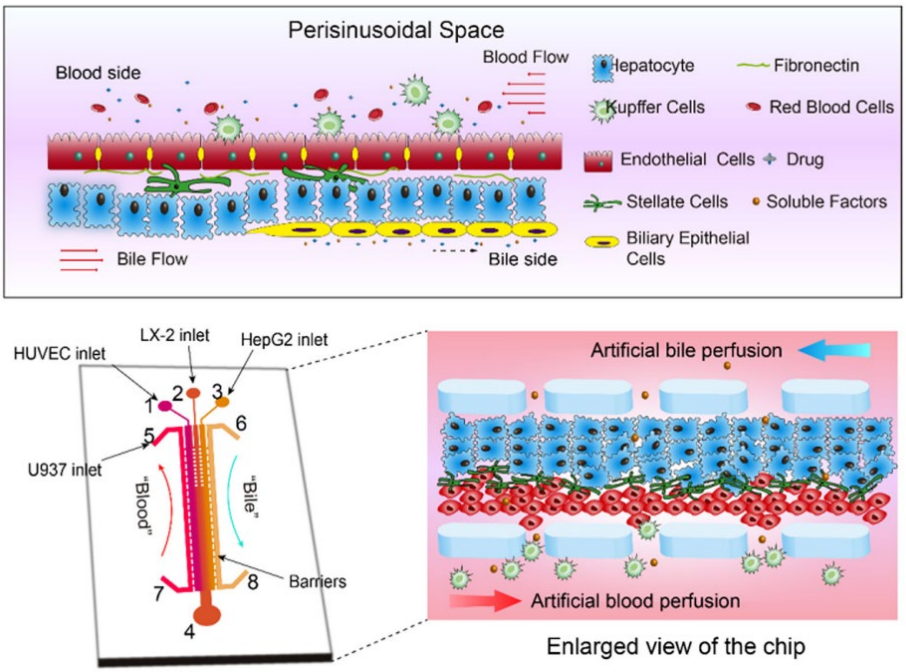

Figure 22. Example of a liver on a chip [173].

The liver, which is the largest and major metabolic organ of the body, plays a key role in a number of vital functions required to sustain normal physiological processes. These activities include the management of glucose and ammonia levels in the blood, the creation of several hormones, and the detoxification of endogenous and foreign chemicals. It has a complex structure that is mostly composed of two primary cell types known as parenchymal cells and nonparenchymal cells. Since parenchymal cells, also known as hepatocytes, are functional cells, scientists have studied the biochemical and functional processes that occur in liver in vitro systems utilising these cells [94], [171]. The liver tumour chip has the potential to serve as a basis for liver cancer treatment. Cytotoxicity testing is a crucial component of drug discovery and screening. They can predict

either the direct toxicity of the medication as a whole or the indirect toxicity of the drug's metabolites to the liver or other organs. As a result of unfavourable effects caused by the metabolism of pharmaceuticals, hepatocytes play an increasingly crucial role in organ-on-a-chip systems. Two prominent instances of drug metabolism that occur in the liver are the conversion of prodrugs to metabolite drugs, which produces hepatotoxicity and liver injury, and the metabolism of doxorubicin to doxorubicin, which causes hematotoxicity, such as cardiotoxicity and myeloid toxicity. Each of these mechanisms can result in liver damage. Due to this, the liver must be cocultured with other cells in a microscale cell culture in order to study the pharmacological properties of anticancer drugs [172]. *Figure 22* shows a proper representation of this system.

3.2.4.5. BRAIN TUMOR-ON-A-CHIP

Glioma is the most prevalent and deadly form of brain tumour. Glioma researchers utilise the transwell-based cell culture model because it is a good tool for examining the mobility and interactions of cells, as it permits cell culture to occur in relatively little fluid. When investigating the in vitro kinetics of brain tumour stem cells, scientists use a microvascular system on a chip to imitate the cells' perivascular environment. It has been demonstrated that the diameter of microvascular channels can facilitate the spread of tumours. This model is a novel approach to the study of certain tumours since it may be used to characterise the dynamics and heterogeneity of tumour cells while they are still in vivo. Fan and colleagues designed a three-dimensional brain tumour chip comprising hydrogel as a carrier for the delivery of drugs and biological applications (*Figure 23*). The results indicated that this model has application potential in the field of glioma chip modelling for drug detection and release testing [174]–[176].

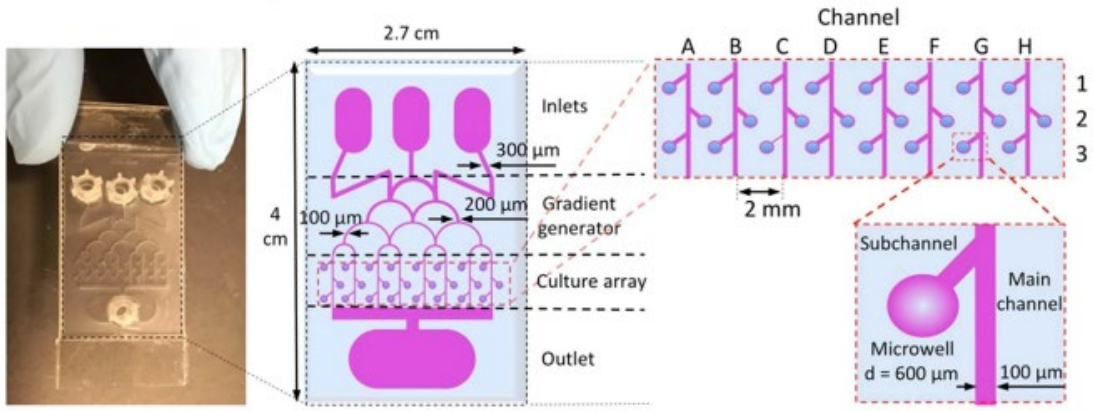

Figure 23. Example of a brain tumor-on-a-chip implementation [174].

3.2.4.6. BREAST TUMOR-ON-A-CHIP

Non-malignant cells cultured in 2D are morphologically comparable to malignant cells when discussing breast cancer cultures. In 3D culture, however, non-malignant breast tissue cells are polarised and grouped in a tube, whereas malignant breast tissue cells form spherical tissue. Researchers such as Hao et al. and Boyle evaluated the effects of different anticancer medications on 2D and 3D grown breast tumour cells and discovered that the response to the drugs was diminished in 3D cultured tumour cells. Therefore, researchers propose that 3D cultured breast tumour chips can be utilised to predict the effectiveness of anticancer drugs [177], [178]. An example of a breast tumor-on-a-chip implementation is shown in *Figure 24.*

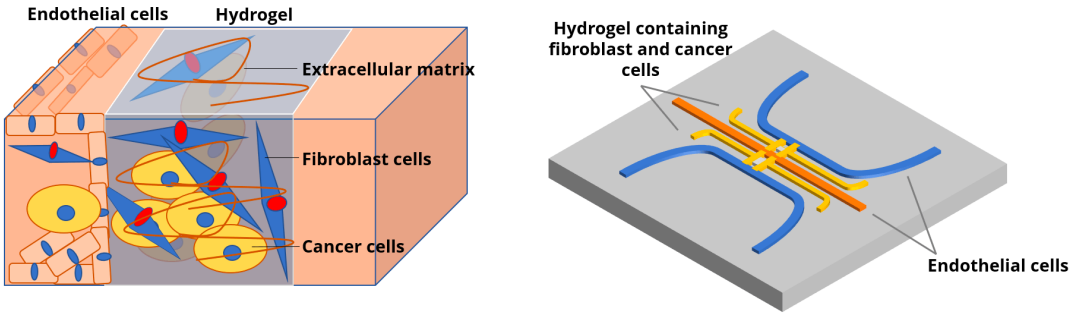

Generation of tumor microenvironment

Representation of microfluidic cell culture device incorporating hydrogel

Figure 24. Example of a breast tumor-on-a-chip implementation [179].

3.2.4.7. TUMOR METASTASIS CHIP

Metastasis is one of the most important concerns that must be addressed in modern clinical cancer treatment, as well as one of the greatest obstacles. This factor is responsible for more than ninety percent of all cancer-related deaths, and it has the potential to increase patient mortality rates significantly. The majority of "tumor-on-a-chip" technologies can only duplicate tumours that are currently present in a patient's body. As a result, the mechanism of tumour cell metastasis is still not entirely comprehended. This is especially true in regards to the variables that initiate tumour cell development and metastasis, as well as the microenvironment's role in regulating these events. Utilizing experimental models to effectively characterise the microenvironment of a disease that has spread to other areas of the body is therefore of the utmost importance [180], [181].

Skardal et al. created one of the earliest metastatic tumour chips. Utilizing microfluidics to supply circulating flow via an organoid system, they demonstrated the applicability of a metastasis-on-a-chip platform. This was one of the first instances of metastasis-on-a-chip. In this scenario, cancer cells multiply in the focal area and then spread via the circulatory system to the rest of the body. In order to mimic the process of cancer cell dissemination, this model was used to simulate the metastatic spread of cancer cells from a three-dimensional parent tissue to a three-dimensional target tissue [182].

The application of more traditional analytic approaches has facilitated research into the migration and invasion of tumours in tumor-on-a-chip models. Toh et al. described a microfluidic tumor-on-a-chip cell migration model after Skardal's model was published. This model utilised microfluidic technology to comprehend the progression of cell intravasation. It combines a three-dimensional microenvironment, which plays a key role in the invasiveness of cancer cells, with an attractive model for testing anti-migration and anti-invasive cancer medicines, which may be utilised to explore biological processes in greater depth [181]. Wang et al. constructed one of the most recently described models. They proved that by building an organ-specific extracellular matrix, hepatocytes can continuously produce albumin and urea, thus duplicating the biological processes that occur in the liver. According to these findings, biomimetic liver microtissues may replicate the organ-specific extracellular matrix, allowing researchers to analyse the evolution of kidney cancer metastasis to the liver [183]. *Figure 25* shows the graphical concept of a metastasis chip implementation.

If we want to enhance both the treatment of cancer and the prognosis for cancer patients, it is essential that novel tumour models be produced. As a result, the use of such models could potentially lead to cost savings in the healthcare industry.

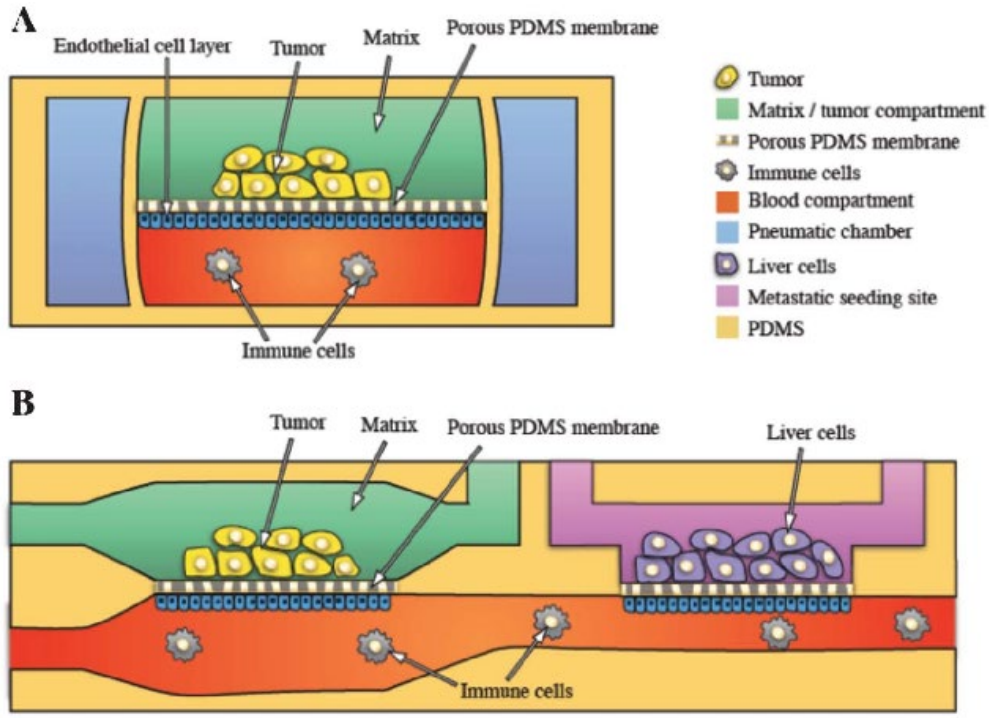

Figure 25. On-chip conceptualization of cancer metastasis. Invasion of tumor cells from the original tumor into the surrounding matrix and then into blood vessels, followed by extravasation and seeding of a possible metastatic location [184].

3.3. CONCLUSION

This section investigates published studies on microfluidics technology for cell culture, organ-on-a-chip, and to a greater extent, tumor-on-a-chip. The design, production, assembly, and culture of these devices, as well as the benefits and limitations of this technology, have been analysed. This section provides a summary of the conclusions gained from the bibliography.

Tumor-on-a-chip systems can imitate the complexity of in vivo tumour masses far more accurately than typical in vitro planar cell models and in vivo animal models, a factor considered reliable for the development of drugs. The superiority of tumor-on-a-chip platforms as candidates for conventional preclinical models has attracted the attention of scientists worldwide, resulting in substantial scientific advancement. Numerous tumor-on-chip platforms simulating lung, liver, breast, or brain tumours have been developed. In order to study the molecular basis of cancer, they are largely employed to identify anticancer drugs and undertake basic research on cancer's spread. As an alternative to traditional preclinical models, tumor-on-a-chip technologies have the potential to revolutionise basic drug research and development across multiple fields.

However, tumor-on-a-chip systems are based on abstract design and microfabrication technologies, and it is essential to research how to rationally develop microfluidic devices for precise control of chips' physicochemical features. In addition, not all researchers are proficient in fabrication facilities or methods; therefore, it is essential to develop easy-to-use chip systems that can generate standardizable data so that non-experts can use these emerging models for research and obtain results that are meaningful for clinical translation. Currently, the production and implementation costs are extremely high, which inhibits its widespread use; therefore, the components must be inexpensive and easy to remove. The more expensive components must be recyclable. In addition, the usage of varied designs and unique materials could provide extra boost

for creating simplification hypotheses that will be used to create a viable chip. Due to the constraints imposed by microfabrication, there is always a trade-off between the concepts engaged in the design process, biological aspects and materials; consequently, these cannot be addressed in their entirety. As a result, there is a great demand for the development of multidisciplinary research in order to expand design options while reducing costs. In addition, a universal cell culture medium that is compatible with all organs is required.

No design was found during the literature search that offered hardware manufacture (culture chips and peripherals) using only fused filament fabrication, which is the project's purpose. This is due to the limitations of this technology, such as the moisture absorbance of certain polymers, the difficulty in obtaining a model with sufficient layer adhesion to prevent liquid leakage, the chip miniaturisation factor, the potential cell adherence to the printed models because of the lack of a smooth wall surface, and the unfavourable chemical interaction of cell culture products with certain polymers. These challenges must be overcome during the development of the project. As has been seen, the benefits of obtaining positive results from the to-be-designed model would include the ability to self-manage and automate the manufacture of culture chips, to have hardware for cell culture based on the use of inexpensive microfluidic systems and disposable parts, to be able to conceptualise and test designs for organ emulation more easily and thus move faster toward model standardisation and cannon creation, or to open the door to this technology’s use decentralisation.

4. HYPOTHESIS AND OBJECTIVES

4.1. RESEARCH QUESTION

Is it possible to fabricate a microfluidic system for the in vitro cell culture of tumor-like structures inspired by the technological concept of organ-on-a-chip and specifically tumor-on-a-chip using fused filament fabrication as the primary manufacturing method and inexpensive electronic components?

4.2. HYPOTHESIS

Manufacture of an in-vitro cell culture device incorporating a microfluidics system using cost-effective components and fused filament fabrication as the primary technology in the manufacturing process is possible by adapting the conceptualization of the models to the limitations of machinery and material and applying the appropriate post-processing.

4.3. OBJECTIVES

4.3.1. MAIN OBJECTIVE

Open interest in 3D design, the use of biocompatible polymers, and fused filament fabrication in the conceptualization and manufacture of devices for cell culture using microfluidics, providing a system that overcomes the major restrictions previously connected with this technique of production in terms of the manufacture of organs-on-a-chip and tumors-on-a-chip.

4.3.2. BROKEN DOWN GOALS

- Conceptualize and construct the culture system, which must consist of a tank for the environment, an infusion pump, and the cultivation devices as its primary components.
- Determine how to connect the culture chips to the tank so that no liquid leaks and the liquid flows appropriately.
- Examine methods for enhancing the layer adhesion of printed models in order to prevent liquid leaks.
- Examine techniques for modifying the surfaces of channels that will hold or convey cells to prevent undesirable cell adhesion.
- To prevent cells or cellular structures from invading other culture zones or coming into touch with our infusion pump, design a filtration system that may be easily tailored to the specific application.
- When employed, the device should be placed in an incubator to replicate the temperature of the human body; hence, a low-cost infusion system that does not require a direct connection to the mains should be devised.

5. MATERIALS AND METHODS

REQUIREMENTS AND SPECIFICATIONS			
Proposal *= D: Design, F: Fabrication, U: User;* ***R / D*** *= R: Requirement, D: Desire*			
CONCEPT	PROPOSAL	R / D	DESCRIPTION
Function	U	R	- Cell culture chip housing as the primary function.
	U / F	R	- Withstand the internal pressures inherent to the perfusion of liquids and the strain inherent to system construction.
	F	R	- Demonstrate watertightness.
	U / D	R	- Possess a filtering and management system.
	U / F / D	R	- Permit simple monitoring of chips using microscopy.
	D	D	- Permit modularity of devices.
Dimensions	U / D	R	- The device must be contained within a culture chamber; hence its maximum height cannot exceed 10 cm (it must be adapted to the incubator).
	F / D	R	- The size of the chips must strike a balance between miniaturisation and the strength achieved by the manufacturing process.
Stress	F /D	R	- Assembly-required components must be able to endure the stresses involved.
Materials	F	R	- They must fall within the spectrum of commercial materials that an FFF printer can handle.
	U	R	- They must possess biological compatibility.
	U / F	R	- They must be capable of post-treatment to enhance their surface finish.
	U	R	- When it comes to chips, they must be clear.
	U	D	- They should be inexpensive and accessible.
Control	U	R	- It must permit visual crop inspection.
	U / D	R	- It must have a filtration space to prevent the presence of tumour clusters in the surrounding environment.
Cost	U	D	- The overall cost of development must be lower than the cost of a commercial implementation: 20,000 €.
	U	D	- A device's manufacturing net cost must be less than 100 €.

Figure 26*. Table of requirements and specifications for the fabrication of a microfluidic device for cell culture employing FFF.*

5.1. DESIGN

One of the most important aspects of the project's development was the design of the device, which not only had to meet biomedical requirements, such as the resemblance to extracellular structures, but also manufacturing technology and, therefore, material requirements. Due to the fact that FFF printers predominantly use polymers, a compromise had to be made between the intended miniaturisation factor, the strength of the materials used, and the level of detail provided by the production process in these smaller components. In addition, other variables had to be considered, such as the size constraints of the incubator, the modularity of the devices, and the thickness of specific surfaces that would allow light to pass through when printed with transparent filament.

The developed microfluidics system is comprised of multiple interconnected components. For the conception of the culture chips, the state-of-the-art models served as inspiration, and they were reinterpreted so that they could be applied to the FFF with the highest miniaturisation factor conceivable. On the one hand, we have a chip engineered to survive photometry testing,

microscope examination, and, in general, more straightforward monitoring. This chip intends to have a more universal design that may be comparable to breast cancer chips (*Figure 24*), colorectal cancer chips (*Figure 21*), liver cancer chips (*Figure 22*), or lung cancer chips (*Figure 20*). On the other side, we have a chip inspired by the metastasis tumor-on-a-chip, whose design attempts to more closely resemble the microstructure and cell distribution of this phenomena (*Figure 25*). The tank was designed to be large enough to accommodate the pump, yet small enough to prevent the loss of culture medium or blood. The remaining parts were made to fit these two primary components. Keep in mind that the proposed dimensions in this section are approximations, as they were obtained from the printed models. Due to factors such as the expansion/contraction of the material when it melts or adjustments that Cura may have made when doing the slicing to accommodate the desired detail and nozzle size, the actual measurements may differ slightly from the theoretical ones. The theoretical dimensions of the designs are available in Annex E.

5.1.1. CULTURE CHIPS

For the design of the chips, there were three major obstacles to overcome: the connections with the pump, the level of detail that could be achieved when printing the internal channels, and getting the bottom layer of the cultivation area to pass the light of a microscope and the top layer to be transparent so that the crop could be studied. Adapting the size of the chips to the current limits has resulted in a culture device that is smaller than a traditional culture plate but larger than the existing organs-on-a-chip. The chips are 4 x 4 x 0.9 cm^3 (general purpose) and 4 x 4 x 1.7 cm^3(metastasis), while the culture chamber occupies a volume measuring 2 x 3.2 x 0.73 cm^3 (general purpose chip) / 1.8 x 3.5 x 0.75 cm^3 (metastasis chip). As for the connections, it was determined that needles would not provide a tight connection with the polymer device (we would have leaks) and that the perfusion of medium through them would not be an efficient method due to the size of the chip. Therefore, it was decided to print the connections on the same piece, allowing a medium transport tube to be connected directly without the need for additional accessories. The external and internal diameters of these connectors were modified so that they could fit inside a tube with a small diameter while remaining sturdy. The tests conducted will be mentioned later, however the external diameter of the connections ended up being 5mm and the interior diameter 2mm, and 1 cm its height.

5.1.1.1. GENERAL PURPOSE

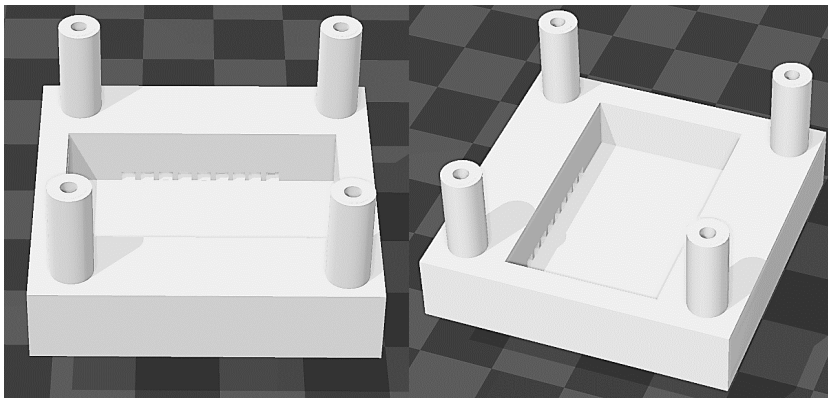

Figure 27. General purpose chip model overview. The four cylinders are medium inputs and outputs, while the region in the middle is the cultural area. The medium enters the camera through each side's nine apertures.

It is a single-layer chip for cultivation designed for various applications and as a base for further adaptations, the medium perfusion is direct (the culture chamber is an intermediate point for

liquid entry and exit), and it is intended to be used in conjunction with a hydrogel that capillaries the flow received or with a scaffold that has been previously seeded and to which cells are already adhered. It comprises of two infusion channels attached to the culture chamber's 3.2 cm sidewalls. From a medium inlet to a medium outlet, microchannels follow an arc. The inputs/outputs are situated 3.5 mm from each of the four vertices of the exterior wall, and the channels extend 7 mm from the outer wall into the interior of the chip. At this time, the canal-chamber of cultivation connections were incorporated, consisting of 0.9 x 1.9 x 1 mm^3 structures that control the amount of medium that enters the chamber; a total of eight of these structures are put along the 2 cm length of the channel's opening. *Figure 26* shows the external design of the chip, while *Figure 27* shows the internal channels.

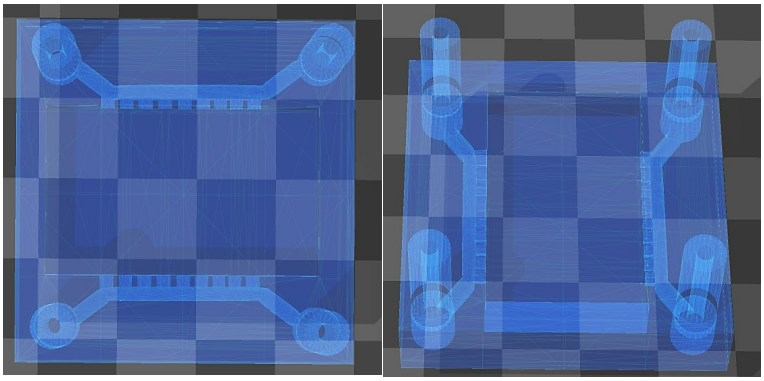

Figure 28. General purpose chip model internal view. Between the intake and outflow on each side is an arch-shaped perfusion channel.

5.1.1.2. METASTASIS

This is a two-layer chip inspired by metastasis. The perfusion of the medium is indirect, as we attempt to directly emulate the capillary nature of the blood without the need for hydrogels or other structures. The path that microchannels take from a medium input to an output is U-shaped. The entrance and exit are centred on the 3 cm side of the growth region, 6 mm from the exterior wall. The channel enters for 1.6 cm till it reaches the lower chamber that joins the two tracks and extends for 3.3 cm with a 5.3 mm diameter. Along the top of this lower channel are eight 1.3 mm-diameter openings that link to the culture chamber. *Figure 28* shows the external design of the chip, while *Figure 29* shows the internal channels.

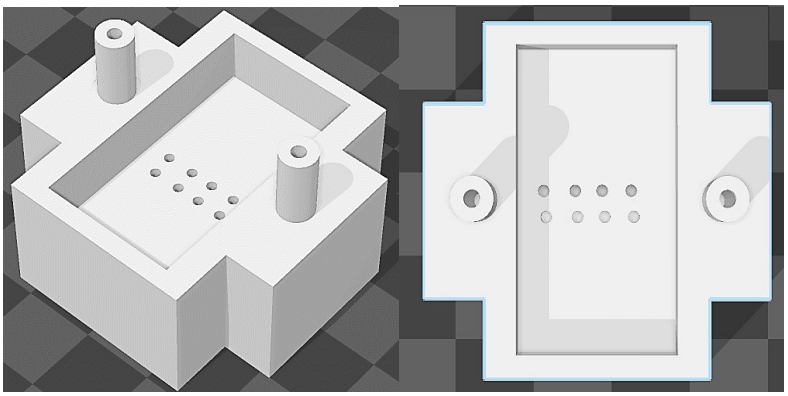

Figure 29. Metastasis chip model overview. The two cylinders are the inlet and outlet for the medium, while the central portion is the culture area. The medium enters the chamber via the eight apertures at the chamber's base that are connected to the lower channel.

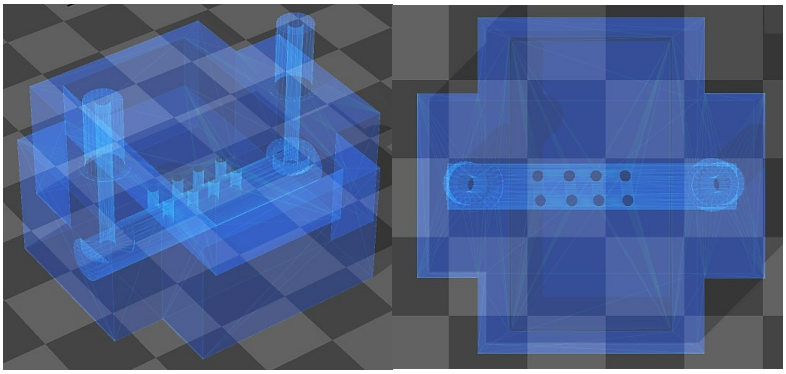

Figure 30. Metastasis chip model internal view. Under the culture chamber, the U-shaped perfusion channel is located.

5.1.1.3. COVERS

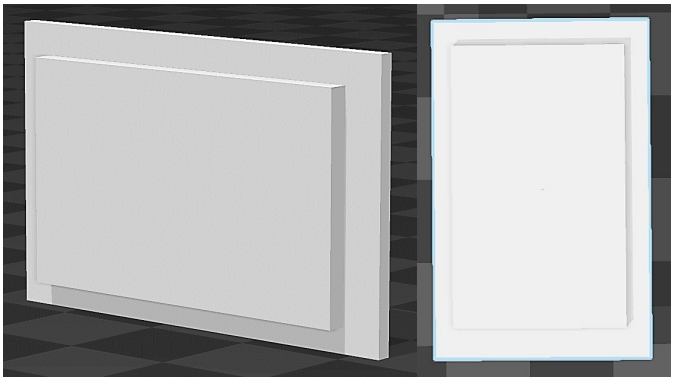

Figure 31. Chip cover.

Using AutoCAD's "Difference" method, coverings that properly fit the chips were designed in order to seal the crop, maintain device pressure, and avoid leaks. The tiny box fits precisely within the 2 x 3.2 / 1.8 x 3.5 cm^2 culture areas, while the large box provides sufficient space to shut or attach the lid without interfering with the previously stated connecting structures. The large box measures 2.1 x 3.9 cm^2 in case of the metastasis chip and 2.5 x 4 cm^2 in case of the general-purpose chip. Both layers have a thickness of 2 mm. *Figure 30* shows the designed cover for the chips.

5.1.2. TANK

Originally, the tank for the culture medium consisted of a single chamber containing the pump. During the design process, problems arose that needed to be resolved, such as adjusting the size of the tank to accommodate different configurations or experiments, sealing the tank to control the concentration of oxygen and carbon dioxide in the cultures, and installing a filtration system prior to closing the microfluidic circuit cycle. Thus, the final design was divided into two models with the same conceptual design, consisting on two chambers, but distinct volumes, allowing this peripheral to be easily adapted to the growing number of chips. A separate lid was designed to seal the tank except for the pump connection opening. So that there are no gas leaks, this can be coated with nonpermanent materials such as Parafilm.

5.1.2.1. INDIVIDUAL

This design has the dimensions of 9.3 x 6 x 10 cm^3, with the large chamber (the one housing the pump) occupying a volume of 5 x 5.5 x 9.45 cm^3 and the small chamber (the one containing the filters) occupying a volume of 3.5 x 5.5 x 9.45 cm^3, with walls of 2.7 mm and a base of 5.5 mm thickness. The pump connection hole in the main chamber is positioned 2.4 centimetres from the

outer wall and measures 0.96 x 0.5 cm^2. The partition wall between the chambers includes three holes; these are the connections for the filters; they are 2.2 cm apart from the ground and from one another to accommodate the use of various medium volumes. The connection holes are positioned in the centre of each compartment, 8 mm from the bottom, with an inner diameter of 8 mm to accommodate the pump connection and an outer diameter of 1.2 cm. The lid is 6.5 x 9.9 x 2.2 cm^3 and has a wall thickness of 2.8 mm (6.5 cm side) and 1.6 mm (9.9 cm side). The pump connection hole is 2.5 centimetres from the wall and measures 1.8 x 0.5 cm^2. The design is shown in *Figure 31.*

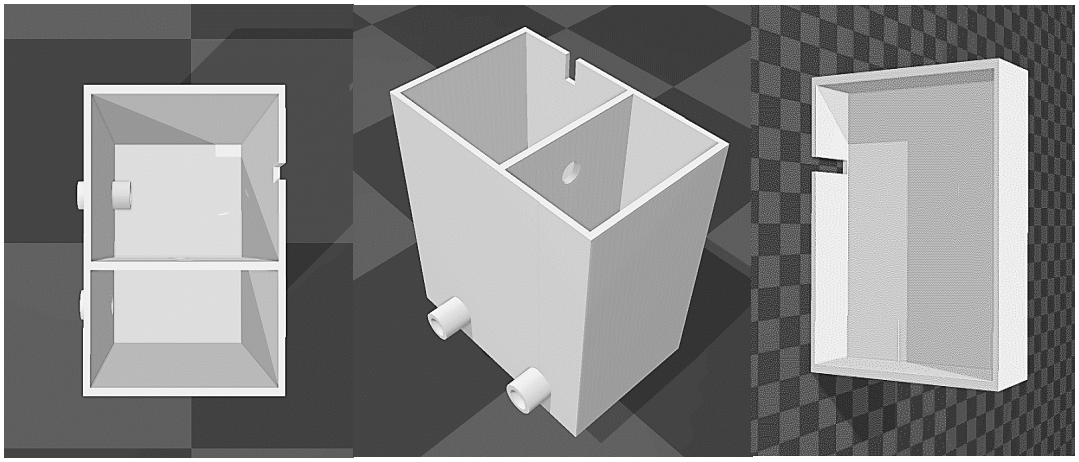

Figure 32. *Tank. Individual culture version. The first image is a top view of the tank; the room above has the pump, while the room below contains the filters. In the second image, one of the filtrate-connecting holes in the partition wall is visible. The third image depicts the tank cover.*

5.1.2.2. EXTENSION

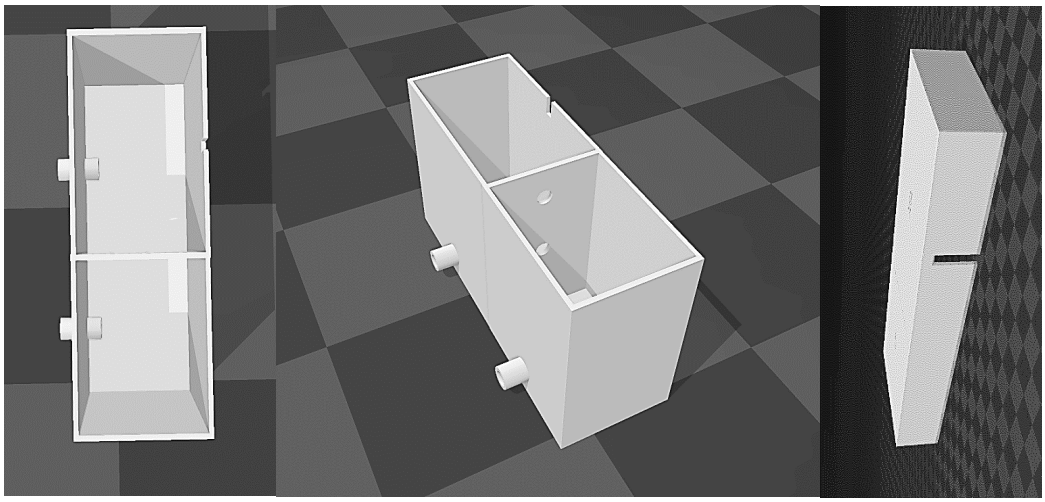

Figure 33*. Tank. Extended culture version. The first image is a top view of the tank; the room above has the pump, while the room below contains the filters. In the second image, one of the filtrate-connecting holes in the partition wall is visible. The third image depicts the tank cover.*

This design has dimensions of 17.6 x 6 x 10 cm^3, with the main chamber (the one housing the pump) occupying a volume of 9.5 x 5.6 x 9.45 cm^3 and the tiny chamber (the one containing the filters) occupying a volume of 7.5 x 5.6 x 9.45 cm^3, with 2 mm walls and a 5.5 mm base thickness. The hole for attaching the pump to the huge chamber is positioned 4.8 centimetres from the outer wall and measures 0.96 x 0.5 cm^2. The partition wall between the chambers includes three holes; these are the connections for the filters; they are 2.2 cm apart from the ground and from one another to accommodate the use of various medium volumes. The connection holes are

positioned in the centre of each compartment, 8 mm from the bottom, with an inner diameter of 8 mm to accommodate the pump connection and an outer diameter of 1.2 cm. The dimensions of the lid are 6.55 x 18.35 x 2.2 cm^3, and the wall thickness is 3 mm (6.55 cm side) and 2 mm (18.35 cm side). The pump connection hole is 5.2 centimetres from the wall and is 1.8 x 0.5 cm^2. The design is shown in *Figure 32*.

5.1.3. CHANNELS MODULE

This device, which began as a support for the chips, was simply intended to hold injection tubing through integrated holes and stabilise the chip and its connections. Later, it was realised that the two principles could be combined, and so the piece might be designed as a method of uniform distribution and collecting of the pumped medium. Thus, it features two 8 mm-diameter internal channels that branch into 5 mm channels. It includes a method for cultivating a single chip as well as a method for cultivating up to three chips to replicate a body-on-a-chip, more sophisticated combinations, or a bioreactor. The two connections to the 8mm channels are centred in the vertical half of the model's front, 1 mm from the bottom and 2 mm from the top. They measure 1.5 cm in length, 1.4 cm in external diameter, and 8 mm in interior diameter. The device is designed to be modular, and with an adapter to be represented later, the connections can be unified without the need for multiple tanks. Of each configuration, two models are available depending on the used chip.

5.1.3.1. INDIVIDUAL APPLICATION

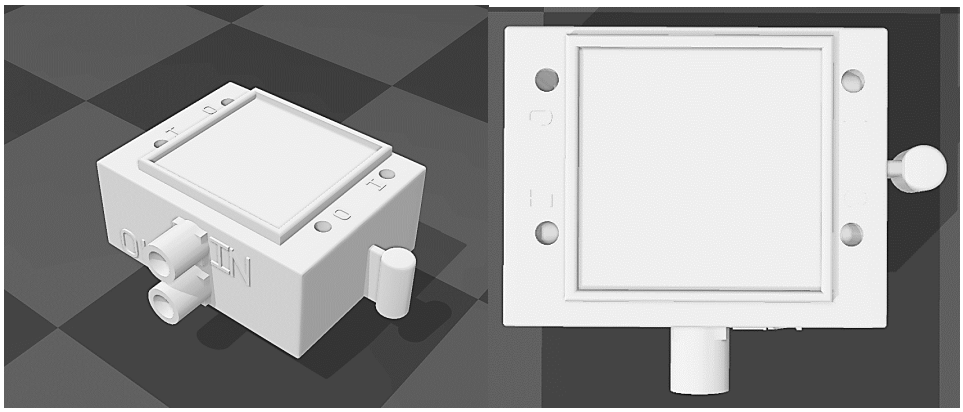

***Figure 34**. "Channels module" overview. Configuration for the general-purpose chip. One-chip-only application. In the side openings, adapters to connect with the chips are inserted. Within the implemented boxes, the chips are arranged.*

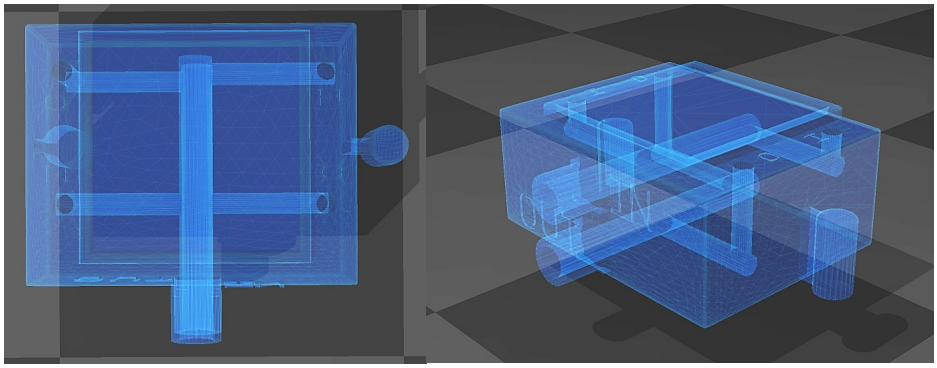

***Figure 35**. "Channels module" internal view. Configuration for the general-purpose chip. One-chip-only application. The branching of 8mm channels into 5mm channels is simple to appreciate.*

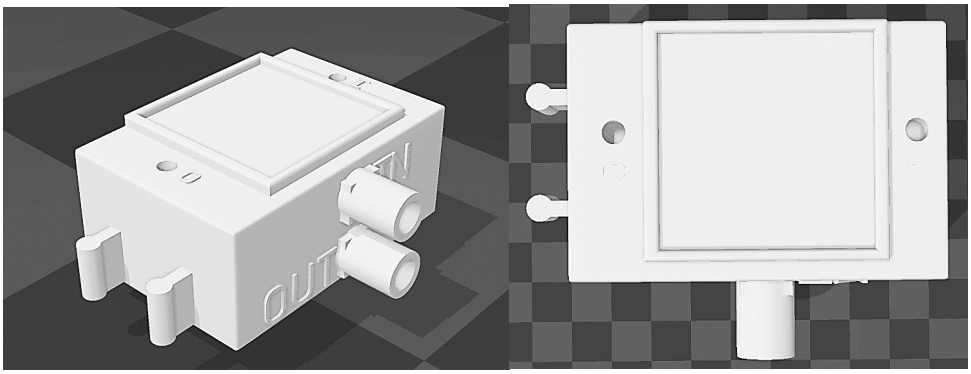

Figure 36. "Channels module" overview. Configuration for the metastasis chip. One-chip-only application. In the side openings, adapters to connect with the chips are inserted. Within the implemented boxes, the chips are arranged.

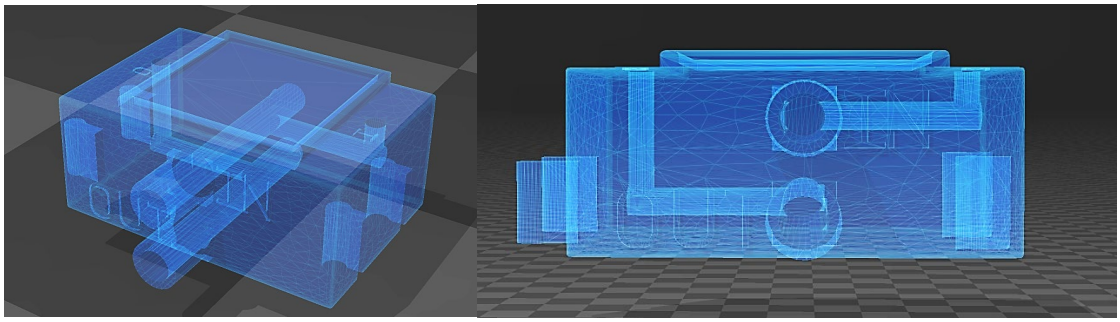

Figure 37. "Channels module" intern view. Configuration for the metastasis chip. One-chip-only application. The branching of 8mm channels into 5mm channels is simple to appreciate.

This model's dimensions are 6.2 x 8 x 3.5 cm^3(general purpose chip) / 5.25 x 7.95 x 3.25 cm^3(metastasis chip). *Figure 33* shows the external design of the channels module's individual application for the general-purpose chip, while *Figure 34* shows the internal structure. *Figure 35* shows the external design of the channels module's individual application for the metastasis chip, while *Figure 36* shows the internal structure.

5.1.3.2. BODY-ON-A-CHIP / BIOREACTOR APPLICATION

This model's dimensions are 14.9 x 7.95 x 3.25 cm^3 (general purpose chip) / 14.85 x 7.95 x 3.16 cm^3(metastasis chip). *Figure 37* shows the external design of the channels module's bioreactor application for the metastasis chip, while *Figure 38* shows the internal structure. *Figure 39* shows the external design of the channels module's bioreactor application for the general-purpose chip, while *Figure 40* shows the internal structure.

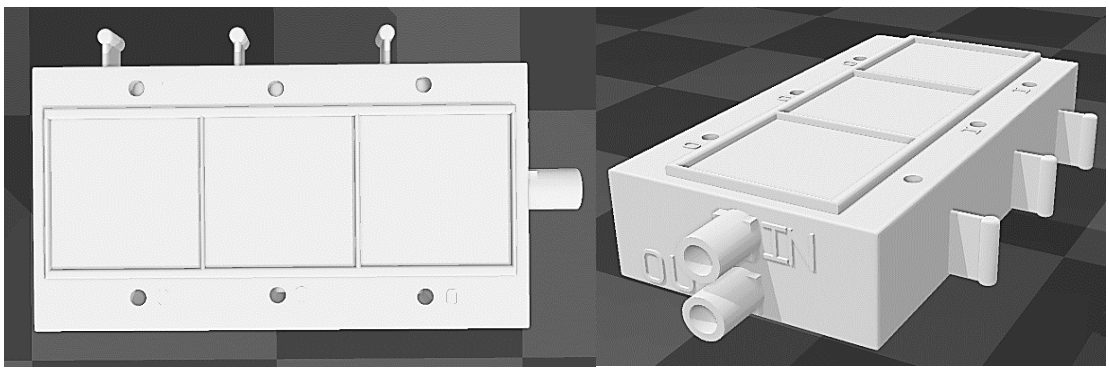

Figure 38. "Channels module" overview. Configuration for the metastasis chip. Multiple-chip application. In the side openings, adapters to connect with the chips are inserted. Within the implemented boxes, the chips are arranged.

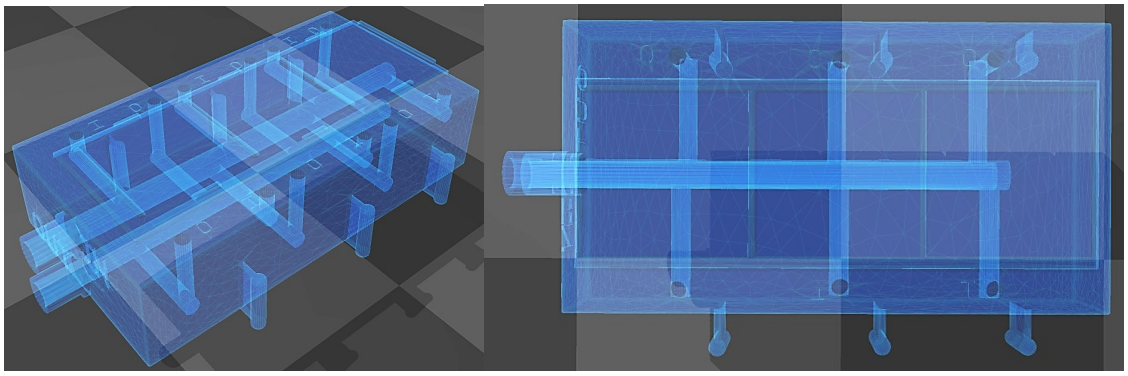

Figure 39. "Channels module" internal view. Configuration for the metastasis chip. Multiple-chip application. The branching of 8mm channels into 5mm channels is simple to appreciate.

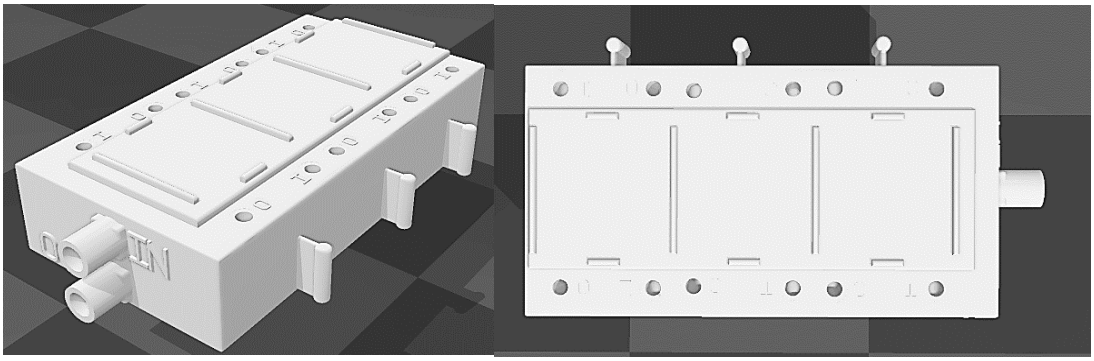

Figure 40. "Channels module" overview. Configuration for the general-purpose chip. Multiple-chip application. In the side openings, adapters to connect with the chips are inserted. Within the implemented boxes, the chips are arranged.

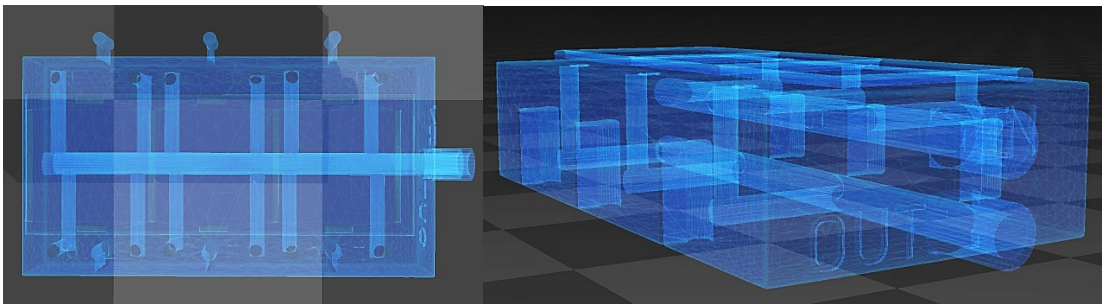

Figure 41. "Channels module" internal view. Configuration for the general-purpose chip. Multiple-chip application. The branching of 8mm channels into 5mm channels is simple to appreciate.

5.1.3.3. ADAPTERS

Adapters are components that are designed to accommodate infusion tubes and allow us to expand the functionality of our design. Two different models with different functionalities were designed: the adapter that connects the 5 mm channels of the channels module with the tubes that will lead to the chips (its use is required for proper device operation) and the adapter that can be installed between the tank and the channel module so that more than one of these can be used (its use is optional).

5.1.3.3.1. 5 mm CHANNELS TO CHIP

It measures 2.9 centimetres. The short section measures 9 mm and the long section measures 1.5 cm, so the separator and support structure between the two sections measures 5 mm. The outer diameter of the main tube is 5 mm and the inner diameter is 1.5 mm. 1 cm is the diameter of the centre section. *Figure 41* shows the external and internal structure of the model.

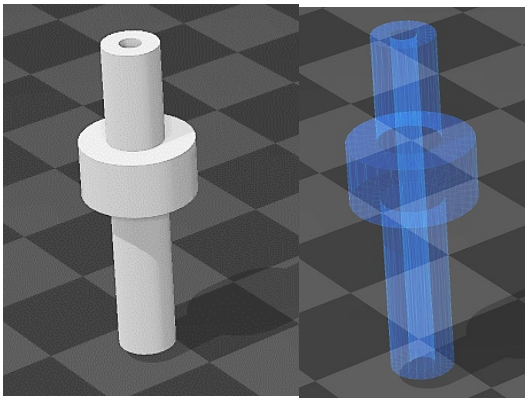

Figure 42. Adapter between the 5 mm channels of the channels module and the chips. The 9 cm section is connected to the channel module's apertures, while the 1.5 cm section is connected to the medium perfusion tubes leading to the chip.

5.1.3.3.2. TANK TO CHANNEL MODULE

This component is intended to divide the flow of the medium pump symmetrically. The volume of the core rectangle is 1,3 x 3 x 1 cm^3. The connections have a height of 1 cm and an external diameter of 1.2 cm and an interior diameter of 6 mm. This one is centred at 1.5 cm on the side of the piece where the entry is located (one connection). On the side of the piece where the exits are placed (two connections), they are joined to the 1 cm outer wall, leaving a space of 6 mm between them. *Figure 42* shows the external and internal structure of the model.

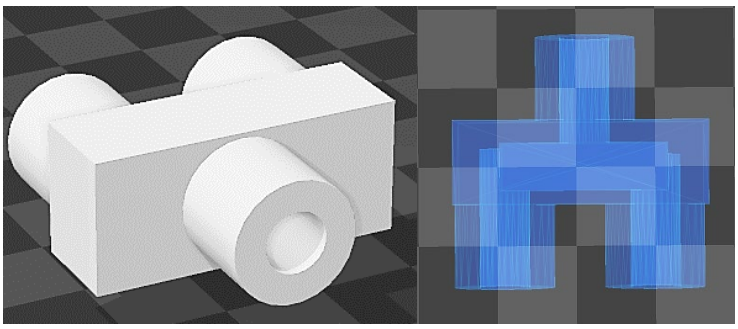

Figure 43. Adapter between the tank and the channels module. The tank tube is connected to the single input, while the inputs of the utilised channel modules are connected to the two outputs.

5.1.4. FILTERS

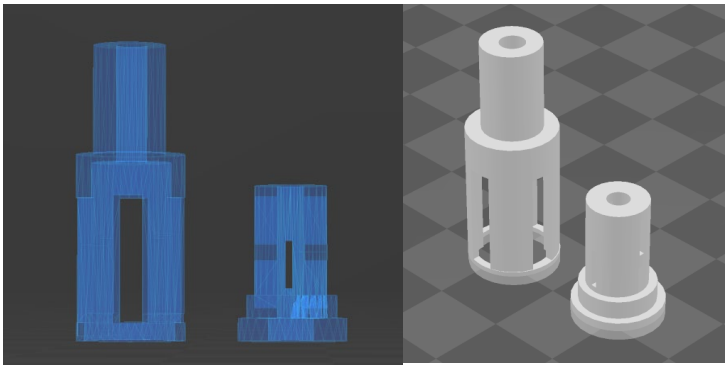

Figure 44. Filter for tumoroids / spheroids. One fibrous scaffold is positioned within the opening of the little component, while another is positioned surrounding it. Finally, it fits the larger section.

The filter consists of two pieces and is designed to manage the connection between the two parts of the tank, retaining for further investigation any tumour spheroids that may be present in the

environment. It is intended to house fibre scaffolds that serve as filtering membranes. It is optimally installed in the secondary chamber because it fits into the slots in the tank chamber partition wall. *Figure 43* shows the external and internal structure of the model.

5.1.5. BATTERY

Because the device will be kept inside of an incubator, a battery casing has been constructed. This casing has been designed to permit airflow between the culture basin and the battery, and it also encloses the battery once it has been packed to prevent condensation from forming. A hole has been made at the back so that moisture can be easily detected. The two parts of the casing (case and lock) are represented in *Figure 44*.

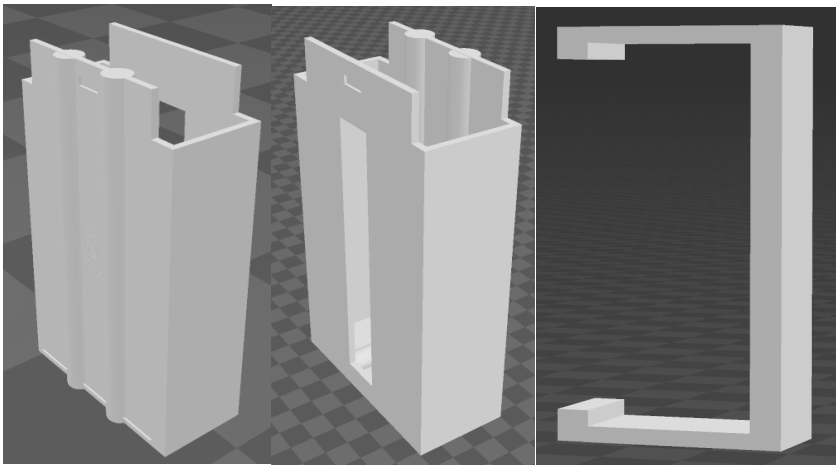

Figure 45. Battery case and lock.

5.2. MATERIALS

Because the used materials will come into contact with organic matter, they must be biocompatible. Therefore, PDMS, glass, and thermoplastic polymers would be the most viable options given the current state of the art. Due to the manufacturing procedure, only the third item meets the standards. Therefore, the most frequent thermoplastic polymers for usage in an FFF printer are PLA, ABS, PET, PETG, Nylon, TPU, polycarbonate, PCTG, PETT, carbon fibre, and PP (polypropylene). As one of the key requirements was that the models be able to be printed by non-experts, the ease of printing of the polymer was a crucial element in its selection. In addition to being biocompatible and biodegradable, PLA is the easiest material to print with an FFF printer, therefore it was initially considered. It was decided not to use ABS, which is difficult to print, extremely sensitive to temperature changes, and easily warps, as well as PET, which, in certain cases, produces toxic vapours when printed. PETG and PCTG, on the other hand, are non-toxic, easy to print, and biocompatible; thus, they were chosen for utilisation. Nylon absorbs a great deal of moisture, is extremely sensitive to temperature fluctuations, and printing it is difficult, thus its use was abandoned . Because TPU is the flexible and biocompatible material that is easier to print, it was selected for usage in some portions, while PP was discarded due to its lack of printability. Carbon fibre filaments are not necessarily biocompatible, they are difficult to print (requiring an aluminium nozzle and high printing temperatures), and expensive, hence their use has been abandoned. Since PETT has the same properties as PETG but it is less transparent, it was not used. PMMA has been utilised due to its biocompatibility, manufacturing simplicity, and transparency. Due to its biocompatibility, flexibility, and transparency, silicone has been utilised. Chloroform has been used because it is a solvent utilised in numerous biomedical laboratory procedures.

5.2.1. PLA, PETG/PCTG

PLA and PETG (and their derivative PCTG) have been used interchangeably to print the majority of models. However, there are several factors to consider:

- To allow light to pass through, the chips must be printed with transparent filament. On the other hand, PETG has proven to be more durable and ideal for the production of this component, as we need to be able to apply pressure to the connecting pipes when we are installing the medium distribution tubes; however, a functional assembly has been achieved using PLA for printing the piece.
- When printing the channel module, the 5 mm channel adapter to the media distribution tubes must be considered. The adapter and module will be connected and sealed to prevent leaks; thus, if we need to remove the adapters because they are broken or we want to seal the entry for a specific application, we will need to apply heat to remove the part without causing damage to the channel module. Therefore, it is recommended to print this model in PETG, which has a higher melting point than PLA. If the adapters are printed in this other polymer, the channel module will not be deteriorated when the PLA is melted.

5.2.2. TPU

As PLA / PETG printing was too hard to allow for easy mounting and installation of the device, TPU has been used for filter printing. For this material, we must take into account that it has a higher liquid absorption than other polymers; consequently, it is anticipated that it will degrade faster than other polymers, and printed parts will need to be replaced more frequently than PLA/PETG parts.

5.2.3. PMMA

PMMA has been utilised to create a totally transparent chip cover. Despite the positive results, the lack of access to a laser cutter necessitated the use of a cutter to cut the polymer plates for these tests. As a result, the resulting pieces did not fit perfectly in the crop area hole, and the set up did not withstand the same pressures as the configuration with a printed lid. To obtain optimal outcomes and functioning, it is anticipated that PMMA would be used when setting up the cell cultures.

5.2.4. SEALING

Various compounds, including silicone, glue, and acetone, have been tested for use in the connecting and sealing of pieces; however, the best results have been obtained with chloroform. The general treatment of the parts with this solvent has proven to be the most effective way to improve the layer adhesion, making the models more durable and less brittle, and it is believed that the texture created by the manufacturing method on the walls of the infusion channels can also be improved to prevent cell adhesion in undesirable areas [185], [186]. It evaporates more slowly than acetone, allowing us more time to work, has a bigger impact on the polymers we've employed, and, unlike silicone or adhesives, leaves very little behind after evaporation.

5.2.5. SILICONE

The used cellular medium transport tubes are constructed of silicone. These connect the channel module, the tank, and the chips; for the “channels module – chip” connection, the tube has a diameter of 4 mm and a length of 8 cm, while for the “tank – channels module” connection, it has a diameter of 1 cm and a length of 10 cm. The silicone utilised is food/medical grade and was

purchased from distributors for aquaponics circuit replacement parts (4 mm) and respirator replacement parts (1 cm).

5.2.6. RESIN

In an effort to improve the miniaturisation factor, resin was used to create the standard and 75 percent scale versions of the chips. However, the resulting pieces had extremely brittle connecting tubes that could not resist the tension applied to them during silicone tube assembly. This, along with the fact that the polymers utilised are less hazardous than photocuring resin and that the production of resin is more costly and requires greater knowledge, led to the conclusion that it was not the optimal material for this application.

5.3. PRINTING

5.3.1. PRINTER

Figure 46. Used printer: Artillery Genius Pro.

The manufacturer of the project utilised an Artillery Genius Pro printer. This printer uses direct extrusion and has a maximum consume of 700 W. To survive the melting temperature of PETG/PCTG, the standard Teflon tube fitted between the filament pulling gear and the nozzle is replaced with a high-temperature-resistant Teflon Capricorn tube. The models were printed with a 0.4 mm diameter nozzle, as a 0.2 mm nozzle did not provide sufficient detail improvement to justify the additional printing time, and a 0.6 mm nozzle lost too much resolution in small details, especially of the chips. Assembling, calibrating, and printing the machine in the author's residence demonstrates that the system can be used in places and by individuals who are not manufacturing science specialists. To prevent the deposition of bacteria or undesired residues between model layers, it is advised to clean the extrusion system with a solvent before each use and, ideally, to keep the printer in a box/cubicle or at least work in a clean atmosphere. However, post-treatment with chloroform should eliminate any undesirable residues.

5.3.2. SLICER PARAMETRITZATION

The software utilised for slicing is Ultimaker Cura. Here, the Artillery Genius printer model has been chosen, and the Printer Settings have been adjusted to accommodate the upgraded version. Using a predetermined template eliminates the need to insert initialization and end-of-print g-code manually. Width (220 mm), Depth (220 mm), and Height (250 mm), which pertain to the dimensions of the print tray, have been modified. To configure the print settings for the various materials, the Standard Quality profile was used as a starting point, and only the essential fields were modified. To parameterize the slicer parameters, temperature, retraction, flow rate, and ventilation benchmarks have been downloaded and executed from 3D printing support blogs.

5.3.2.1. PLA

- **Wall Thickness**: 3 mm.
- **Top Surface Skin Layers**: 1.
- **Top Thickness**: 1 mm.
- **Bottom Thickness**: 1 mm.
- **Infill**: 40 %.
- **Printing Temperature**: 200 ºC.
- **Build Plate Temperature**: 60 ºC.
- **Flow**: 98%.
- **Print Speed**: 90 mm/s.
- **Wall Speed**: 70 mm/s.
- **Build Plate Adhesion Type**: Brim.

5.3.2.2. PETG / PCTG

- **Wall Thickness**: 3 mm.
- **Top Surface Skin Layers**: 1.
- **Top Thickness**: 1 mm.
- **Bottom Thickness**: 1 mm.
- **Infill**: 40 %.
- **Printing Temperature**: 245 ºC.
- **Build Plate Temperature**: 80 ºC.
- **Flow**: 97%.
- **Print Speed**: 60 mm/s.
- **Wall Speed**: 50 mm/s.
- **Build Plate Adhesion Type**: Brim.
- **Retraction Speed**: 30 mm/s.

5.3.2.3. TPU

- **Wall Thickness**: 3 mm.
- **Top Surface Skin Layers**: 1.
- **Top Thickness**: 1 mm.
- **Bottom Thickness**: 1 mm.
- **Infill**: 40 %.
- **Printing Temperature**: 220 ºC.
- **Build Plate Temperature**: 60 ºC.
- **Flow**: 100%.
- **Print Speed**: 60 mm/s.
- **Wall Speed**: 30 mm/s.
- **Retraction Distance**: 3 mm.

5.4. PUMPING SYSTEM

Figure 47. Perfusion pump scheme.

Due to the available time and electronic circuit design skills at the time the work was developed, it was determined that designing a control circuit for the cultivation device was not viable. Therefore, it was determined to conceptually simplify as much as feasible the initial project's requirements for electronic components until just two remained: the pump and the portable power source. Four primary criteria were considered while selecting the pump: adjustable flow rate, USB power supply, minimum feasible size, and minimum possible cost. Thus, a water pump for smaller aquasystems manufactured by Flintronic was selected. That provides a variable supply between 3.5 and 9 V and between 1 and 3 watts of power. The selected battery has a 20.000mAh capacity and a 5V and 9V output; consequently, depending on the consumption numbers and the voltage used, the battery will last between three and four days of continuous use. In most situations, cell cultures are tested every three days; therefore, we should incorporate the replacement of the battery with a fully charged one in our check schedule.

5.5. REGULATIONS AND LEGAL ASPECTS

No personal information, biological materials, or other resources requiring review and approval by a Medical Ethics Committee were utilised in the production of this project. Regarding the environmental impact of its manufacture, despite the fact that recycled filament cannot be used due to the risk that it contains traces of polluting microparticles that may interfere with the subsequent development of cell cultures, we have chosen a main filament manufacturer that allows us to return the finished spools for recycling, such as Smart Materials (for PLA spools) and,

in cases where it has been possible (PETG/PCTG), the unwound filament from Fillamentum and Fiberology has been used by printing a reusable spool. With the exception of the printer, all resources were obtained locally or nationally in order to minimise the carbon footprint.

Regarding the intellectual property of the device, despite being designed as an open-source platform so that users can adapt it to their needs, explicit permission from the author is required to use the platform as a foundation for future projects so as not to create a conflict of interest with any future projects that the owner may undertake.

6. RESULTS

Figure 48. Final results. Images depict: (1,2) Assembly of the circuit in bioreactor mode; (3) individual culture channels module; (4) individual tank, lid, pump, and battery; and (5) assembly of the circuit in bioreactor mode utilising two channels modules and the extended tank.

Due to the four-month development period and the lack of a cell culture laboratory with the resources to test the device's quality, the gold standards established to ensure the correct evolution of the project design and the tests conducted do not include a cytotoxicity or cell viability study, although this will be presented as a necessary extension. To ensure that the

solvent is not deposited in the culture chamber, a chip-sealing test with chloroform is added to the previously mentioned tests for adjusting the sizes of the various parts of the device, for determining the device's ability to be watertight, and for determining the pieces' resistance.

In the instance of the size adaption test, the first two iterations of the chips had a 3 × 3 cm^2 and 5 x 5 cm^2 base area, respectively. The first version did not allow for simple integration and the connections for the medium distribution pipes could not survive the stress of the assembly process; the second version was too large and did not conform to the concept of downsizing. As previously stated, we utilised an intermediate version with a 4 x 4 cm^2 foundation. Concerning the connections with the medium tubes, testing with external diameters of 4, 5, and 6 mm and internal diameters of 1 and 2 mm have been conducted. The 1-mm internal diameter did not enable enough medium to pass, thus it was decided to increase it to 2 mm. The 4mm outside diameter resulted in channels that were too fragile, while the 6mm outer diameter took up too much area on the chip, so it was determined that the optimal outer diameter was 5mm. These measures have proven optimal and permit a decent but controlled liquid circulation and adequate resistance to withstand the assembly process without difficulty.

The adapters between the channel module and the chips were subjected to a similar evaluation. To fit with the same tubes as the chips, the exterior diameter had to be 5 mm, but because this piece had to be mechanically fitted within another tough polymer model, it required greater mechanical resistance than the chips, therefore the internal diameter was decreased to 1.5 mm. If good layer adhesion is not obtained during printing, these parts will not survive the channel module assembly procedure.

The devices' watertightness was tested by connecting the system and leaving it running for an extended period of time on a surface that absorbs water, such as paper. By adding a dye to the water used for the perfusion test, it was simple to determine if there had been any liquid loss, no matter how minor. During the development of these, it was discovered that preparing the external walls of the various printed connection tubes with a solvent such as chloroform facilitates the insertion of silicone tubes and avoids liquid leakage. Using 100 x 2.5 mm^2 flanges, the connections between the printed components and the silicone tubes have been secured. Thus, a gadget with no discernible liquid leakage has been achieved.

Although the resistance of the parts had already been evaluated and parameterized, it was desired to determine whether the chloroform treatment had resulted in an improvement, particularly in the connections or parts that had to endure the most stress. Thus, lateral stresses were applied to the chip connections and channel module collectors in order to compare their performance prior to and after chloroform application. In the case of untreated pieces, they supported an average of 15 kg, whereas treated pieces, after allowing the chloroform to evaporate for 24 hours, gained resistance to weights up to 30 kg, and the rupture exhibited a significantly greater proportion of plastic deformation. These tests were conducted by suspending predetermined weights from the connections; consequently, to acquire more precise resistance values, a study using the right equipment would be required.

To confirm that sealing the chip with chloroform would not result in contamination of the culture, a dried pigment that interacted with the solvent was placed on the internal border of the lid and the culture chamber. If the cap was the correct size, well-fitted to the chip, and the time required for the solvent to react with the polymer was allowed between applications (at least two applications of chloroform are advised for optimal results), there was no detectable chloroform transfer in the culture zone. Regarding the sealing with chloroform and the use of PMMA caps, it

must be kept in mind that, in order to preserve the material's transparency, it is imperative to avoid applying solvent to the upper portion of the cap at all costs. Therefore, precise applicators, such as a syringe with a small-diameter needle, are required for this application.

The experimentally determined flow rate between input and output for the maximum power configuration of the pump is 0.1 l/min, yielding a liquid velocity inside the chip of approximately 100 mm/s, whereas for the minimum power configuration, the flow rate is 0.02 l/min, yielding a liquid velocity inside the chip of approximately 25 mm/s. Final results can be seen in *Figure 47*.

7. DISCUSSION

In response to the research question, "Is it possible to fabricate a microfluidic system for the in vitro cell culture of tumor-like structures inspired by the technological concept of organ-on-a-chip and specifically tumor-on-a-chip using fused filament fabrication as the primary manufacturing method and inexpensive electronic components? ", we can confirm that it is feasible to produce a dynamic cell culture device using FFF as the primary manufacturing method. This has been possible due to the adaption of the models to the limits of the printer and the parameterization of the optimal post-processing, confirming the hypothesis. Thus, in accordance with the proposed objectives, the models that would comprise the cultivation device have been designed and adapted; watertightness has been achieved through chloroform treatment of the pieces; a filtration system has been developed; and low-cost electronic components that do not require a connection to the main have been incorporated.

7.1. LIMITATIONS

The primary restriction of the obtained data was the inability to test the device by cultivating cells. Due to the time spent on the design, the resolution of obstacles that arose during its development, the printing time required by the parts, and the complexity of designing a cultivation procedure for a new device and research methodology, a collaboration project with a biomedical laboratory to test the effectiveness of the resulting product could not be conceived. A cell viability study would serve as the gold standard for finalising the adaptation of parameters such as the average flow rate within the chips or the efficacy of the post-processing done to prevent cell adherence to undesirable locations.

However, it has proven able to design a device that overcomes the primary limitations of FFF as a manufacturing technique for organ-on-chip / tumor-on-chip applications. Such are miniaturisation issues or the difficulty of achieving optimal layer adhesion. With a thorough expansion of the study, it will be possible to personalise the designs of the models and the electrical equipment used to achieve successful application and control of culture parameters on par with much more expensive devices.

7.2. CONTRIBUTIONS TO THE UNITED NATIONS SUSTAINABLE DEVELOPMENT GOALS

The project intends to contribute to the Sustainable Development Goals of the United Nations on two fronts. First, it promotes aim 3, "Good Health and Well-Being," because one of the primary objectives of the research is to accomplish more cheap, individualised, and trustworthy scientific research. On the other hand, it aims to contribute to objective 12, "Responsible consumption and production," by centralising the production of cultivation hardware in the same research laboratories and on demand. By doing so, we will avoid the environmental impact caused by the transport of goods and we will not have an excess of unused growing materials. In addition, the capability of extending the lifespan of crops leads to the decreased use of cell seed plates. These elements contribute to a smaller environmental footprint.

Figure 49. United Nations' sustainable development goals.

8. CONCLUSIONS

This research has proposed a platform that intends to be the first venture into the creation of microfluidic devices for cell culture, inspired by the technological ideas of organ-on-a-chip and tumor-on-a-chip and made mostly by fused filament fabrication. This innovative method promises to simplify and reduce manufacturing costs, to make it easier to adapt culture chips to the current application, to be watertight, to have an adjustable flow, to be wire-free, and to serve as a foundation for the development of new bio-inspired designs. To make the models workable despite the required miniaturisation factor for the intended use, the sizes of the various components and pieces have been adjusted through the use of stress testing. To establish optimal sealing of the parts and ensure that the system was impermeable, chloroform was employed; it was also used to increase the layer adhesion (and hence the strength) and to smooth the texture of the pieces, which was intrinsic to the manufacturing process, in order to reduce cell adhesion. TPU is used to make the filters, whereas PLA, PETG, and PCTG are utilised to make the other models.

Before performing culture tests, PMMA caps for the chips need to be produced in order to monitor the cells accurately. These will be cut from a sheet of material using a laser cutter, and the lid's two components will be connected with chloroform. On the other hand, cell culture and viability testing are essential for establishing the device's efficacy and future potential. Consequently, it will be necessary to build a culture approach and modify procedures such as chip sealing and cell seeding for the new device.

After evaluating the current device, three major enhancement recommendations are presented. The initial step is to construct a control circuit utilising an open-source electrical platform, such as Arduino boards, as the primary module and a pH sensor, an oxygen sensor, a carbon dioxide sensor, a temperature sensor, a pressure sensor, a humidity sensor, and a thermistor, among others. We would be able to monitor the crop without needing to examine it under a microscope or be there in the laboratory. In contrast, the thermistor would allow us to manage the temperature of the culture medium without using an incubator. In addition, we would be able to add an additional pump in order to create more complex O_2 gradients. The second suggestion would be to merge sensor data into a prediction model employing artificial intelligence, notably machine learning, to automate the process of managing cell culture and forecast when it will no longer be viable. The third and simplest improvement would be to use a 4 x 4 cm^2 piece of PMMA as the bottom of the chips to increase transparency and simplify microscopic examination. As a last supplementary project, a chamber for equally applying chloroform to the printed components could be constructed.

Thus, we can conclude that an intersection between the disciplines of biology, materials science, industrial engineering, and electronic engineering is essential towards the development of economical, innovative, personalised, and intelligent medicine.

9. BIBLIOGRAPHY

[1] W. H. Organization, "Cáncer," 2020. https://www.who.int/es/news-room/fact-sheets/detail/cancer (accessed Aug. 31, 2021).

[2] S. E. de O. Médica, "Cáncer España," 2021. https://seom.org/images/Cifras_del_cancer_en_Espnaha_2021.pdf (accessed Aug. 31, 2021).

[3] N. Catherine Sánchez, "Conociendo y comprendiendo la célula cancerosa: Fisiopatología del cáncer," *Revista Médica Clínica Las Condes*, vol. 24, no. 4, pp. 553–562, Jul. 2013, doi: 10.1016/s0716-8640(13)70659-x.

[4] C. P. Segeritz and L. Vallier, "Cell Culture: Growing Cells as Model Systems In Vitro," *Basic Science Methods for Clinical Researchers*, pp. 151–172, Apr. 2017, doi: 10.1016/B978-0-12-803077-6.00009-6.

[5] M. W. Hess, K. Pfaller, H. L. Ebner, B. Beer, D. Hekl, and T. Seppi, "3D Versus 2D Cell Culture: Implications for Electron Microscopy," *Methods in Cell Biology*, vol. 96, no. C, pp. 649–670, Jan. 2010, doi: 10.1016/S0091-679X(10)96027-5.

[6] I. Padmalayam and M. J. Suto, "3D Cell Cultures: Mimicking In Vivo Tissues for Improved Predictability in Drug Discovery," *Annual Reports in Medicinal Chemistry*, vol. 47, pp. 367–378, Jan. 2012, doi: 10.1016/B978-0-12-396492-2.00024-2.

[7] J. Hansmann, D. Egger, and C. Kasper, "Advanced Dynamic Cell and Tissue Culture," *Bioengineering*, vol. 5, no. 3, p. 65, Sep. 2018, doi: 10.3390/BIOENGINEERING5030065.

[8] P. Aishwarya, G. Agrawal, J. Sally, and M. Ravi, "Dynamic three-dimensional cell-culture systems for enhanced in vitro applications," *CURRENT SCIENCE*, vol. 122, no. 2, 2022.

[9] "Tumoroid | Encyclopedia." https://encyclopedia.pub/2504 (accessed Sep. 01, 2021).

[10] A. K. Badekila, S. Kini, and A. K. Jaiswal, "Fabrication techniques of biomimetic scaffolds in three-dimensional cell culture: A review," *Journal of Cellular Physiology*, vol. 236, no. 2, pp. 741–762, Feb. 2021, doi: 10.1002/JCP.29935.

[11] B. P. Chan and K. W. Leong, "Scaffolding in tissue engineering: general approaches and tissue-specific considerations," *European Spine Journal*, vol. 17, no. Suppl 4, p. 467, Dec. 2008, doi: 10.1007/S00586-008-0745-3.

[12] P. Tomlins, "Material types for tissue scaffolds," *Characterisation and Design of Tissue Scaffolds*, pp. 1–21, Jan. 2016, doi: 10.1016/B978-1-78242-087-3.00001-8.

[13] W. Cai, R. B. Gupta, and Updated by Staff, "Hydrogels," *Kirk-Othmer Encyclopedia of Chemical Technology*, pp. 1–20, Jul. 2012, doi: 10.1002/0471238961.0825041807211620.A01.PUB2.

[14] S. K. H. Gulrez, S. Al-Assaf, and G. O. Phillips, "Hydrogels: Methods of Preparation, Characterisation and Applications," *Progress in Molecular and Environmental Bioengineering - From Analysis and Modeling to Technology Applications*, Aug. 2011, doi: 10.5772/24553.

[15] S. R. Caliari and J. A. Burdick, "A practical guide to hydrogels for cell culture," *Nature Methods 2016 13:5*, vol. 13, no. 5, pp. 405–414, Apr. 2016, doi: 10.1038/nmeth.3839.

[16] S. R. Caliari and J. A. Burdick, "A practical guide to hydrogels for cell culture," *Nature Methods 2016 13:5*, vol. 13, no. 5, pp. 405–414, Apr. 2016, doi: 10.1038/nmeth.3839.

[17] M. W. Tibbitt and K. S. Anseth, "Hydrogels as extracellular matrix mimics for 3D cell culture," *Biotechnology and Bioengineering*, vol. 103, no. 4, pp. 655–663, Jul. 2009, doi: 10.1002/BIT.22361.

[18] E. M. Ahmed, "Hydrogel: Preparation, characterization, and applications: A review," *Journal of Advanced Research*, vol. 6, no. 2, pp. 105–121, Mar. 2015, doi: 10.1016/J.JARE.2013.07.006.

[19] Jon. Stanger, Nick. Tucker, and Mark. Staiger, "Electrospinning," 2008.

[20] "Electrospinning - Wikipedia, la enciclopedia libre." https://es.wikipedia.org/wiki/Electrospinning (accessed May 07, 2022).

[21] A. L. Yarin, S. Koombhongse, and D. H. Reneker, "Taylor cone and jetting from liquid droplets in electrospinning of nanofibers," *Journal of Applied Physics*, vol. 90, no. 9, pp. 4836–4846, Nov. 2001, doi: 10.1063/1.1408260.

[22] "What is 3D Modeling & What's It Used For?" https://conceptartempire.com/what-is-3d-modeling/ (accessed May 07, 2022).

[23] "What is 3D Modeling? | Siemens Software." https://www.plm.automation.siemens.com/global/ru/our-story/glossary/3d-modeling/17977 (accessed May 07, 2022).

[24] "What is 3D Modeling? | How 3D Modeling is Used Today." https://www.takeoffpros.com/2020/04/27/guide-to-3d-modeling/ (accessed May 07, 2022).

[25] "Additive manufacturing, explained | MIT Sloan." https://mitsloan.mit.edu/ideas-made-to-matter/additive-manufacturing-explained (accessed May 08, 2022).

[26] "3D printing scales up | The Economist." https://www.economist.com/technology-quarterly/2013/09/05/3d-printing-scales-up (accessed May 07, 2022).

[27] "The rise of additive manufacturing." https://www.theengineer.co.uk/content/in-depth/the-rise-of-additive-manufacturing (accessed May 07, 2022).

[28] "Homepage - Stratasys." https://www.stratasys.com/ (accessed May 08, 2022).

[29] A. Zolfaghari, T. Chen, and A. Y. Yi, "Additive manufacturing of precision optics at micro and nanoscale," *International Journal of Extreme Manufacturing*, vol. 1, no. 1, Apr. 2019, doi: 10.1088/2631-7990/AB0FA5.

[30] "Fused Deposition Modeling: Most Common 3D Printing Method | Live Science." https://www.livescience.com/39810-fused-deposition-modeling.html (accessed May 08, 2022).

[31] "FDM (FUSED DEPOSITION MODELING)." https://web.archive.org/web/20130812014856/http://rpworld.net/cms/index.php/addit

ive-manufacturing/rp-rapid-prototyping/fdm-fused-deposition-modeling-.html (accessed May 08, 2022).

[32] "Category:Extruders - RepRap." https://reprap.org/wiki/Category:Extruders (accessed May 08, 2022).

[33] C. K. Chua, K. F. Leong, and C. S. Lim, "Rapid Prototyping," Mar. 2003, doi: 10.1142/5064.

[34] "Bioplastics Report: Industry Analysis, Market Forecast 2030." https://www.ceresana.com/en/market-studies/plastics/bioplastics/ (accessed May 08, 2022).

[35] V. Nagarajan, A. K. Mohanty, and M. Misra, "Perspective on Polylactic Acid (PLA) based Sustainable Materials for Durable Applications: Focus on Toughness and Heat Resistance," *ACS Sustainable Chemistry and Engineering*, vol. 4, no. 6, pp. 2899–2916, Jun. 2016, doi: 10.1021/ACSSUSCHEMENG.6B00321/ASSET/IMAGES/LARGE/SC-2016-00321X_0014.JPEG.

[36] A. Södergård and M. Stolt, "Industrial Production of High Molecular Weight Poly(Lactic Acid)," *Poly(Lactic Acid): Synthesis, Structures, Properties, Processing, and Applications*, pp. 27–41, Sep. 2010, doi: 10.1002/9780470649848.CH3.

[37] "What Is PLA? – 3D Printing Materials Simply Explained | All3DP." https://all3dp.com/2/what-is-pla-3d-printing-materials-simply-explained/ (accessed May 08, 2022).

[38] "All you need to know about PLA for 3D printing - 3Dnatives." https://www.3dnatives.com/en/pla-3d-printing-guide-190820194/ (accessed May 08, 2022).

[39] L. de Vos, B. van de Voorde, L. van Daele, P. Dubruel, and S. van Vlierberghe, "Poly(alkylene terephthalate)s: From current developments in synthetic strategies towards applications," *European Polymer Journal*, vol. 161, p. 110840, Dec. 2021, doi: 10.1016/J.EURPOLYMJ.2021.110840.

[40] "What is PET? - NAPCOR." https://napcor.com/about-pet/ (accessed May 09, 2022).

[41] F. Brenz, S. Linke, and T. J. Simat, "Linear and cyclic oligomers in PET, glycol-modified PET and Tritan™ used for food contact materials," *https://doi.org/10.1080/19440049.2020.1828626*, vol. 38, no. 1, pp. 160–179, 2020, doi: 10.1080/19440049.2020.1828626.

[42] "Modern Polyesters: Chemistry and Technology of Polyesters and Copolyesters - Google Llibres." https://books.google.es/books?hl=ca&lr=&id=ZgxgZ5vfxTkC&oi=fnd&pg=PR5&dq=pctg+pte&ots=DtHDAsleGu&sig=Gi_iQyqPDO0bggr_s092hWVftBE&redir_esc=y#v=onepage&q&f=false (accessed May 09, 2022).

[43] "PET vs PETg Filament - What's The Difference?" https://www.filamentive.com/pet-vs-petg-filament-whats-the-difference/ (accessed May 09, 2022).

[44] "PET Vs PETG Filament – What Are the Actual Differences? – 3D Printerly." https://3dprinterly.com/pet-vs-petg-filament-what-are-the-actual-differences/ (accessed May 09, 2022).

[45] F. Welle, "Food law compliance of poly(ethylene Terephthalate) (PET) food packaging materials," *ACS Symposium Series*, vol. 1162, pp. 167–195, 2014, doi: 10.1021/BK-2014-1162.CH016.

[46] C. Lambré *et al.*, "Safety assessment of the process Green Loop System, used to recycle polycyclohexylene dimethylene terephthalate glycol-modified (PCTG) plates for use as food contact materials," *EFSA Journal*, vol. 20, no. 1, p. e07002, Jan. 2022, doi: 10.2903/J.EFSA.2022.7002.

[47] "PCTG | Impact resistant filament - your alternative to PET-G | Fiberlogy." https://fiberlogy.com/en/fiberlogy-filaments/pctg/ (accessed May 09, 2022).

[48] J. Y. Liang, S. R. Shin, S. H. Lee, and D. S. Lee, "Self-Healing and Mechanical Properties of Thermoplastic Polyurethane/Eugenol-Based Phenoxy Resin Blends via Exchange Reactions," *Polymers 2020, Vol. 12, Page 1011*, vol. 12, no. 5, p. 1011, Apr. 2020, doi: 10.3390/POLYM12051011.

[49] O. Olabis, "Polymer-Polymer Miscibility," p. 383.

[50] "Applications & Benefits." https://www.americanchemistry.com/industry-groups/center-for-the-polyurethanes-industry-cpi/applications-benefits (accessed May 09, 2022).

[51] "Engineered Polymers Thermoplastic Polyurethane (TPU) - Lubrizol." https://www.lubrizol.com/Engineered-Polymers (accessed May 09, 2022).

[52] W. 1946- Michaeli, *Technologie der Kunststoffe Lern- und Arbeitsbuch für die Aus- und Weiterbildung*.

[53] "Polymethylmethacrylate - Acrylic - PMMA General Purpose." https://www.azom.com/article.aspx?ArticleID=788 (accessed May 09, 2022).

[54] "Polymethylmethacrylate (PMMA, Acrylic) :: MakeItFrom.com." https://www.makeitfrom.com/material-properties/Polymethylmethacrylate-PMMA-Acrylic (accessed May 09, 2022).

[55] "Working with Plexiglas®." https://web.archive.org/web/20150221110921/http://www.science-projects.com/Plastics/PlexiglasWork.htm (accessed May 09, 2022).

[56] "Chloroform | CHCl3 - PubChem." https://pubchem.ncbi.nlm.nih.gov/compound/Chloroform (accessed May 09, 2022).

[57] M. Rossberg *et al.*, "Chlorinated Hydrocarbons," *Ullmann's Encyclopedia of Industrial Chemistry*, Jul. 2006, doi: 10.1002/14356007.A06_233.PUB2.

[58] "Chloroform [MAK Value Documentation, 2000]," *The MAK-Collection for Occupational Health and Safety*, pp. 20–58, Jan. 2012, doi: 10.1002/3527600418.MB6766E0014.

[59] "Improve your 3D prints with chemical smoothing - Original Prusa 3D Printers." https://blog.prusa3d.com/improve-your-3d-prints-with-chemical-smoothing_36268/ (accessed May 09, 2022).

[60] E. W. K. Young and D. J. Beebe, "Fundamentals of microfluidic cell culture in controlled microenvironments," *Chem Soc Rev*, vol. 39, no. 3, pp. 1036–1048, Feb. 2010, doi: 10.1039/B909900J.

[61] S. Shay and S. Shay, "Organs-on-a-Chip: A Future of Rational Drug-Design," *Journal of Biosciences and Medicines*, vol. 5, no. 9, pp. 22–28, Aug. 2017, doi: 10.4236/JBM.2017.59003.

[62] "A short review about organ on chip - Elveflow." https://www.elveflow.com/microfluidic-reviews/organs-on-chip-3d-cell-culture/a-review-about-organ-on-chip/ (accessed May 10, 2022).

[63] "Organs-on-Chips: Applications, Challenges, and the Future | Technology Networks." https://www.technologynetworks.com/drug-discovery/articles/organs-on-chips-applications-challenges-and-the-future-288031 (accessed May 11, 2022).

[64] Y. S. Zhang *et al.*, "Multisensor-integrated organs-on-chips platform for automated and continual in situ monitoring of organoid behaviors," *Proc Natl Acad Sci U S A*, vol. 114, no. 12, pp. E2293–E2302, Mar. 2017, doi: 10.1073/PNAS.1612906114.

[65] J. Theobald *et al.*, "Liver-Kidney-on-Chip To Study Toxicity of Drug Metabolites," *ACS Biomater Sci Eng*, vol. 4, no. 1, pp. 78–89, Jan. 2018, doi: 10.1021/ACSBIOMATERIALS.7B00417.

[66] M. Haddrick and P. B. Simpson, "Organ-on-a-chip technology: turning its potential for clinical benefit into reality," *Drug Discov Today*, vol. 24, no. 5, pp. 1217–1223, May 2019, doi: 10.1016/J.DRUDIS.2019.03.011.

[67] D. H. T. Nguyen *et al.*, "Biomimetic model to reconstitute angiogenic sprouting morphogenesis in vitro," *Proc Natl Acad Sci U S A*, vol. 110, no. 17, pp. 6712–6717, Apr. 2013, doi: 10.1073/PNAS.1221526110.

[68] K. J. Jang, H. S. Cho, D. H. Kang, W. G. Bae, T. H. Kwon, and K. Y. Suh, "Fluid-shear-stress-induced translocation of aquaporin-2 and reorganization of actin cytoskeleton in renal tubular epithelial cells," *Integr Biol (Camb)*, vol. 3, no. 2, pp. 134–141, Feb. 2011, doi: 10.1039/C0IB00018C.

[69] J. Zhou, D. A. Khodakov, A. v. Ellis, and N. H. Voelcker, "Surface modification for PDMS-based microfluidic devices," *Electrophoresis*, vol. 33, no. 1, pp. 89–104, Jan. 2012, doi: 10.1002/ELPS.201100482.

[70] M. P. Tibbe, A. M. Leferink, A. van den Berg, J. C. T. Eijkel, and L. I. Segerink, "Microfluidic Gel Patterning Method by Use of a Temporary Membrane for Organ-On-Chip Applications," *Advanced Materials Technologies*, vol. 3, no. 3, Mar. 2018, doi: 10.1002/ADMT.201700200.

[71] D. Xue, Y. Wang, J. Zhang, D. Mei, Y. Wang, and S. Chen, "Projection-Based 3D Printing of Cell Patterning Scaffolds with Multiscale Channels," *ACS Appl Mater Interfaces*, vol. 10, no. 23, pp. 19428–19435, Jun. 2018, doi: 10.1021/ACSAMI.8B03867.

[72] C. F. Mandenius, "Conceptual Design of Micro-Bioreactors and Organ-on-Chips for Studies of Cell Cultures," *Bioengineering*, vol. 5, no. 3, Sep. 2018, doi: 10.3390/BIOENGINEERING5030056.

[73] J. S. Kwon and J. H. Oh, "Microfluidic Technology for Cell Manipulation," *Applied Sciences 2018, Vol. 8, Page 992*, vol. 8, no. 6, p. 992, Jun. 2018, doi: 10.3390/APP8060992.

[74] D. Huh *et al.*, "A human disease model of drug toxicity-induced pulmonary edema in a lung-on-a-chip microdevice," *Sci Transl Med*, vol. 4, no. 159, Nov. 2012, doi: 10.1126/SCITRANSLMED.3004249.

[75] S. Jalili-Firoozinezhad *et al.*, "Modeling radiation injury-induced cell death and countermeasure drug responses in a human Gut-on-a-Chip," *Cell Death Dis*, vol. 9, no. 2, Feb. 2018, doi: 10.1038/S41419-018-0304-8.

[76] B. A. Hassell *et al.*, "Human Organ Chip Models Recapitulate Orthotopic Lung Cancer Growth, Therapeutic Responses, and Tumor Dormancy In Vitro," *Cell Rep*, vol. 21, no. 2, pp. 508–516, Oct. 2017, doi: 10.1016/J.CELREP.2017.09.043.

[77] A. Ozkan, N. Ghousifam, P. J. Hoopes, T. E. Yankeelov, and M. N. Rylander, "In vitro vascularized liver and tumor tissue microenvironments on a chip for dynamic determination of nanoparticle transport and toxicity," *Biotechnol Bioeng*, vol. 116, no. 5, pp. 1201–1219, May 2019, doi: 10.1002/BIT.26919.

[78] H. J. Kim, H. Li, J. J. Collins, and D. E. Ingber, "Contributions of microbiome and mechanical deformation to intestinal bacterial overgrowth and inflammation in a human gut-on-a-chip," *Proc Natl Acad Sci U S A*, vol. 113, no. 1, pp. E7–E15, Jan. 2016, doi: 10.1073/PNAS.1522193112.

[79] M. A. Mofazzal Jahromi *et al.*, "Microfluidic Brain-on-a-Chip: Perspectives for Mimicking Neural System Disorders," *Mol Neurobiol*, vol. 56, no. 12, pp. 8489–8512, Dec. 2019, doi: 10.1007/S12035-019-01653-2.

[80] M. Shi *et al.*, "Glia co-culture with neurons in microfluidic platforms promotes the formation and stabilization of synaptic contacts," *Lab on a Chip*, vol. 13, no. 15, pp. 3008–3021, Jul. 2013, doi: 10.1039/C3LC50249J.

[81] H. J. Kim, D. Huh, G. Hamilton, and D. E. Ingber, "Human gut-on-a-chip inhabited by microbial flora that experiences intestinal peristalsis-like motions and flow," *Lab Chip*, vol. 12, no. 12, pp. 2165–2174, Jun. 2012, doi: 10.1039/C2LC40074J.

[82] K. H. Dodson, F. D. Echevarria, D. Li, R. M. Sappington, and J. F. Edd, "Retina-on-a-chip: a microfluidic platform for point access signaling studies," *Biomed Microdevices*, vol. 17, no. 6, pp. 1–10, Dec. 2015, doi: 10.1007/S10544-015-0019-X.

[83] D. Bennet, Z. Estlack, T. Reid, and J. Kim, "A microengineered human corneal epithelium-on-a-chip for eye drops mass transport evaluation," *Lab on a Chip*, vol. 18, no. 11, pp. 1539–1551, May 2018, doi: 10.1039/C8LC00158H.

[84] M. Wufuer *et al.*, "Skin-on-a-chip model simulating inflammation, edema and drug-based treatment," *Scientific Reports 2016 6:1*, vol. 6, no. 1, pp. 1–12, Nov. 2016, doi: 10.1038/srep37471.

[85] Q. Ramadan and F. C. W. Ting, "In vitro micro-physiological immune-competent model of the human skin," *Lab on a Chip*, vol. 16, no. 10, pp. 1899–1908, May 2016, doi: 10.1039/C6LC00229C.

[86] D. T. T. Phan *et al.*, "A vascularized and perfused organ-on-a-chip platform for large-scale drug screening applications," *Lab on a Chip*, vol. 17, no. 3, pp. 511–520, Jan. 2017, doi: 10.1039/C6LC01422D.

[87] J. Park, B. K. Lee, G. S. Jeong, J. K. Hyun, C. J. Lee, and S. H. Lee, "Three-dimensional brain-on-a-chip with an interstitial level of flow and its application as an in vitro model of Alzheimer's disease," *Lab on a Chip*, vol. 15, no. 1, pp. 141–150, Jan. 2015, doi: 10.1039/C4LC00962B.

[88] B. M. Maoz *et al.*, "A linked organ-on-chip model of the human neurovascular unit reveals the metabolic coupling of endothelial and neuronal cells," *Nat Biotechnol*, vol. 36, no. 9, pp. 865–877, Oct. 2018, doi: 10.1038/NBT.4226.

[89] A. Herland, A. D. van der Meer, E. A. FitzGerald, T. E. Park, J. J. F. Sleeboom, and D. E. Ingber, "Distinct Contributions of Astrocytes and Pericytes to Neuroinflammation Identified in a 3D Human Blood-Brain Barrier on a Chip," *PLOS ONE*, vol. 11, no. 3, p. e0150360, Mar. 2016, doi: 10.1371/JOURNAL.PONE.0150360.

[90] J. A. Brown *et al.*, "Recreating blood-brain barrier physiology and structure on chip: A novel neurovascular microfluidic bioreactor," *Biomicrofluidics*, vol. 9, no. 5, Sep. 2015, doi: 10.1063/1.4934713.

[91] S. P. Deosarkar, B. Prabhakarpandian, B. Wang, J. B. Sheffield, B. Krynska, and M. F. Kiani, "A Novel Dynamic Neonatal Blood-Brain Barrier on a Chip," *PLOS ONE*, vol. 10, no. 11, p. e0142725, Nov. 2015, doi: 10.1371/JOURNAL.PONE.0142725.

[92] X. Yang *et al.*, "Nanofiber membrane supported lung-on-a-chip microdevice for anti-cancer drug testing," *Lab on a Chip*, vol. 18, no. 3, pp. 486–495, Jan. 2018, doi: 10.1039/C7LC01224A.

[93] D. Bovard *et al.*, "A lung/liver-on-a-chip platform for acute and chronic toxicity studies," *Lab Chip*, vol. 18, no. 24, pp. 3814–3829, Dec. 2018, doi: 10.1039/C8LC01029C.

[94] C. H. Beckwitt *et al.*, "Liver 'organ on a chip,'" *Exp Cell Res*, vol. 363, no. 1, pp. 15–25, Feb. 2018, doi: 10.1016/J.YEXCR.2017.12.023.

[95] E. M. Materne, A. G. Tonevitsky, and U. Marx, "Chip-based liver equivalents for toxicity testing – organotypicalness versus cost-efficient high throughput," *Lab on a Chip*, vol. 13, no. 18, pp. 3481–3495, Aug. 2013, doi: 10.1039/C3LC50240F.

[96] M. Jang, I. Koh, S. J. Lee, J. H. Cheong, and P. Kim, "Droplet-based microtumor model to assess cell-ECM interactions and drug resistance of gastric cancer cells," *Sci Rep*, vol. 7, Jan. 2017, doi: 10.1038/SREP41541.

[97] M. J. Wilmer, C. P. Ng, H. L. Lanz, P. Vulto, L. Suter-Dick, and R. Masereeuw, "Kidney-on-a-Chip Technology for Drug-Induced Nephrotoxicity Screening," *Trends Biotechnol*, vol. 34, no. 2, pp. 156–170, 2016, doi: 10.1016/J.TIBTECH.2015.11.001.

[98] N. Huebsch *et al.*, "Miniaturized iPS-Cell-Derived Cardiac Muscles for Physiologically Relevant Drug Response Analyses," *Scientific Reports 2016 6:1*, vol. 6, no. 1, pp. 1–12, Apr. 2016, doi: 10.1038/srep24726.

[99] A. G. Sciancalepore, F. Sallustio, S. Girardo, L. Gioia Passione, and A. Camposeo, "Correction: A Bioartificial Renal Tubule Device Embedding Human Renal Stem/Progenitor Cells," *PLOS ONE*, vol. 9, no. 6, p. e100141, Jun. 2014, doi: 10.1371/JOURNAL.PONE.0100141.

[100] A. Aung *et al.*, "3D cardiac μtissues within a microfluidic device with real-time contractile stress readout," *Lab Chip*, vol. 16, no. 1, pp. 153–162, 2016, doi: 10.1039/C5LC00820D.

[101] S. J. Hachey and C. C. W. Hughes, "Applications of tumor chip technology," *Lab Chip*, vol. 18, no. 19, pp. 2893–2912, Oct. 2018, doi: 10.1039/C8LC00330K.

[102] H. F. Tsai, A. Trubelja, A. Q. Shen, and G. Bao, "Tumour-on-a-chip: microfluidic models of tumour morphology, growth and microenvironment," *J R Soc Interface*, vol. 14, no. 131, Jun. 2017, doi: 10.1098/RSIF.2017.0137.

[103] W. Sun *et al.*, "Organ-on-a-Chip for Cancer and Immune Organs Modeling," *Adv Healthc Mater*, vol. 8, no. 4, Feb. 2019, doi: 10.1002/ADHM.201801363.

[104] M. Shang, R. H. Soon, C. T. Lim, B. L. Khoo, and J. Han, "Microfluidic modelling of the tumor microenvironment for anti-cancer drug development," *Lab Chip*, vol. 19, no. 3, pp. 369–386, Feb. 2019, doi: 10.1039/C8LC00970H.

[105] N. Kashaninejad *et al.*, "Organ-Tumor-on-a-Chip for Chemosensitivity Assay: A Critical Review," *Micromachines (Basel)*, vol. 7, no. 8, Jul. 2016, doi: 10.3390/MI7080130.

[106] Y. Wang, F. Cuzzucoli, A. Escobar, S. Lu, L. Liang, and S. Wang, "Tumor-on-a-chip platforms for assessing nanoparticle-based cancer therapy," *Nanotechnology*, vol. 29, no. 33, Jun. 2018, doi: 10.1088/1361-6528/AAC7A4.

[107] D. Caballero, S. Kaushik, V. M. Correlo, J. M. Oliveira, R. L. Reis, and S. C. Kundu, "Organ-on-chip models of cancer metastasis for future personalized medicine: From chip to the patient," *Biomaterials*, vol. 149, pp. 98–115, Dec. 2017, doi: 10.1016/J.BIOMATERIALS.2017.10.005.

[108] J. Y. Kim *et al.*, "3D spherical microtissues and microfluidic technology for multi-tissue experiments and analysis," *J Biotechnol*, vol. 205, pp. 24–35, Jul. 2015, doi: 10.1016/J.JBIOTEC.2015.01.003.

[109] A. van den Berg, C. L. Mummery, R. Passier, and A. D. van der Meer, "Personalised organs-on-chips: functional testing for precision medicine," *Lab on a Chip*, vol. 19, no. 2, pp. 198–205, Jan. 2019, doi: 10.1039/C8LC00827B.

[110] R. Portillo-Lara and N. Annabi, "Microengineered cancer-on-a-chip platforms to study the metastatic microenvironment," *Lab Chip*, vol. 16, no. 21, pp. 4063–4081, 2016, doi: 10.1039/C6LC00718J.

[111] M. A. Swartz *et al.*, "Tumor microenvironment complexity: emerging roles in cancer therapy," *Cancer Res*, vol. 72, no. 10, pp. 2473–2480, May 2012, doi: 10.1158/0008-5472.CAN-12-0122.

[112] M. Wang *et al.*, "Role of tumor microenvironment in tumorigenesis," *J Cancer*, vol. 8, no. 5, p. 761, 2017, doi: 10.7150/JCA.17648.

[113] M. Romero-López *et al.*, "Recapitulating the human tumor microenvironment: Colon tumor-derived extracellular matrix promotes angiogenesis and tumor cell growth," *Biomaterials*, vol. 116, pp. 118–129, Feb. 2017, doi: 10.1016/J.BIOMATERIALS.2016.11.034.

[114] S. J. Hachey and C. C. W. Hughes, "Applications of tumor chip technology," *Lab Chip*, vol. 18, no. 19, pp. 2893–2912, Oct. 2018, doi: 10.1039/C8LC00330K.

[115] L. Wan, C. A. Neumann, and P. R. Leduc, "Tumor-on-a-chip for integrating a 3D tumor microenvironment: chemical and mechanical factors," *Lab Chip*, vol. 20, no. 5, pp. 873–888, Mar. 2020, doi: 10.1039/C9LC00550A.

[116] Y. A. Chen *et al.*, "Generation of oxygen gradients in microfluidic devices for cell culture using spatially confined chemical reactions," *Lab Chip*, vol. 11, no. 21, pp. 3626–3633, Nov. 2011, doi: 10.1039/C1LC20325H.

[117] M. D. Brennan, M. L. Rexius-Hall, L. J. Elgass, and D. T. Eddington, "Oxygen control with microfluidics," *Lab Chip*, vol. 14, no. 22, pp. 4305–4318, Nov. 2014, doi: 10.1039/C4LC00853G.

[118] N. Bhattacharjee, A. Urrios, S. Kang, and A. Folch, "The upcoming 3D-printing revolution in microfluidics," *Lab on a Chip*, vol. 16, no. 10, pp. 1720–1742, May 2016, doi: 10.1039/C6LC00163G.

[119] W. Aljohani, M. W. Ullah, X. Zhang, and G. Yang, "Bioprinting and its applications in tissue engineering and regenerative medicine," *Int J Biol Macromol*, vol. 107, no. Pt A, pp. 261–275, Feb. 2018, doi: 10.1016/J.IJBIOMAC.2017.08.171.

[120] A. v. Nielsen, M. J. Beauchamp, G. P. Nordin, and A. T. Woolley, "3D Printed Microfluidics," *Annu Rev Anal Chem (Palo Alto Calif)*, vol. 13, no. 1, pp. 45–65, Jun. 2020, doi: 10.1146/ANNUREV-ANCHEM-091619-102649.

[121] A. A. Yazdi, A. Popma, W. Wong, T. Nguyen, Y. Pan, and J. Xu, "3D printing: an emerging tool for novel microfluidics and lab-on-a-chip applications," *Microfluidics and Nanofluidics 2016 20:3*, vol. 20, no. 3, pp. 1–18, Feb. 2016, doi: 10.1007/S10404-016-1715-4.

[122] S. v. Murphy and A. Atala, "3D bioprinting of tissues and organs," *Nature Biotechnology 2014 32:8*, vol. 32, no. 8, pp. 773–785, Aug. 2014, doi: 10.1038/nbt.2958.

[123] J. W. Stansbury and M. J. Idacavage, "3D printing with polymers: Challenges among expanding options and opportunities," *Dent Mater*, vol. 32, no. 1, pp. 54–64, Jan. 2016, doi: 10.1016/J.DENTAL.2015.09.018.

[124] J. Jang, H. G. Yi, and D. W. Cho, "3D Printed Tissue Models: Present and Future," *ACS Biomaterials Science and Engineering*, vol. 2, no. 10, pp. 1722–1731, Oct. 2016, doi: 10.1021/ACSBIOMATERIALS.6B00129/ASSET/IMAGES/LARGE/AB-2016-00129N_0004.JPEG.

[125] "(PDF) Development of a Capillary-driven, Microfluidic, Nucleic Acid Biosensor." https://www.researchgate.net/publication/288818484_Development_of_a_Capillary-driven_Microfluidic_Nucleic_Acid_Biosensor (accessed May 11, 2022).

[126] S. H. Ng, R. T. Tjeung, and Z. Wang, "Hot embossing on polymethyl methacrylate," *Proceedings of the Electronic Packaging Technology Conference, EPTC*, pp. 615–621, 2006, doi: 10.1109/EPTC.2006.342784.

[127] L. J. Kricka, P. Fortina, N. J. Panaro, P. Wilding, G. Alonso-Amigo, and H. Becker, "Fabrication of plastic microchips by hot embossing," *Lab on a Chip*, vol. 2, no. 1, pp. 1–4, Feb. 2002, doi: 10.1039/B109775J.

[128] H. Becker and U. Heim, "Hot embossing as a method for the fabrication of polymer high aspect ratio structures," *Sensors and Actuators A: Physical*, vol. 83, no. 1–3, pp. 130–135, May 2000, doi: 10.1016/S0924-4247(00)00296-X.

[129] C. S. Chen, S. C. Chen, W. H. Liao, R. der Chien, and S. H. Lin, "Micro injection moulding of a micro-fluidic platform," *International Communications in Heat and Mass Transfer*, vol. 37, no. 9, pp. 1290–1294, Nov. 2010, doi: 10.1016/J.ICHEATMASSTRANSFER.2010.06.032.

[130] Y. C. Su, J. Shah, and L. Lin, "Implementation and analysis of polymeric microstructure replication by micro injection moulding," *Journal of Micromechanics and Microengineering*, vol. 14, no. 3, p. 415, Dec. 2003, doi: 10.1088/0960-1317/14/3/015.

[131] Y. Lee *et al.*, "Microfluidics within a well: an injection-molded plastic array 3D culture platform," *Lab on a Chip*, vol. 18, no. 16, pp. 2433–2440, Aug. 2018, doi: 10.1039/C8LC00336J.

[132] D. B. Weibel, W. R. DiLuzio, and G. M. Whitesides, "Microfabrication meets microbiology," *Nature Reviews Microbiology 2007 5:3*, vol. 5, no. 3, pp. 209–218, Mar. 2007, doi: 10.1038/nrmicro1616.

[133] E. Ferrari, F. Nebuloni, M. Rasponi, and P. Occhetta, "Photo and Soft Lithography for Organ-on-Chip Applications," *Methods Mol Biol*, vol. 2373, pp. 1–19, 2022, doi: 10.1007/978-1-0716-1693-2_1.

[134] O. Kilic *et al.*, "Brain-on-a-chip model enables analysis of human neuronal differentiation and chemotaxis," *Lab Chip*, vol. 16, no. 21, pp. 4152–4162, 2016, doi: 10.1039/C6LC00946H.

[135] R. Paoli and J. Samitier, "Mimicking the Kidney: A Key Role in Organ-on-Chip Development," *Micromachines (Basel)*, vol. 7, no. 7, Jul. 2016, doi: 10.3390/MI7070126.

[136] A. Choe, S. K. Ha, I. Choi, N. Choi, and J. H. Sung, "Microfluidic Gut-liver chip for reproducing the first pass metabolism," *Biomed Microdevices*, vol. 19, no. 1, Mar. 2017, doi: 10.1007/S10544-016-0143-2.

[137] S. Torino, B. Corrado, M. Iodice, and G. Coppola, "PDMS-Based Microfluidic Devices for Cell Culture," *Inventions 2018, Vol. 3, Page 65*, vol. 3, no. 3, p. 65, Sep. 2018, doi: 10.3390/INVENTIONS3030065.

[138] K. Raj M and S. Chakraborty, "PDMS microfluidics: A mini review," *Journal of Applied Polymer Science*, vol. 137, no. 27, p. 48958, Jul. 2020, doi: 10.1002/APP.48958.

[139] S. B. Campbell, Q. Wu, J. Yazbeck, C. Liu, S. Okhovatian, and M. Radisic, "Beyond Polydimethylsiloxane: Alternative Materials for Fabrication of Organ-on-a-Chip Devices and Microphysiological Systems," *ACS Biomaterials Science and Engineering*, vol. 7, no. 7, pp. 2880–2899, Jul. 2021, doi: 10.1021/ACSBIOMATERIALS.0C00640/ASSET/IMAGES/MEDIUM/AB0C00640_0008.GIF.

[140] J. Zhou, A. V. Ellis, and N. H. Voelcker, "Recent developments in PDMS surface modification for microfluidic devices," *Electrophoresis*, vol. 31, no. 1, pp. 2–16, Jan. 2010, doi: 10.1002/ELPS.200900475.

[141] E. Holczer and P. Fürjes, "Effects of embedded surfactants on the surface properties of PDMS; applicability for autonomous microfluidic systems," *Microfluidics and Nanofluidics 2017 21:5*, vol. 21, no. 5, pp. 1–14, Apr. 2017, doi: 10.1007/S10404-017-1916-5.

[142] G. T. Roman and C. T. Culbertson, "Surface engineering of poly(dimethylsiloxane) microfluidic devices using transition metal sol-gel chemistry," *Langmuir*, vol. 22, no. 9, pp. 4445–4451, Apr. 2006, doi: 10.1021/LA053085W.

[143] W. H. Chin and J. J. Barr, "Phage research in 'organ-on-chip' devices," *Microbiol Aust*, vol. 40, no. 1, pp. 28–32, 2019, doi: 10.1071/MA19006.

[144] K. T. L. Trinh, D. A. Thai, W. R. Chae, and N. Y. Lee, "Rapid Fabrication of Poly(methyl methacrylate) Devices for Lab-ona-Chip Applications Using Acetic Acid and UV Treatment," *ACS Omega*, vol. 5, no. 28, pp. 17396–17404, Jul. 2020, doi: 10.1021/ACSOMEGA.0C01770/SUPPL_FILE/AO0C01770_SI_001.PDF.

[145] H. Becker and C. Gärtner, "Polymer microfabrication technologies for microfluidic systems," *Analytical and Bioanalytical Chemistry 2007 390:1*, vol. 390, no. 1, pp. 89–111, Nov. 2007, doi: 10.1007/S00216-007-1692-2.

[146] H. Becker and C. Gärtner, "Polymer microfabrication technologies for microfluidic systems," *Analytical and Bioanalytical Chemistry*, vol. 390, no. 1, pp. 89–111, Jan. 2008, doi: 10.1007/S00216-007-1692-2.

[147] K. Ren, J. Zhou, and H. Wu, "Materials for microfluidic chip fabrication," *Accounts of Chemical Research*, vol. 46, no. 11, pp. 2396–2406, Nov. 2013, doi: 10.1021/AR300314S/ASSET/IMAGES/MEDIUM/AR-2012-00314S_0007.GIF.

[148] B. Giri, "Laboratory methods in microfluidics," *Laboratory Methods in Microfluidics*, pp. 1–178, May 2017.

[149] C. Iliescu, H. Taylor, M. Avram, J. Miao, and S. Franssila, "A practical guide for the fabrication of microfluidic devices using glass and silicon," *Biomicrofluidics*, vol. 6, no. 1, p. 016505, Mar. 2012, doi: 10.1063/1.3689939.

[150] M. R. Haq *et al.*, "Fabrication of all glass microfluidic device with superior chemical and mechanical resistances by glass moulding with vitreous carbon mold," *JMiMi*, vol. 29, no. 7, p. 075010, May 2019, doi: 10.1088/1361-6439/AB1F99.

[151] R. O. Rodrigues, R. Lima, H. T. Gomes, and A. M. T. Silva, "Polymer microfluidic devices: an overview of fabrication methods," *U.Porto Journal of Engineering*, vol. 1, no. 1, pp. 67–79, Oct. 2015, doi: 10.24840/2183-6493_001.001_0007.

[152] X. Zhang, L. Li, and C. Luo, "Gel integration for microfluidic applications," *Lab Chip*, vol. 16, no. 10, pp. 1757–1776, 2016, doi: 10.1039/C6LC00247A.

[153] N. Y. C. Lin *et al.*, "Renal reabsorption in 3D vascularized proximal tubule models," *Proc Natl Acad Sci U S A*, vol. 116, no. 12, pp. 5399–5404, 2019, doi: 10.1073/PNAS.1815208116/-/DCSUPPLEMENTAL.

[154] M. E. Sakalem, M. T. de Sibio, F. A. da S. da Costa, and M. de Oliveira, "Historical evolution of spheroids and organoids, and possibilities of use in life sciences and medicine," *Biotechnology Journal*, vol. 16, no. 5, May 2021, doi: 10.1002/BIOT.202000463.

[155] Y. Fang and R. M. Eglen, "Three-Dimensional Cell Cultures in Drug Discovery and Development," *Slas Discovery*, vol. 22, no. 5, p. 456, Jun. 2017, doi: 10.1177/1087057117696795.

[156] V. Velasco, S. A. Shariati, and R. Esfandyarpour, "Microtechnology-based methods for organoid models," *Microsystems & Nanoengineering 2020 6:1*, vol. 6, no. 1, pp. 1–13, Oct. 2020, doi: 10.1038/s41378-020-00185-3.

[157] M. Kasendra *et al.*, "Development of a primary human Small Intestine-on-a-Chip using biopsy-derived organoids," *Scientific Reports 2018 8:1*, vol. 8, no. 1, pp. 1–14, Feb. 2018, doi: 10.1038/s41598-018-21201-7.

[158] S. Swaminathan, Q. Hamid, W. Sun, and A. M. Clyne, "Bioprinting of 3D breast epithelial spheroids for human cancer models," *Biofabrication*, vol. 11, no. 2, 2019, doi: 10.1088/1758-5090/AAFC49.

[159] S. Sant and P. A. Johnston, "The production of 3D tumor spheroids for cancer drug discovery," *Drug Discov Today Technol*, vol. 23, pp. 27–36, Mar. 2017, doi: 10.1016/J.DDTEC.2017.03.002.

[160] A. S. Nunes, A. S. Barros, E. C. Costa, A. F. Moreira, and I. J. Correia, "3D tumor spheroids as in vitro models to mimic in vivo human solid tumors resistance to therapeutic drugs," *Biotechnol Bioeng*, vol. 116, no. 1, pp. 206–226, Jan. 2019, doi: 10.1002/BIT.26845.

[161] B. Patra, C. C. Peng, W. H. Liao, C. H. Lee, and Y. C. Tung, "Drug testing and flow cytometry analysis on a large number of uniform sized tumor spheroids using a microfluidic device," *Scientific Reports 2016 6:1*, vol. 6, no. 1, pp. 1–12, Feb. 2016, doi: 10.1038/srep21061.

[162] M. Rothbauer, H. Zirath, and P. Ertl, "Recent advances in microfluidic technologies for cell-to-cell interaction studies," *Lab on a Chip*, vol. 18, no. 2, pp. 249–270, Jan. 2018, doi: 10.1039/C7LC00815E.

[163] L. B. Weiswald, D. Bellet, and V. Dangles-Marie, "Spherical cancer models in tumor biology," *Neoplasia*, vol. 17, no. 1, pp. 1–15, Jan. 2015, doi: 10.1016/J.NEO.2014.12.004.

[164] A. Jain *et al.*, "Primary Human Lung Alveolus-on-a-chip Model of Intravascular Thrombosis for Assessment of Therapeutics," *Clin Pharmacol Ther*, vol. 103, no. 2, pp. 332–340, Feb. 2018, doi: 10.1002/CPT.742.

[165] D. Bovard *et al.*, "A lung/liver-on-a-chip platform for acute and chronic toxicity studies," *Lab Chip*, vol. 18, no. 24, pp. 3814–3829, Dec. 2018, doi: 10.1039/C8LC01029C.

[166] B. A. Hassell *et al.*, "Human Organ Chip Models Recapitulate Orthotopic Lung Cancer Growth, Therapeutic Responses, and Tumor Dormancy In Vitro," *Cell Rep*, vol. 21, no. 2, pp. 508–516, Oct. 2017, doi: 10.1016/J.CELREP.2017.09.043.

[167] M. R. Carvalho *et al.*, "Colorectal tumor-on-a-chip system: A 3D tool for precision onco-nanomedicine," *Sci Adv*, vol. 5, no. 5, 2019, doi: 10.1126/SCIADV.AAW1317.

[168] H. Jiang *et al.*, "Targeting focal adhesion kinase renders pancreatic cancers responsive to checkpoint immunotherapy," *Nat Med*, vol. 22, no. 8, pp. 851–860, Aug. 2016, doi: 10.1038/NM.4123.

[169] A. Nishiguchi *et al.*, "In vitro 3D blood/lymph-vascularized human stromal tissues for preclinical assays of cancer metastasis," *Biomaterials*, vol. 179, pp. 144–155, Oct. 2018, doi: 10.1016/J.BIOMATERIALS.2018.06.019.

[170] M. R. Haque, C. R. Wessel, D. D. Leary, C. Wang, A. Bhushan, and F. Bishehsari, "Patient-derived pancreatic cancer-on-a-chip recapitulates the tumor microenvironment," *Microsystems & Nanoengineering 2022 8:1*, vol. 8, no. 1, pp. 1–13, Mar. 2022, doi: 10.1038/s41378-022-00370-6.

[171] J. Deng *et al.*, "Engineered Liver-On-A-Chip Platform to Mimic Liver Functions and Its Biomedical Applications: A Review," *Micromachines (Basel)*, vol. 10, no. 10, Oct. 2019, doi: 10.3390/MI10100676.

[172] N. Kashaninejad *et al.*, "Organ-Tumor-on-a-Chip for Chemosensitivity Assay: A Critical Review," vol. 7, no. 8, p. 130, Jul. 2016, doi: 10.3390/MI7080130.

[173] J. Deng *et al.*, "A liver-on-a-chip for hepatoprotective activity assessment," *Biomicrofluidics*, vol. 14, no. 6, Nov. 2020, doi: 10.1063/5.0024767.

[174] Y. Fan, D. T. Nguyen, Y. Akay, F. Xu, and M. Akay, "Engineering a Brain Cancer Chip for High-throughput Drug Screening," *Sci Rep*, vol. 6, May 2016, doi: 10.1038/SREP25062.

[175] J. Saliba, A. Daou, S. Damiati, J. Saliba, M. El-Sabban, and R. Mhanna, "Development of Microplatforms to Mimic the In Vivo Architecture of CNS and PNS Physiology and Their Diseases," *Genes 2018, Vol. 9, Page 285*, vol. 9, no. 6, p. 285, Jun. 2018, doi: 10.3390/GENES9060285.

[176] Y. Fan, D. T. Nguyen, Y. Akay, F. Xu, and M. Akay, "Engineering a Brain Cancer Chip for High-throughput Drug Screening," *Sci Rep*, vol. 6, May 2016, doi: 10.1038/SREP25062.

[177] S. Hao *et al.*, "A Spontaneous 3D Bone-On-a-Chip for Bone Metastasis Study of Breast Cancer Cells," *Small*, vol. 14, no. 12, Mar. 2018, doi: 10.1002/SMLL.201702787.

[178] P. Boyle, "Triple-negative breast cancer: epidemiological considerations and recommendations," *Ann Oncol*, vol. 23 Suppl 6, no. SUPPL. 6, 2012, doi: 10.1093/ANNONC/MDS187.

[179] "Tumor-on-a-chip to study breast cancer with microfluidics : MTOAC." https://www.elveflow.com/microfluidics-research-horizon-europe/european-projects/organ-chip-multi-compartmental-tumor-chip-study-breast-cancer-mtoac-project/ (accessed May 14, 2022).

[180] J. Aleman and A. Skardal, "A multi-site metastasis-on-a-chip microphysiological system for assessing metastatic preference of cancer cells," *Biotechnol Bioeng*, vol. 116, no. 4, pp. 936–944, Apr. 2019, doi: 10.1002/BIT.26871.

[181] Y. C. Toh, A. Raja, H. Yu, and D. van Noort, "A 3D Microfluidic Model to Recapitulate Cancer Cell Migration and Invasion," *Bioengineering (Basel)*, vol. 5, no. 2, Jun. 2018, doi: 10.3390/BIOENGINEERING5020029.

[182] A. Skardal, M. Devarasetty, S. Forsythe, A. Atala, and S. Soker, "A reductionist metastasis-on-a-chip platform for in vitro tumor progression modeling and drug screening," *Biotechnol Bioeng*, vol. 113, no. 9, pp. 2020–2032, Sep. 2016, doi: 10.1002/BIT.25950.

[183] Y. Wang *et al.*, "Metastasis-on-a-chip mimicking the progression of kidney cancer in the liver for predicting treatment efficacy," *Theranostics*, vol. 10, no. 1, p. 300, 2020, doi: 10.7150/THNO.38736.

[184] A. van de Stolpe and J. den Toonder, "Workshop meeting report Organs-on-Chips: Human disease models," *Lab on a Chip*, vol. 13, no. 18, pp. 3449–3470, Sep. 2013, doi: 10.1039/C3LC50248A.

[185] C. Y. Yang, L. Y. Huang, T. L. Shen, and J. Andrew Yeh, "Cell adhesion, morphology and biochemistry on nano-topographic oxidized silicon surfaces," *Eur Cell Mater*, vol. 20, pp. 415–430, 2010, doi: 10.22203/ECM.V020A34.

[186] A. Ranella, M. Barberoglou, S. Bakogianni, C. Fotakis, and E. Stratakis, "Tuning cell adhesion by controlling the roughness and wettability of 3D micro/nano silicon structures," *Acta Biomaterialia*, vol. 6, no. 7, pp. 2711–2720, 2010, doi: 10.1016/J.ACTBIO.2010.01.016.

[187] "3D Cell Culture for Biological-Relevant, Neuroscientific, In Vitro Environments - Advanced Science News." https://www.advancedsciencenews.com/3d-cell-culture-towards-realistic-biological-environments-cell-culture/ (accessed May 07, 2022).

[188] "File:Extruder lemio.svg - RepRap." https://reprap.org/wiki/File:Extruder_lemio.svg (accessed May 08, 2022).

[189] "File:Polylactides Formulae V.1.svg - Wikimedia Commons." https://commons.wikimedia.org/wiki/File:Polylactides_Formulae_V.1.svg (accessed May 08, 2022).

[190] A. K. van der (Anne K. Vegt and L. E. (Leonard E. Govaert, *Polymeren : van keten tot kunststof*, 5e dr. Delft: DUP Blue Print, 2003.

[191] N. Baydogan and F. Gul, "Synthesis of Poly (methyl methacrylate) with borax Decahydrate Addition for Energy Applications," Oct. 2020, doi: 10.5281 /zenodo.4084573.

[192] "Polydimethylsiloxane - American Chemical Society." https://www.acs.org/content/acs/en/molecule-of-the-week/archive/p/polydimethylsiloxane.html (accessed May 12, 2022).

[193] Y. Lee *et al.*, "Microfluidics within a well: an injection-molded plastic array 3D culture platform," *Lab on a Chip*, vol. 18, no. 16, pp. 2433–2440, Aug. 2018, doi: 10.1039/C8LC00336J.

[194] "Organ-on-a-Chip | Cell Cultivation / Imaging / Analysis / Preservation | Life Science | KYODO INTERNATIONAL INC. /Japan." https://www.kyodo-inc.co.jp/english/bio/cell_cultivation/organ/index.html (accessed May 12, 2022).

[195] I. A. Carrete *et al.*, "Failure Analysis of Additively Manufactured Polyester Test Specimens Exposed to Various Liquid Media," *Journal of Failure Analysis and Prevention*, vol. 19, no. 2, pp. 418–430, Apr. 2019, doi: 10.1007/S11668-019-00614-0/FIGURES/19.

ANNEX A. PLANIFICATION

1. *INITIAL PLANIFICATION*

	Task Name	Duration	Start	ETA
1	Complete project execution	114 days	07.02.22	31.05.22
2	Research	21 days	07.02.22	28.02.22
3	Organ-on-a-chip / Tumor-on-a-chip bibliography study	14 days	07.02.22	21.02.22
4	Comercial filaments research	7 days	21.02.22	28.02.22
5	Design of the models	31 days	28.02.22	31.03.22
6	Fabrication	20 days	31.03.22	20.04.22
7	Calibration of printing parameters	7 days	31.03.22	07.04.22
8	Printing of the models	13 days	07.04.22	20.04.22
9	Testing	18 days	20.04.22	07.05.22
10	Model testing: resistance	7 days	20.04.22	27.04.22
11	Model testing: watertightness	11 days	27.04.22	07.05.22
12	Report development	24 days	07.05.22	31.05.22

Figure 50. Tasks to be developed.

This section of the appendix provides a preliminary outline for structuring the tasks to be completed throughout the project (see *Figure 50*). There will be five major sections: project inspiration research, device design, device fabrication, resistance and watertightness testing, and report writing. The complete Gantt chart is shown in *Figure 52* This plan will be revised and expanded after the conclusion of the project so that it precisely reflects the actual tasks performed.

2. *REAL PLANIFICATION*

	Task Name	Duration	Start	ETA
1	Complete project execution	112 days	07.02.22	29.05.22
2	Research	20 days	07.02.22	27.02.22
3	Organ-on-a-chip / Tumor-on-a-chip bibliography study	7 days	07.02.22	14.02.22
4	State of the art conceptualitzation	5 days	14.02.22	19.02.22
5	Training in FFF	3 days	19.02.22	22.02.22
6	Filament tryouts	5 days	22.02.22	27.02.22
7	Design, manufacture and testing	51 days	28.02.22	20.04.22
8	Model design	7 days	28.02.22	07.03.22
9	Printing batch of models	5 day	07.03.22	12.03.22
10	Model testing 1 (resistance)	1 day	12.03.22	13.03.22
11	Model redesign	7 days	13.03.22	20.03.22
12	Printing batch of models	5 days	20.03.22	25.03.22
13	Model testing 2 (resistance)	1 day	25.03.22	26.03.22
14	Mounting equipment	1 day	26.03.22	27.03.22
15	Sealing of the chips and connections (hot glue)	1 day	27.03.22	28.03.22
16	Test for watertight quality 1	1 day	28.03.22	29.03.22
17	Sealing of the chips and connections (silicone)	1 day	29.03.22	30.03.22
18	Test for watertight quality 2	1 day	30.03.22	31.03.22
19	Sealing of the chips and connections (chloroform)	2 days	31.03.22	02.04.22
20	Test for watertight quality 3	1 day	02.04.22	03.04.22
21	Design of non fundamental adapters and model variations	7 days	03.04.22	10.04.22
22	Printing batch of models	2 days	10.04.22	12.04.22
23	PMMA chip covers manufacture	5 days	12.04.22	17.04.22
24	PMMA chip covers testing	1 day	17.04.22	18.04.22
25	Final model testing (resistance + watertight quality)	2 days	18.04.22	20.04.22
26	Report development	38 days	21.04.22	29.05.22
27	Previos concepts	3 days	21.04.22	24.04.22
28	State of the art	10 days	24.04.22	04.05.22
29	Hipothesis + objectives	1 day	04.05.22	05.05.22
30	Materials and methods	5 days	05.05.22	10.05.22
31	Results	1 day	10.05.22	11.05.22
32	Discussion	1 day	11.05.22	12.05.22
33	Conclusion	1 day	12.05.22	13.05.22
34	Annexes	7 days	13.05.22	20.05.22
35	Final adaptation and revision of the bibliograpgy	3 days	20.05.22	23.05.22
36	Final revision of the document	3 days	23.05.22	26.05.22
37	Revision after tutor's evaluation	3 days	26.05.22	29.05.22

Figure 51. Developed tasks.

This section of the Annex provides a breakdown of the real tasks performed throughout the project (broken down in *Figure 51*). Despite being an approximation of actual development and not necessarily having devoted an identical number of hours per day throughout these months, the development times defined for each activity are proportional to their complexity and work volume. Thus, the project was completed by performing 33 tasks organised into 3 blocks: preliminary study; design, manufacturing, and testing; and report writing.

In many cases, it is evident that the tasks are brief and concrete, and that the tests and improvements have been developed in a cyclical manner, i.e., once a model has been

printed, the corresponding testing has been conducted; with the test results, the designs have been improved, they have been printed, and from the new designs, new tests have been developed. This approach consists of two rounds for resistance and three iterations for watertightness until a feasible model is achieved.

The duration of the study project has been extended by 112 days, from 07.02.22 to 5.29.22. As part of the project planning, we can consider the approximate printing time for each component of the basic setup:

- Breast cancer chip: 1h (12g).
- Metastasis chip: 1h 10min (19g).
- Chip cover: 10min (4g).
- Channel module (1 chip): 5h 20min (100g).
- Channel module (3 chips): 14h (290 g).
- Adapter for the channel module (required): 11min (1g).
- Individual tank: 5h 45min (126g).
- Individual tank lid: 2h (44g).
- Extended tank: 7h (190g).
- Extended tank lid: 2h 30min (65g).
- Battery enclosure: 4h (92g).
- Filter: 22 min (3g).

It should be emphasized that the printing time is dependent on the parameterization of the polymers used, mainly the infill and movement and extrusion speeds that are set. Calculated by Ultimaker, the information supplied corresponds to the amount of time and filament each piece will require. Caution In this instance, the prints have been made in a group, i.e., multiple pieces have been produced at the same time, so that the machinery does not require as frequent maintenance/revision as if they were printed individually. The complete Gantt chart is shown in *Figure 53*.

	Task Name	Duration	Start	ETA
1	Complete project execution	114 days	07.02.22	31.05.22
2	Research	21 days	07.02.22	28.02.22
3	Organ-on-a-chip / Tumor-on-a-chip bibliography study	14 days	07.02.22	21.02.22
4	Comercial filaments research	7 days	21.02.22	28.02.22
5	Design of the models	31 days	28.02.22	31.03.22
6	Fabrication	20 days	31.03.22	20.04.22
7	Calibration of printing parameters	7 days	31.03.22	07.04.22
8	Printing of the models	13 days	07.04.22	20.04.22
9	Testing	18 days	20.04.22	07.05.22
10	Model testing: resistance	7 days	20.04.22	27.04.22
11	Model testing: watertightness	11 days	27.04.22	07.05.22
12	Report development	24 days	07.05.22	31.05.22

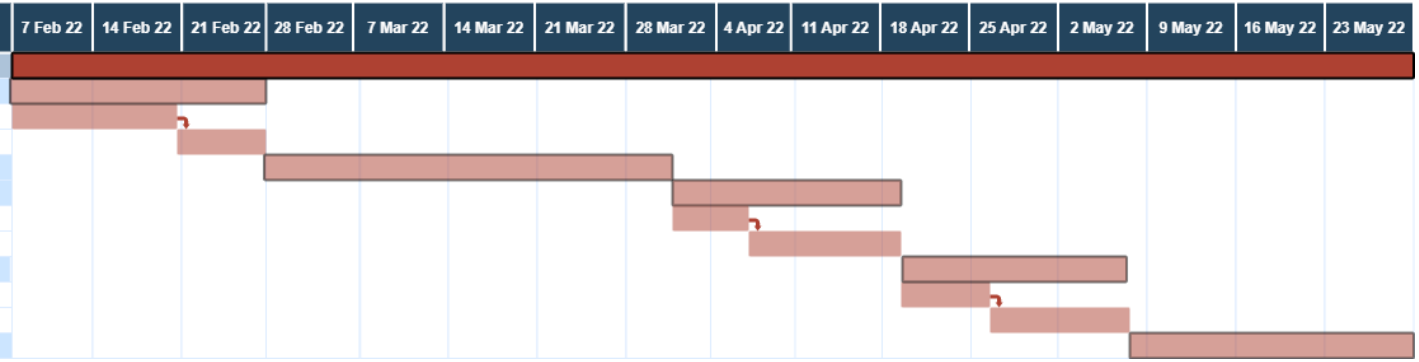

Figure 52. Initial Gantt chart.

	Task Name	Duration	Start	ETA
1	Complete project execution	112 days	07.02.22	29.05.22
2	Research	20 days	07.02.22	27.02.22
3	Organ-on-a-chip / Tumor-on-a-chip bibliography study	7 days	07.02.22	14.02.22
4	State of the art conceptualitzation	5 days	14.02.22	19.02.22
5	Training in FFF	3 days	19.02.22	22.02.22
6	Filament tryouts	5 days	22.02.22	27.02.22
7	Design, manufacture and testing	51 days	28.02.22	20.04.22
8	Model design	7 days	28.02.22	07.03.22
9	Printing batch of models	5 day	07.03.22	12.03.22
10	Model testing 1 (resistance)	1 day	12.03.22	13.03.22
11	Model redesign	7 days	13.03.22	20.03.22
12	Printing batch of models	5 days	20.03.22	25.03.22
13	Model testing 2 (resistance)	1 day	25.03.22	26.03.22
14	Mounting equipment	1 day	26.03.22	27.03.22
15	Sealing of the chips and connections (hot glue)	1 day	27.03.22	28.03.22
16	Test for watertight quality 1	1 day	28.03.22	29.03.22
17	Sealing of the chips and connections (silicone)	1 day	29.03.22	30.03.22
18	Test for watertight quality 2	1 day	30.03.22	31.03.22
19	Sealing of the chips and connections (chloroform)	2 days	31.03.22	02.04.22
20	Test for watertight quality 3	1 day	02.04.22	03.04.22
21	Design of non fundamental adapters and model variations	7 days	03.04.22	10.04.22
22	Printing batch of models	2 days	10.04.22	12.04.22
23	PMMA chip covers manufacture	5 days	12.04.22	17.04.22
24	PMMA chip covers testing	1 day	17.04.22	18.04.22
25	Final model testing (resistance + watertight quality)	2 days	18.04.22	20.04.22
26	Report development	38 days	21.04.22	29.05.22
27	Previos concepts	3 days	21.04.22	24.04.22
28	State of the art	10 days	24.04.22	04.05.22
29	Hipothesis + objectives	1 day	04.05.22	05.05.22
30	Materials and methods	5 days	05.05.22	10.05.22
31	Results	1 day	10.05.22	11.05.22
32	Discussion	1 day	11.05.22	12.05.22
33	Conclusion	1 day	12.05.22	13.05.22
34	Annexes	7 days	13.05.22	20.05.22
35	Final adaptation and revision of the bibliograpgy	3 days	20.05.22	23.05.22
36	Final revision of the document	3 days	23.05.22	26.05.22
37	Revision after tutor's evaluation	3 days	26.05.22	26.05.22

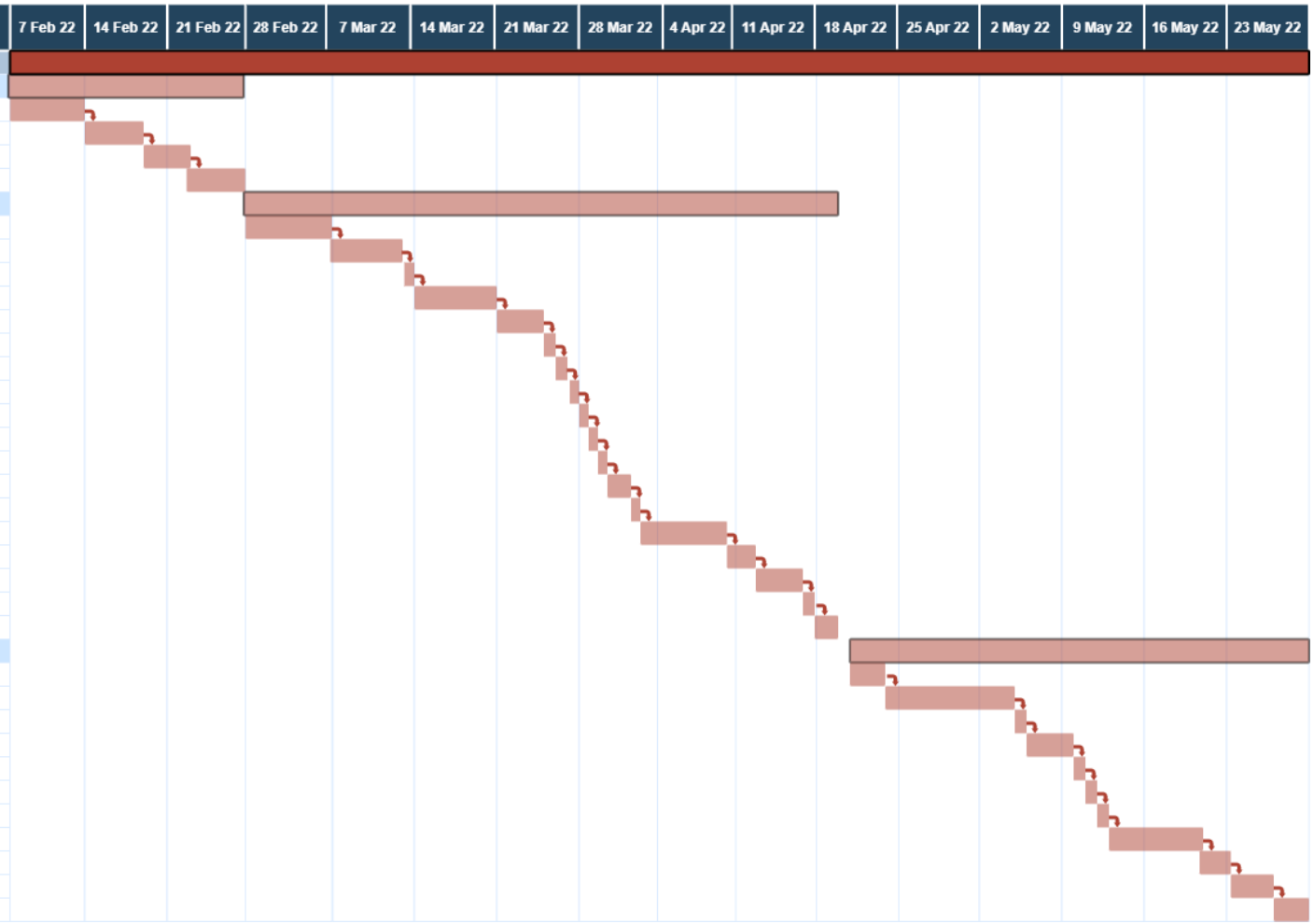

Figure 53. Final Gantt chart.

ANNEX B. SOFTWARE / PROGRAMS

When discussing the programs used to construct the project, three apps stand out:

·**AutoCAD (AutoDesk) 2022/2023**: Autodesk AutoCAD is a CAD (Computer Aided Design) application for 2D and 3D drawing. AutoCAD has a number of characteristics that distinguish it from competing tools for assisted design:

Figure 54. AutoCAD logo.

- It has fundamental geometry for two-dimensional drawing, which enables the addition of figures in layer format.
- The layering technique allows for a great deal of flexibility when working, as the parts of the piece or plan being developed are properly organised.
- Through octagonal vision and rendering, it is possible to draw in three dimensions.

This application is the ideal ally for architects, engineers, and graphic designers. There are various classes that allow the user to train to master the fundamentals of this design application, in which it is possible to create everything from simple projects and sketches to blueprints, engineering presentations, and architectural models. Logo shown in *Figure 52*.

·**AutoDesk Inventor Professional 2023:** The AutoDesk software company produces the 3D parametric solid modelling application Autodesk Inventor. Users begin by developing components that can be assembled. By modifying individual components and assemblies, numerous versions can be produced. As a parametric modeller, it is not comparable to conventional CAD software. In engineering design, Inventor is used to create and enhance new things, whereas AutoCAD drives only dimensions. A parametric modeller permits the modelling of geometry, dimension, and material in such a way that if the dimensions are changed, the geometry is automatically updated to account for the change. Unlike non-parametric modelling, which is more analogous to a "digital sketch board," this allows the designer to preserve their calculating knowledge within the model.

Figure 55. Inventor logo.

·**Ultimaker Cura:** Application for 3D printers that allows the printing parameters to be adjusted and then converted to G code. Ultimaker Cura operates by dividing a user's model file into multiple levels and creating G code for the 3D printer. When the procedure is complete, the G code is transmitted to the printer via a storage device or by connecting the printer to the programme, and the printer then creates the physical object. Logo shown in *Figure 53*.

Figure 56. Cura logo.

This open-source software is compatible with the majority of desktop 3D printers that support the most popular 3D file formats, including STL, OBJ, X3D, and 3MF, among others. Image formats including BMP, GIF, JPG, and PNG are also compatible.

·**3D Builder**: Microsoft's 3D modelling software that makes it simple to create, modify, and visualise 3D models. It is a free solution that is installed by default on all Windows 10 computers. 3D Builder facilitates 3D printing by allowing the export of models in STL, OBJ, and 3MF formats. Logo shown in *Figure 54*.

Figure 57. 3D Builder logo.

When discussing the project's coding, we can only mention the G-codes processed by Cura that provide the manufacturing instructions for each sliced model. Multiple versions of G-code, also known as RS-274, are the most extensively used programming language in numerical control. It is mostly utilised for automation and is a component of computer-aided engineering.

G-code is a language that allows people to instruct computer-controlled machine tools on what to do and how to do it. In other words, it will carry information on the printer's movements and the amount of filament it will extrude.

ANNEX C. BUDGET

COST OF THE PROJECT				
CONCEPT	DESCRIPTION	QUANTITY	COST	TOTAL
Labour	Work done by an industrial engineer / product designer	450 h	30 €/h	13.500 €
Electricity	Electricity consumed by the printer	145 h	0.235 €/h	34.1 €
FFF Printer	Artillery Genius Pro 3D filament printer	1	339.99 €/u	339.99 €
PLA Spool	1kg of PLA filament by Smart Materials	3	20.31 €/kg	60.93 €
PETG Spool	750kg of PETG filament by Smart Materials	1	30.47 €/kg	22.85 €
PCTG Spool	750g of PCTG filament by Fiberology	1	33.32 €/kg	24.99 €
TPU Spool	500g of TPU filament by Fillamentum	1	67.98 €/kg	33.99 €
Teflon tube	Capricorn Teflon tube, especially resistant to hot temperatures	1 m	13.99 €/m	13.99 €
Power bank	20.000 mA capacity battery by Posugear	1	22.99 €/u	22.99 €
Pump	Mini aquatic pump for aquaponic systems by Flintronic	1	12.99 €/u	12.99 €
Brass nozzles set	Set of 8 brass nozzles of different sizes by Durtail	1	16.99 €/u	16.99 €
Silicone tube	4mm interior/ 6mm exterior silicone tube	10 m	0.999 €/m	9.99 €
Silicone tube	10mm interior/ 15mm exterior silicone tube	2 m	6.15 €/m	12.30 €
Chloroform	Chloroform 98% EPR by Labkem	1 l	16.32 €/l	16.32 €
Brush	Precision brush by Stylex for applying chloroform to the models, size 4	3	0.99 €/u	2.97 €
Silicone	Transparent airdry silicone by Pattex, 50ml package	5	5.60 €/u	28 €
Hot glue gun	60W hot glue gun by Dweyka	1	22.99 €/u	22.99 €
Hot glue sticks	Glue sticks for the hot glue gun, by BSTHP	30	0.399 €/u	11.99 €
PMMA plate	2mm thick polymethyl methacrylate sheet	1 x 0.6 m	33.02 €/m²	19.81 €
Cutter	Bosch Professional cutter	1	19.24 €/u	19.24 €
Spatula	3D printer removal metal spatula by Comensal	1	9.69 €/u	9.69 €
Ratchet	Ratchet and socket set by Favengo	1	14.98 €/u	14.98 €
Isopropyl alcohol	Isopropyl alcohol for cleaning the printer by Oblait	1l	4.58 €/l	4.58 €
3DLac	Adhesive spray to improve the adhesion of the impression with the base by 3DLAC	2	10.50 €/u	21 €
Flanges	Flanges to secure connections by Beshine, 100mm x 2.5mm	1000	0.00849 €/u	8.49 €

Total cost of the project	**14286.16 €**

COST OF A DEVICE (BIOREACTOR APLICATION)				
CONCEPT	DESCRIPTION	QUANTITY	COST	TOTAL
Electricity	Electricity consumed by the printer	32 h	0.235 €/h	7.52 €
PLA	PLA filament by Smart Materials	0.64 kg	20.31 €/kg	13 €
TPU	TPU filament by Fillamentum	0.009 kg	67.98 €/kg	0.61 €
Silicone tube	4mm interior/ 6mm exterior silicone tube	1 m	0.999 €/m	0.99 €
Silicone tube	10mm interior/ 15mm exterior silicone tube	0.5 m	6.15 €/m	3.08 €
Flanges	Flanges to secure connections by Beshine, 100mm x 2.5mm	30	0.00849 €/u	0.25 €
Chloroform	Chloroform 98% EPR by Labkem	0.04 l	16.32 €/l	0.65 €

Total cost of the device	**26.1 €**

COST OF A DEVICE (INDIVIDUAL APLICATION)				
CONCEPT	DESCRIPTION	QUANTITY	COST	TOTAL
Electricity	Electricity consumed by the printer	20.9 h	0.235 €/h	4.91 €
PLA	PLA filament by Smart Materials	0.41 kg	20.31 €/kg	8.32 €
TPU Spool	TPU filament by Fillamentum	0.009 kg	67.98 €/kg	0.61 €
Silicone tube	4mm interior/ 6mm exterior silicone tube	0.4 m	0.999 €/m	0.4 €
Silicone tube	10mm interior/ 15mm exterior silicone tube	0.5m	6.15 €/m	3.08 €
Flanges	Flanges to secure connections by Beshine, 100mm x 2.5mm	10	0.00849 €/u	0.09 €
Chloroform	Chloroform 98% EPR by Labkem	0.02 l	16.32 €/l	0.33 €

Total cost of the device	**17.74 €**

ANNEX D. ETHICS COMETEE

As described in section 5.5, no personally identifiable information, biological materials, tests involving living organisms, or other resources needing evaluation and approval by an Ethics Committee were used in the development of this project.

Regarding the environmental impact of its production, despite the fact that recycled filament cannot be used due to the possibility that it contains traces of polluting microparticles that may interfere with the subsequent development of cell cultures, a major filament manufacturer that allows us to return the finished spools for recycling, such as Smart Materials, was chosen for PLA spools and, in cases where it was possible (PETG/PCTG), the unwound filament from Fillamentum and Fiberology. Except for the printer, all materials were sourced locally or nationally in order to reduce the carbon footprint.

Regarding the intellectual property of the device, despite being designed as an open-source platform so that users can adapt it to their needs, explicit permission from the author is required to use the platform as a basis for future projects so as not to conflict with any future projects that the owner may undertake.

ANNEX E. PLANS

1. CULTURE CHIPS

1.1. GENERAL PURPOSE

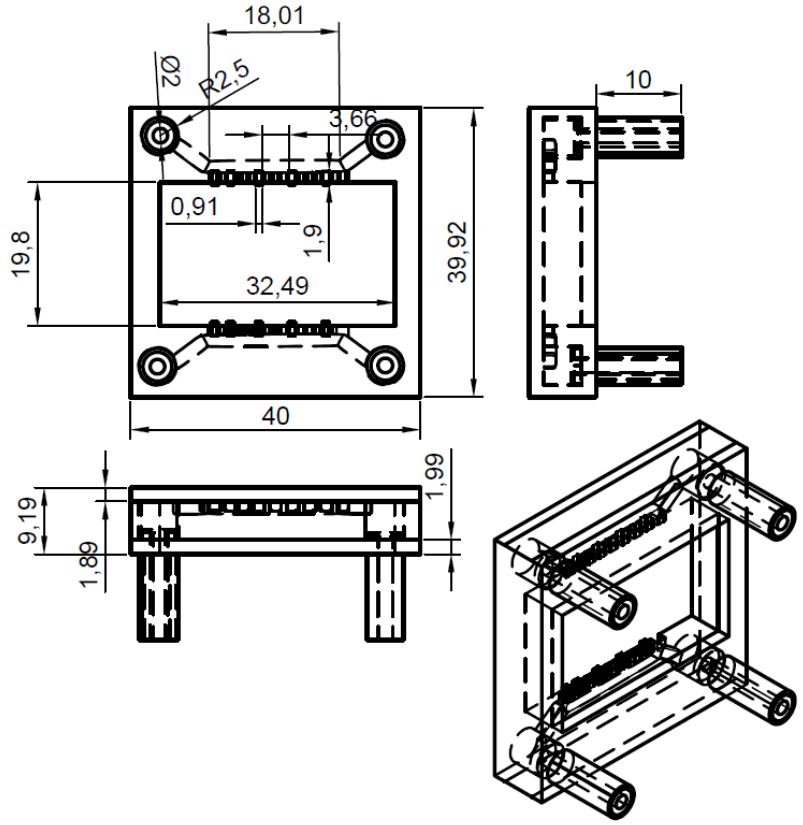

1.2. METASTASIS

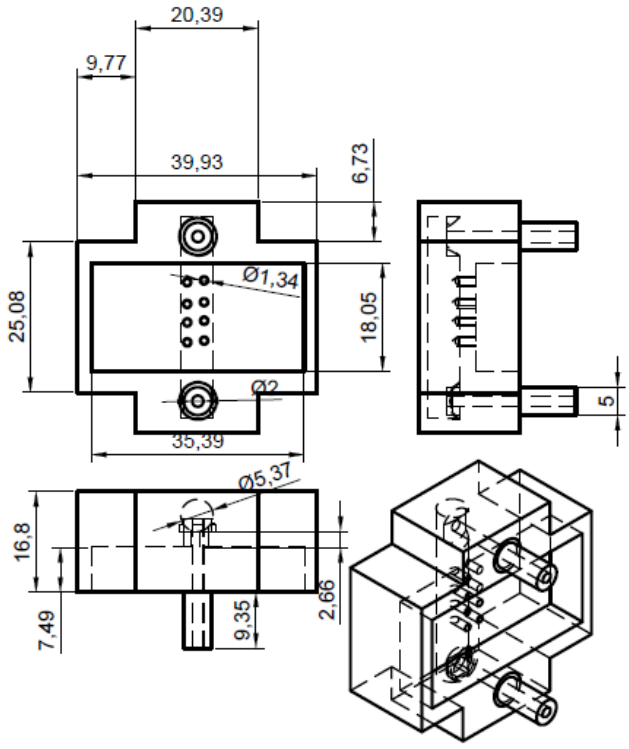

1.3. COVERS

1.3.1. GENERAL PURPOSE

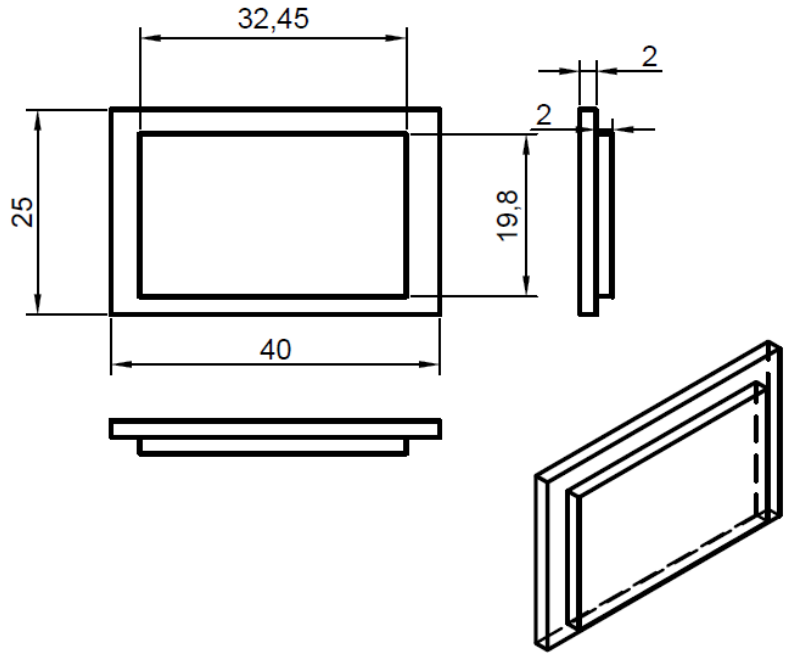

1.3.2. METASTASIS

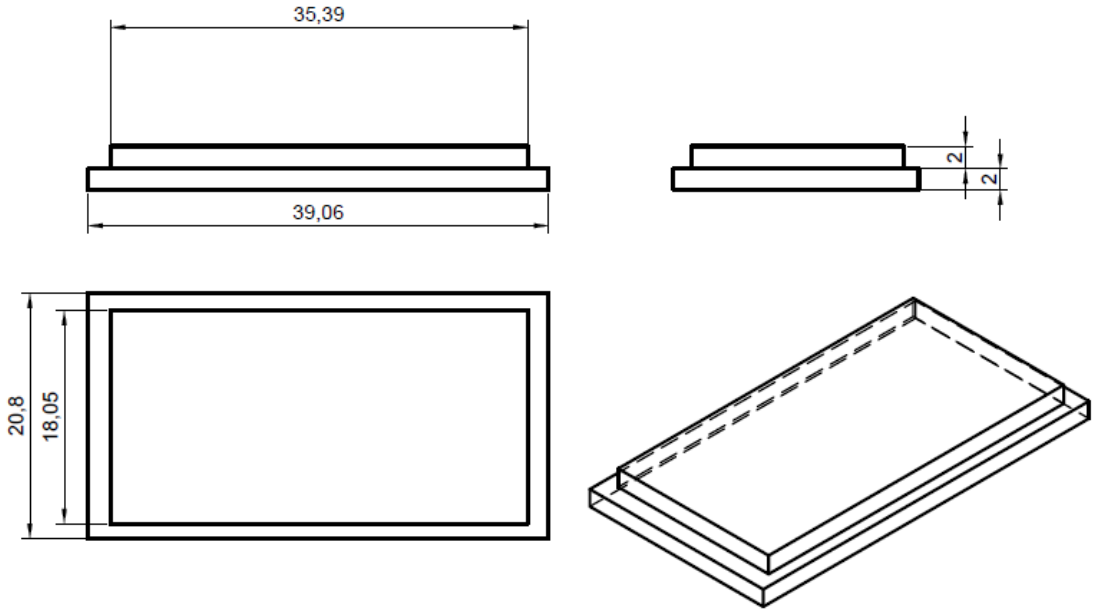

2. TANK

2.1. INDIVIDUAL

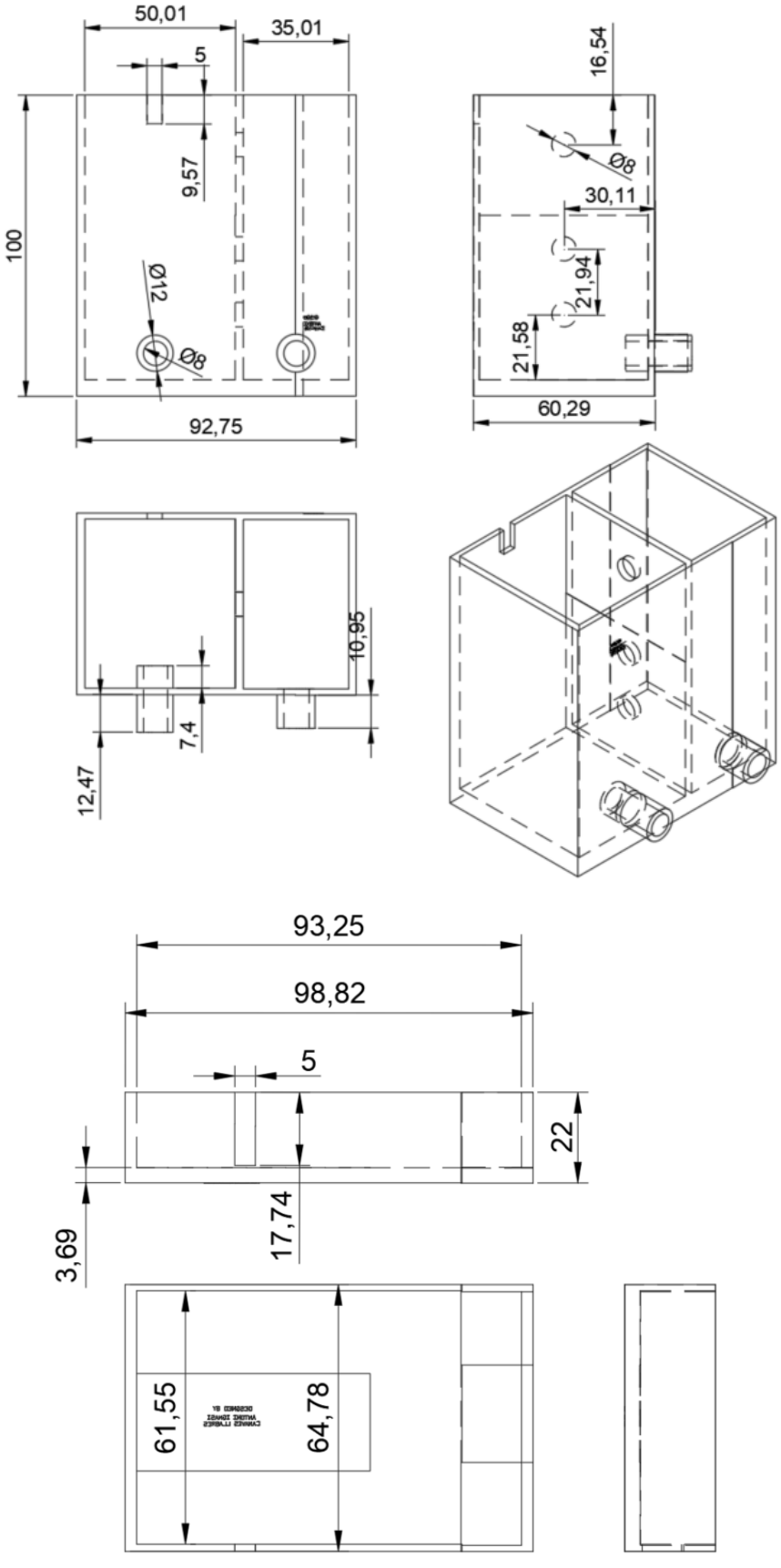

2.2. EXTENSION

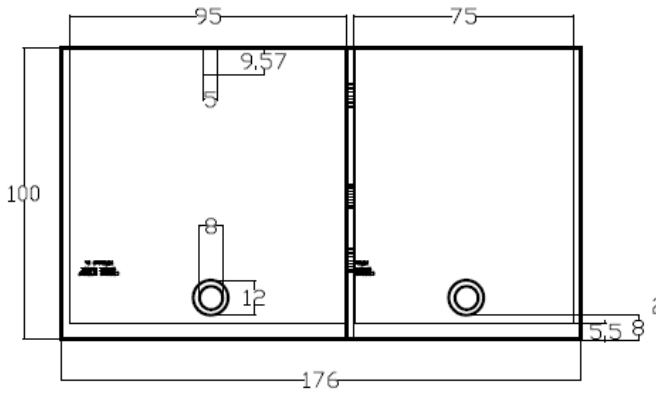

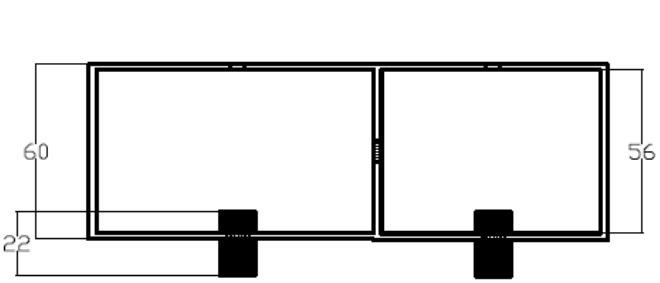

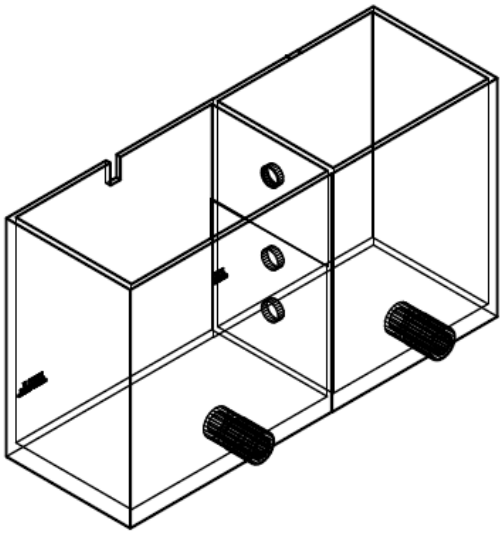

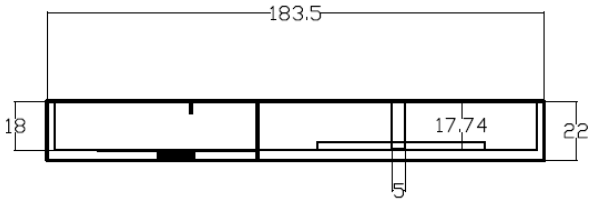

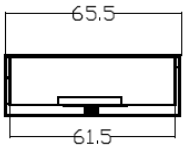

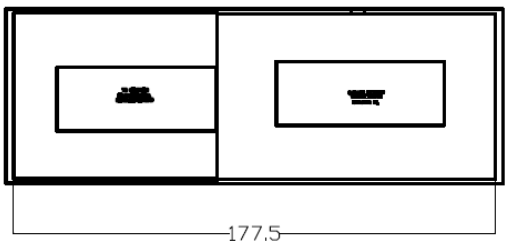

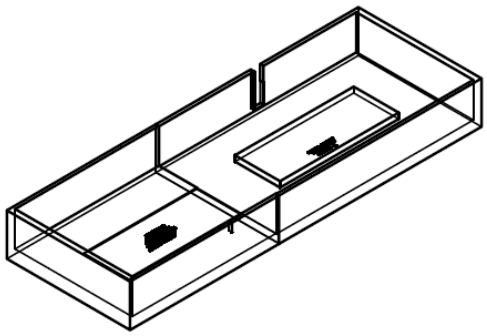

3. CHANNELS MODULE

3.1. INDIVIDUAL APPLICATION

3.1.1. GENERAL PURPOSE CHIP

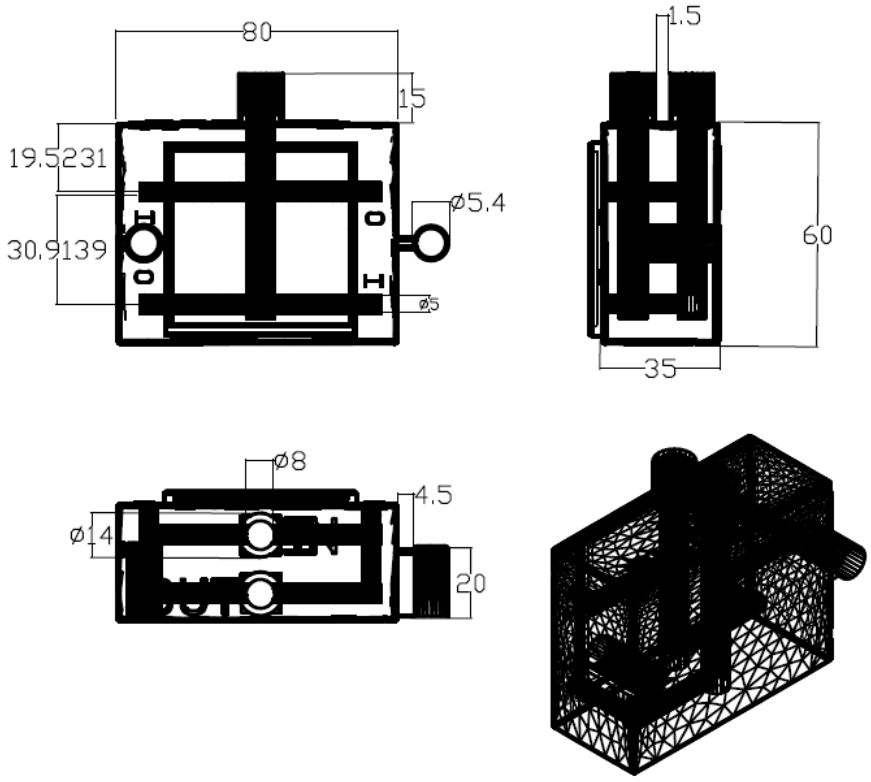

3.1.2. METASTASIS CHIP

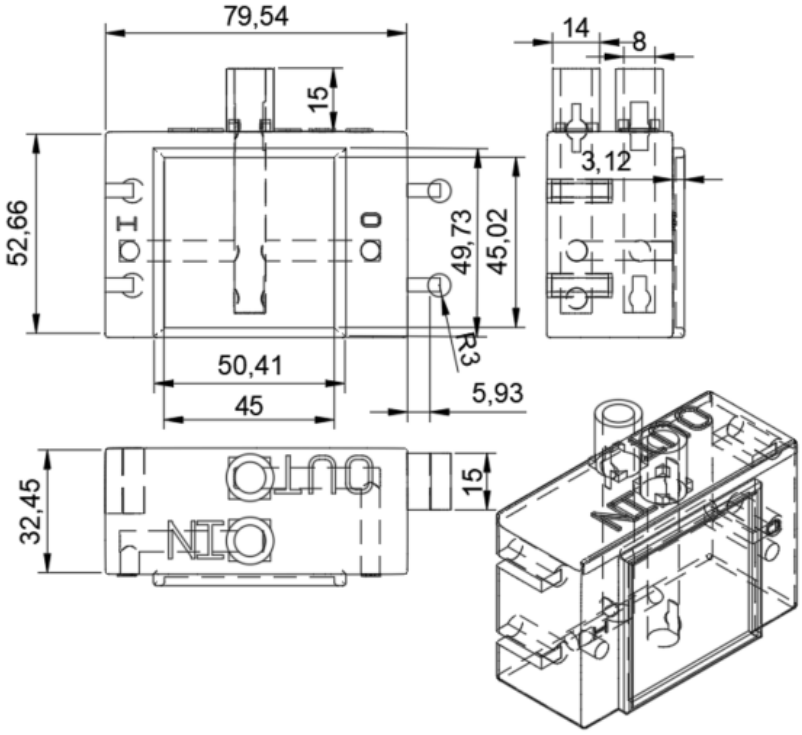

3.2. BODY-ON-A-CHIP / BIOREACTOR APPLICATION

3.2.1. GENERAL PURPOSE CHIP

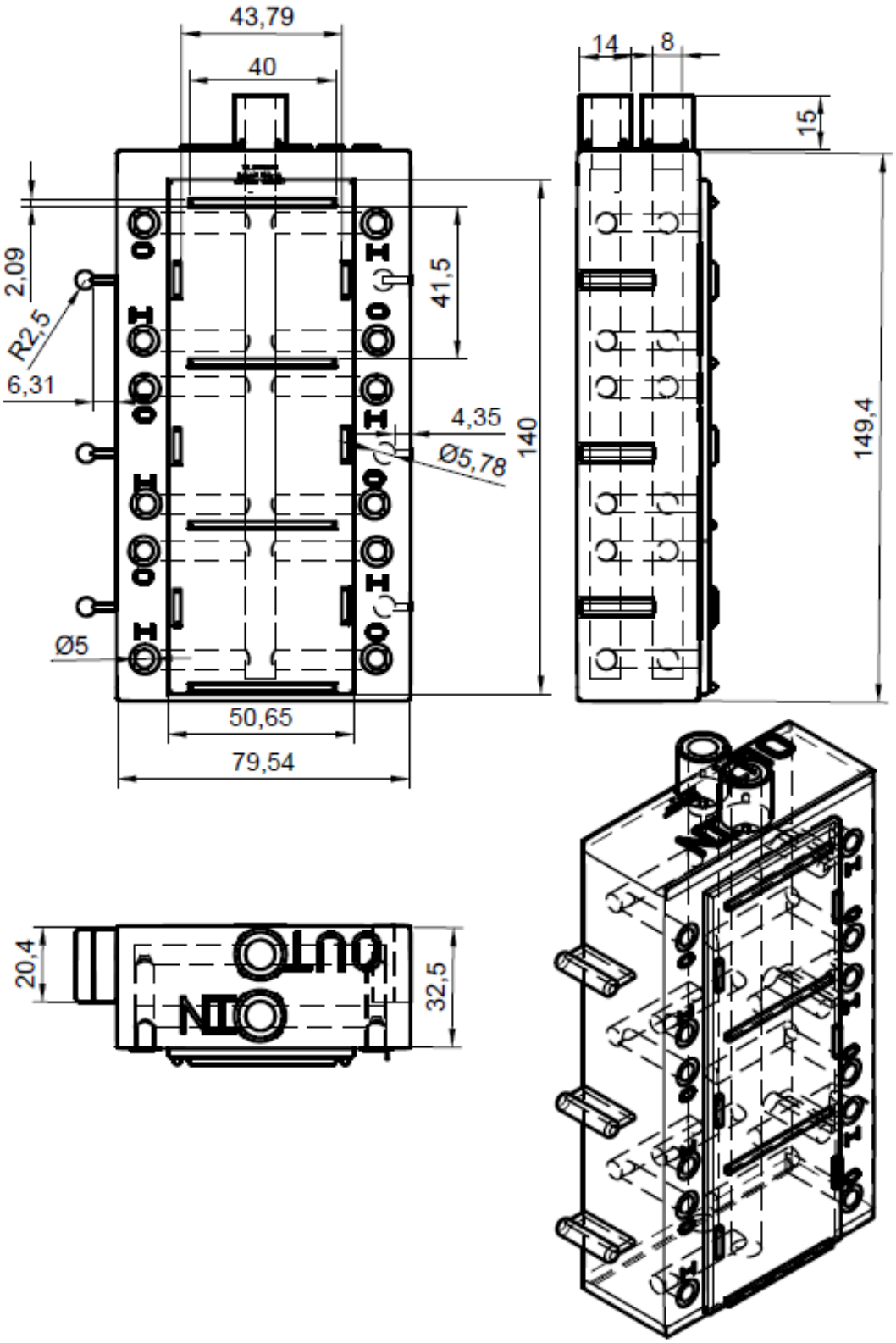

3.2.2. METASTASIS CHIP

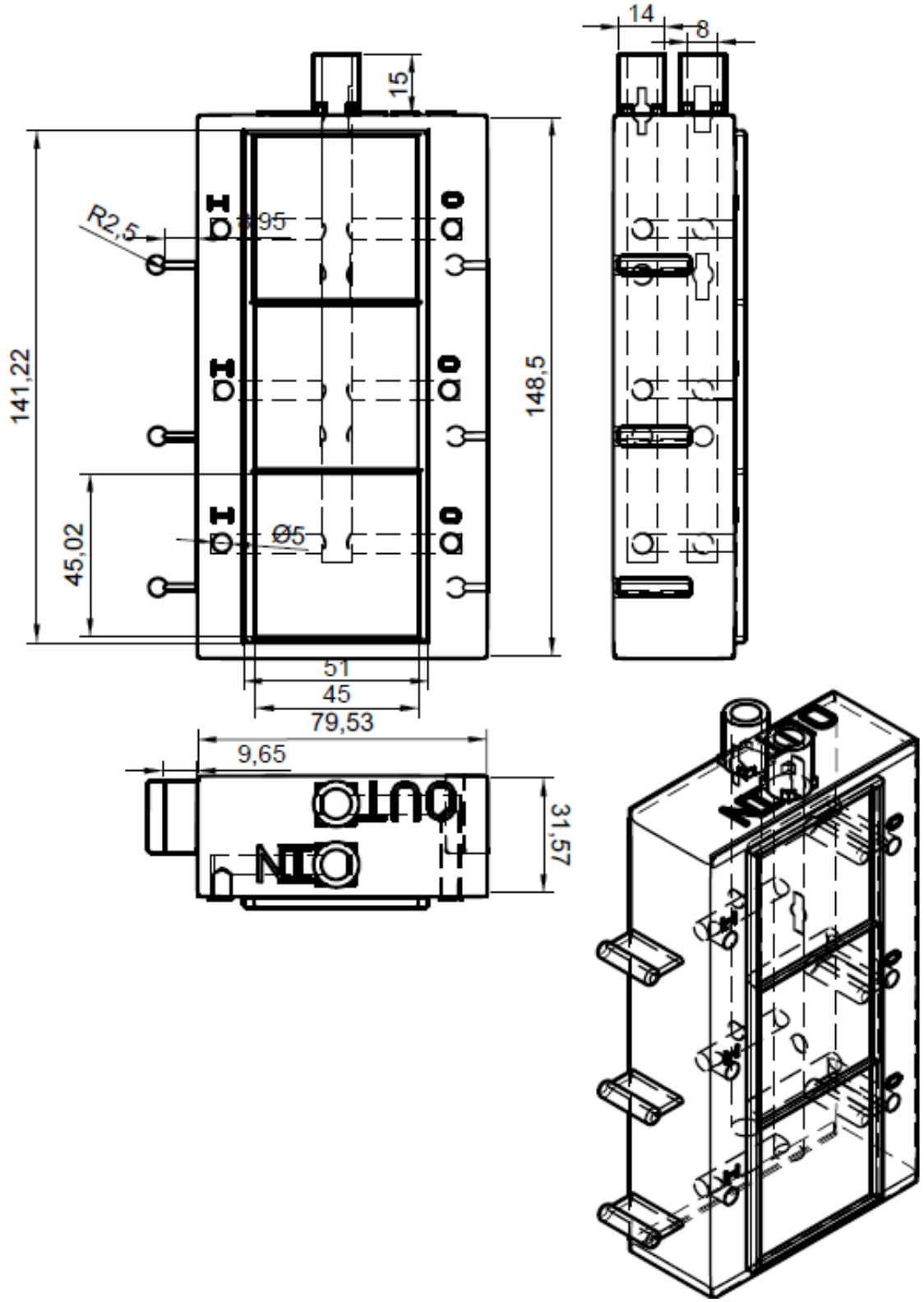

3.3. ADAPTERS

3.3.1. 5 mm CHANNELS TO CHIP

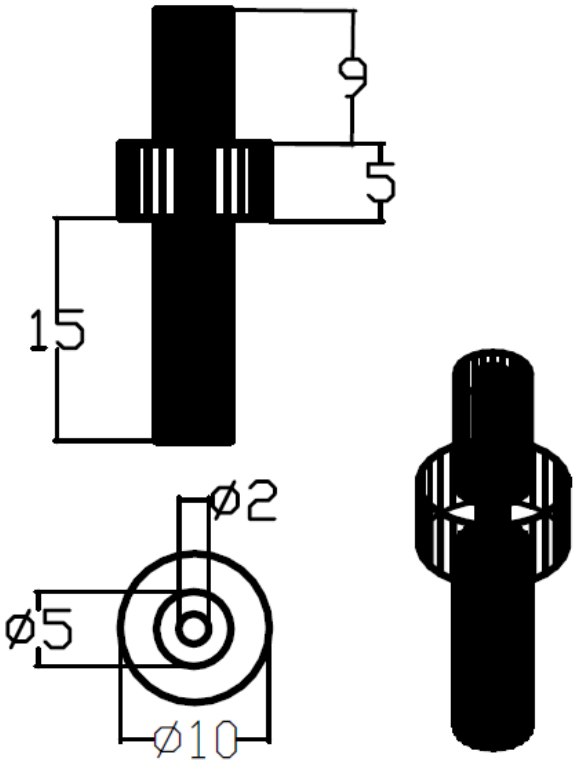

3.3.2. TANK TO CHANNEL MODULE

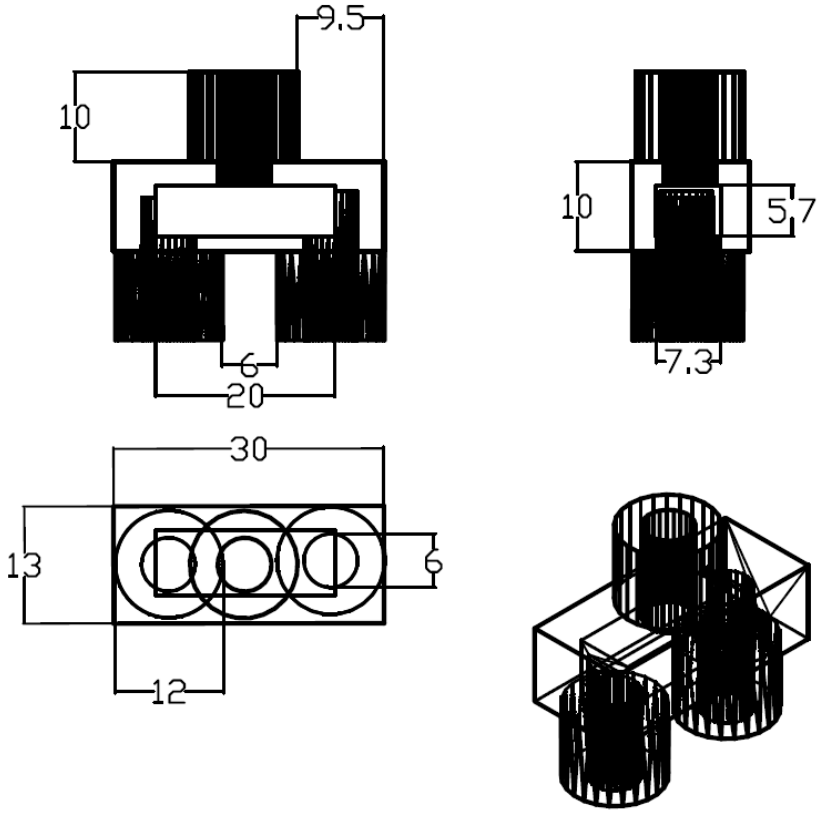

4. *FILTERS*

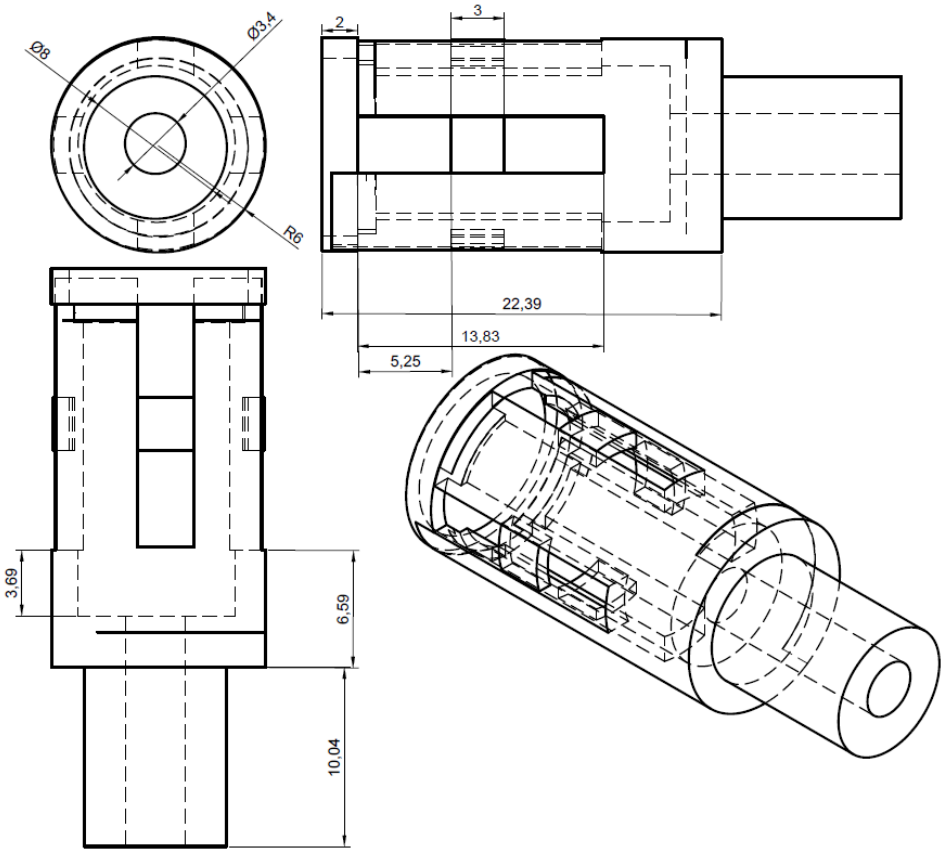
Ø8
Ø3,4
R6
2
3
22,39
13,83
5,25
3,69
6,59
10,04

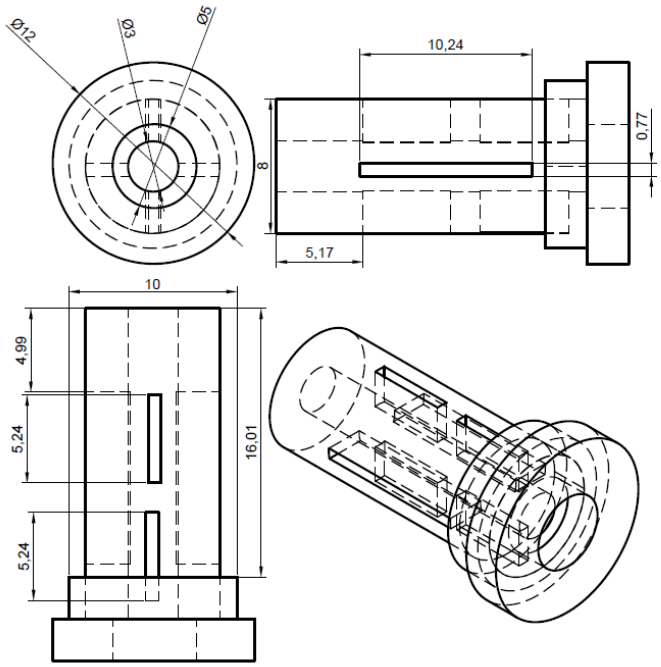
Ø12
Ø3
Ø5
10,24
8
0,77
5,17
10
4,99
5,24
5,24
16,01

5. *BATTERY*

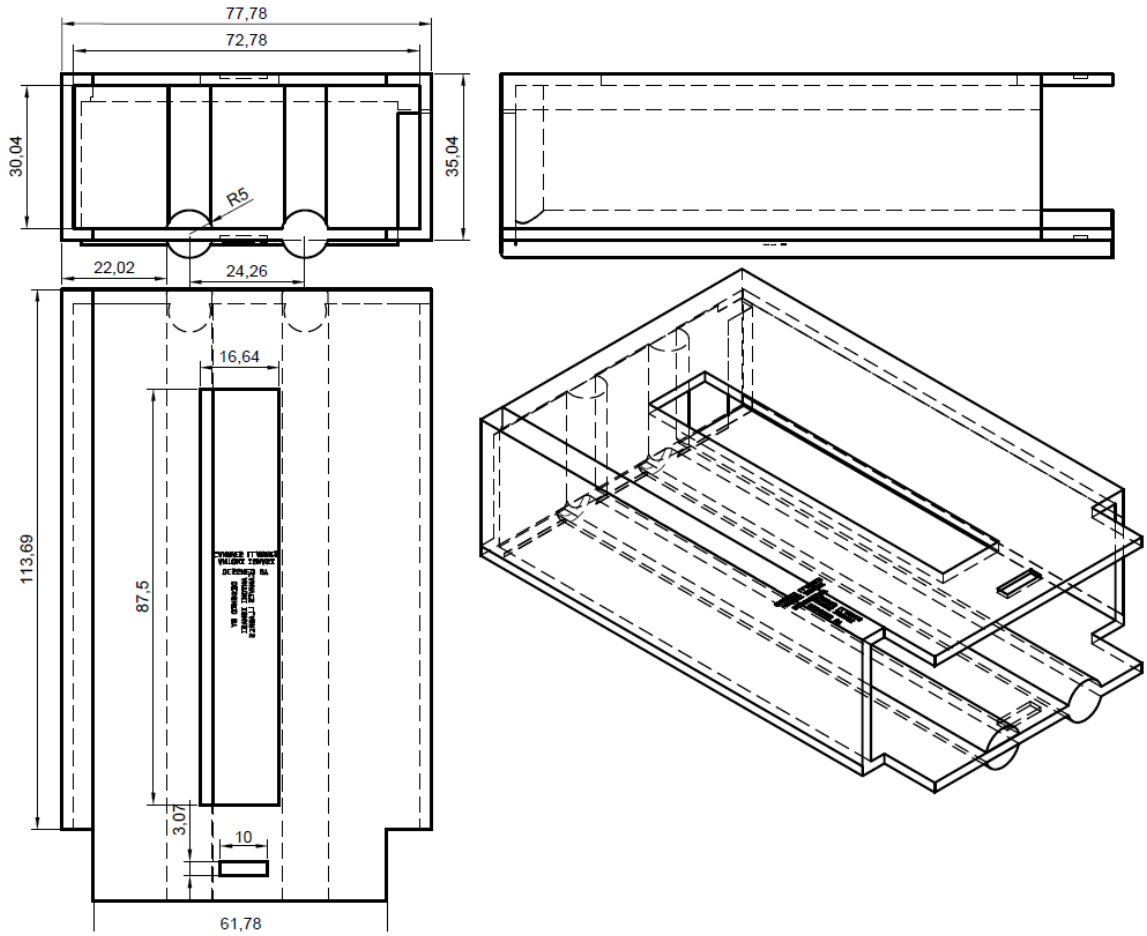
77,78
72,78
30,04
35,04
R5
22,02
24,26
16,64
113,69
87,5
3,07
10
61,78

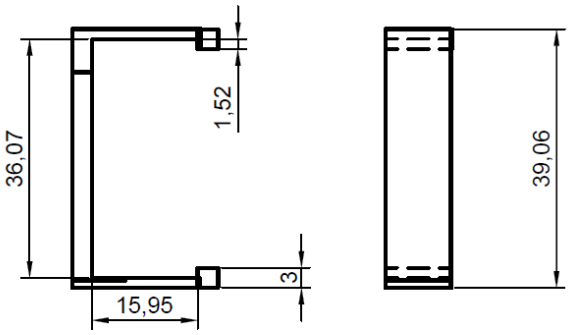
36,07
1,52
3
15,95
39,06

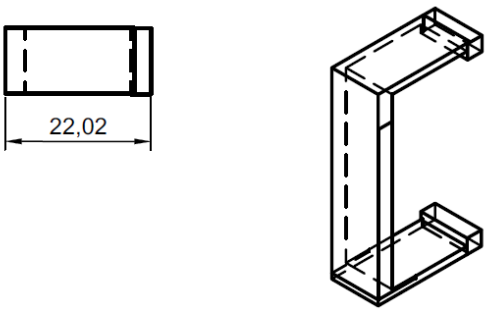
22,02

ANNEX F. ACKNOWLEDGMENTS

First and foremost, I would like to thank all the professors who, over the past four years, have worked to make the Biomedical Engineering degree a space for learning and connection between vastly different fields of study, which, when combined, can revolutionise the future of medicine as we know it. The degree coordinator, Beatriz López, has been an academic and frequently emotional support for all of us during this journey. I would also like to acknowledge Drs. Joaquim de Ciurana Gay and Teresa Puig Miquel for tutoring this project.

I would want to thank my classmates for always prioritising the progress of the group over the egos of individuals and for fostering a non-competitive learning atmosphere in which we have all learned from one another. I would want to call two friends who have been by my side for the past four years. On the one hand, Paula Giménez Almasqué, to whom I owe having taught myself to live day by day, I do not know how I would have gotten out of certain corners of my mind that I am not proud to have been in without you. On the other side, Xavier Beltran Urbano, who despite never having said anything pleasant to me since we met, has always appreciated my work and my inability to clean the coffee cup; Thank you for providing me everyday encouragement to accomplish and be more, I hope we can work together in the future.

I want to thank Dr. David Angelats Lobo for his ability to detour from the topic and start talking for hours about everything he is passionate about, not only because I learned about the concept of Organ-on-a-chip as a result, but also because I met a very close friend as a result.

Finally, I would not be where I am without the support of my family. To my parents, thank you for everything you've done to help me get to this point; we've learnt to support each other, grow and move forward together despite the distance, and this is what I am most proud of after completing my degree. And last but not least, to the one who taught me that the key to being a nice boyfriend is to make supper and discuss social policy at the most inappropriate times: Luismi, I am aware that I have devoted the last few months of my life to completing this project, and that I have not accompanied you as much as I would have liked as you overcame your own obstacles. However, I promise to devote the remaining months of my life to researching how I can love you so much.